Dissipative Structures in Tank Flames

– an experimental study of the dynamic behaviour using several methods, e.g. the holographic real-time interferometry

Axel Schönbucher, Christian Kuhr, Iris Vela

Institute of Chemical Engineering
University of Duisburg-Essen , Campus Essen, Germany

Presentation at the University of Utah, 14th of April 2005

1.0 Introduction: some characteristics of non-reacting and reacting flows

2.0 Experimental work

3.0 Visualisation and interpretation of the dissipative (coherent) structures in space and time

3.1 Interpretation of the interference fringes pattern for transparent objects

3.2 Types of dissipative (coherent) structures

3.3 DVD-Video: "Pool flames, Dynamics of Dissipative Structures"

4.0 Concepts for modeling dissipative (coherent) structures in turbulent reacting flows [flames]

4.1 Present flame models: *modeling of local structures (dissipative structures) is not possible*

4.2 Some aspects of nonlinear science: *modeling of local structures should be possible*

5.0 Properties of dissipative (coherent) structures

5.1 Turbulent length-, time- and velocity scales

5.1.1 Bimodal frequency distributions of length scales of density sources Q and density sinks S

5.1.2 *Borghi* diagram

5.2 Turbulent Pr_t-, Sc_t- and Le_t numbers

5.3 Dynamic properties of density sources Q and density sinks S

5.3.1 Physical meaning of Q and S

5.3.2 Number of Q and S

Scientific co-workers

Bärbel *Arnold-Maurer*
Christoph *Balluff*
Volker *Banhardt*
Manfred *Beck*
Vera *Bieller*
Oliver *Brehm*
Hyunjoo *Chun*
Manfred *Dorn*
Markus *Gawlowski*
Hans-Jürgen *Geiger*
Dietmar *Göck*
Henning *Kasper*
Martin *Kaufmann*
Albrecht *Kettler*
Thomas *Koch*
Dieter *Krattenmacher*
Christian *Kuhr*
Rolf *Lucas*
Achim *Leitzke*
Anna *Luque*
Werner *Müller*
Daniel *Opitz*
Markus *Pulm*
Gunther *Riedel*
Raimund *Schäble*
Volker *Scheller*
Norbert *Schieß*
Rainer *Schuhmacher*
Steffen *Staus*
Peter *Sudhoff*
Dieter *Tschoppe*
Iris *Vela*
Albrecht *Walcher*
Horst *Wehlus*
Thomas *Weihs*

Financial support

Volkswagen-Foundation with the focus „Fundamentals of Technical Combustion Procedures"
Deutsche Forschungsgemeinschaft (DFG)
Fonds der Chemischen Industrie

1.0 Introduction

1.1 Some characteristics of non-reacting flows

- Gas outflow ($\rho < \rho_u$) vertical into the *free* ambient atmosphere

- Initial momentum flow rate << buoyant convective force of inertia

  slow flows: $0.02 < u_{ax}\ (x = 0) < 0.7$ m/s ($d = 4.6$ cm)

- States of fluid flow

  Laminar flow → quasi-periodic flow → (anisotropic) turbulent flow

1.2 Some characteristics of reacting flows (tank/pool flames)

- Free (non-enclosed) laminar coflow nonpremixed flames

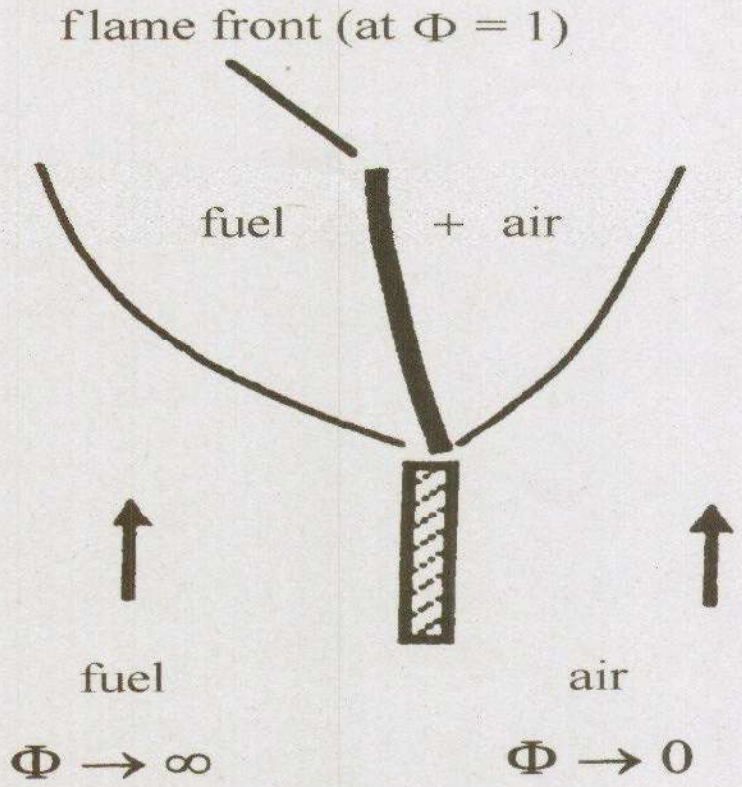

Nonpremixed parallel inflow of fuel and air; variation of the ambient air

Φ: fuel equivalence ratio

- As a pure premixed flame (e.g. CH_4 : $0.5 < \Phi < 1.68$) and also as a transition to a nonpremixed flame (e.g. CH_4 up to $\Phi = 3$)

- Stationary and instationary, nonpremixed flame

- Thermal buoyancy of the flame gases

  Initial momentum flow rate << buoyant convective force of inertia

$\Rightarrow$ *slow flows*: $0.05 < u_{ax} < 2.5$ m/s (d = 4.6 cm, n-hexane)

u_{ax} : axial flow velocity

d : tank diameter

- States of fluid flow: Laminar

- Transport-controlled

  $r_R >> r_T$ (fast chemistry)

  r_R : reaction rate

  r_T : transport rate

- Formation of *soot particles*

  The chemical reaction mechanism is rather complicated; e.g. the temperature decrease due to heat radiation of the soot particles is also to be considered

- *Multiphase* systems

Gaseous fuels: heterogeneous 2-phase system of flame gases and soot particles

Liquid fuels: heterogeneous 3-phase system of liquid fuel, flame gases and soot particles

---

- New concept in tank flames: *Nonlinear science*
  - Tank and pool flames can be characterised as:
    - thermodynamic open systems with a continuous exchange of momentum, heat and matter with the ambient atmosphere
    - (fast) chemistry with finite reaction rates, but controlled by diffusion processes
    - nonlinear chemical reaction kinetics, e.g. chain branching reactions
    - formation of dissipative (coherent, organized) fluid dynamic structures

- Large gradients of temperatures T, mass fractions y_i of the species i, flow velocities $\vec{u}$

  - Axial and radial profiles of T, y_i , $\vec{u}$

  - Axial and radial *dispersion* as well as the heat flow rate (energy feedback) from the flame to the liquid fuel surface

  - Increase in dynamic viscosity [transition to laminar flow] due to the local high flame temperatures

  - Broad residence time distribution (RTD)

In tank and pool flames large deviations from the ideal plug flow exist because the reactor dispersion number is large:

$\frac{D_{ax}}{\bar{u}\ \bar{H}}$ [$\bar{H}$: averaged flame length; $\bar{u}$: averaged flow velocity; D_{ax}: axial *dispersion* coefficient]

CH_4/air - nonpremixed flame (d = 4.6 cm): ≈ 14

n-hexane/air - nonpremixed flame (d = 4.6 cm): ≈ 29

- Formation of dissipative (coherent, organized) fluid dynamic structures [supramolecular organisation to coherent structures]

  - Molecular ensembles of 10^{10} to 10^{20} molecules, which are long-range correlated on macroscopic length- and time scale:

Length - scales:

$\approx$ mm to cm; correlation length $l \approx \sqrt{K\ t_R}$

Time - scales:

$\approx$ ms; $t_R << t_M$, $\tau << t_M$,

τ : space-time

CH_4/air - tank flame (d = 4.6 cm):

$$t_R = \frac{1}{Da_{II}} t_M \approx 0.002\ t_M \approx 0.5 \text{ ms};\ t_M \approx 250 \text{ ms}$$

$$\overline{\tau} \approx 0.2\ t_R \approx 0.1 \text{ ms}$$

n-hexane tank flame (d = 4.6 cm):

$$l \approx \sqrt{K_I t_R} \approx \sqrt{2*10^{-3}\,m^2/s \text{ x } 0.5*10^{-3}\,s} \approx 10^{-3}\,m$$

- Pockets, (density) parcels, lumps
  Self-organized regions with independent movements

- Properties of dissipative structures (in tank flames) different to classic eddies:

  * not only decay but a definite growth (downstream) with increasing vertical distance from the tank rim

  * formation of *multiple* parcels, e.g. « twins », « triples »

  * neither decay nor growth : the geometric sizes of the parcels remain constant

  * Relatively long lifetimes (≈ ms): important for the formation of pollutants, e.g. NO_x, soot particles

2.0 Experimental work

2.1 Experimental methods for the *visualization* of dissipative structures in flames

- *General requirements*

  - Mainly contact-free and inertia-free methods with as high a *spatial* and *temporal* resolution as possible

  - As many methods as possible should be used *simultaneously* since the dissipative structures in flames are very complex phenomena

  - For *visualization* of the dissipative structures preferably 2-D or 3-D measurements should be taken instead of point measurements

- *types of density structures*

  - *Shadow* structures : $\frac{\partial^2 \rho_m}{\partial y^2}$ - *fields*

  - *Schlieren* structures : $\frac{\partial \rho_m}{\partial y}$ - *fields*

  - *Interference fringe* patterns : ρ_m - *fields*

$\rho_m(x, y, z)$: mass density field of the flame gas mixture

Experimental methods (I)

1	**Instantaneous interference fringe patterns**	
	Density structures with [for flames] or without [non-reactive flows] simultaneous radiance structures	*Holographic real-time interferometry*
2	**Instantaneous radiance structures**	
	VIS-radiance structures IR-radiance structures	*High-speed photography* *Thermographic camera system with a video mixing unit, digital image analysis*
3	**Time-averaged radiance structures**	
	VIS-radiance structures	*Time exposures* *Digital image analysis*
4	**Time-averaged irradiances**	
	E(y,d,fuel) from VIS- to IR-spectral region	*Pyroelectrical and ellipsoidal radiometry*

Experimental methods (II)

5	**Sampling methods**	
	$T_F(r,x)$; $u(r,x)$; $\gamma_i(r,x)$; $c_R(r,x)$	*PtRh/Pt thermocouple* *Photoelectric detector* *Gas chromatography*
6	**Frequency spectra**	
	• of the thermal boundary layer $y_G(t)$	*Interferometry*
	• of the number w(t) of density sources and sinks	*Interferometry*
	• of the dynamic pressure $p_{dyn}(t)$	*Differential pressure sensor and spectrum analyzer*
	• of the spectral radiance $L_{\Delta\lambda}(y,x,t)$	*Photoelectric detectors*
7	**Flow velocities**	*Differential pressure sensor, photoelectric detector*
8	**Meteorological parameters**	
	$u_{wi}(t)$; $\bar{u}_{wi}(t)$	*10 m mast with electronic weather station*

2.2 Holographic real-time interferometer with 25 cm Laser beam expanding

Optical paths

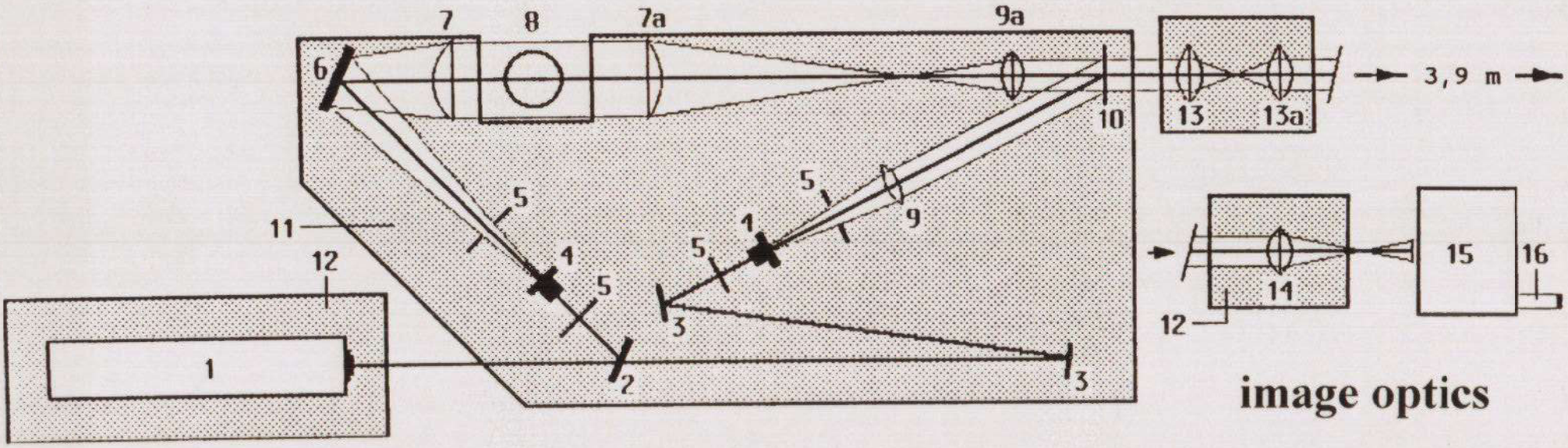

1)	2 W-cw-Argon Laser	9 u. 9a)	7.8 cm achromat, f = 31 cm
2)	beam splitter	10)	hologram
3)	mirror	11)	granite plate
4)	beam expanding	12)	concrete finished products
5)	iris	13 u. 13a)	7.8 cm achromat, f = 16 cm
6)	22 cm plate mirror	14)	7.8 cm achromat, f = 31 cm
7 u. 7a)	25 cm lens (plan convex)	15)	high speed camera (Hycam)
8)	testroom for phase objekt	16)	microscope ocular

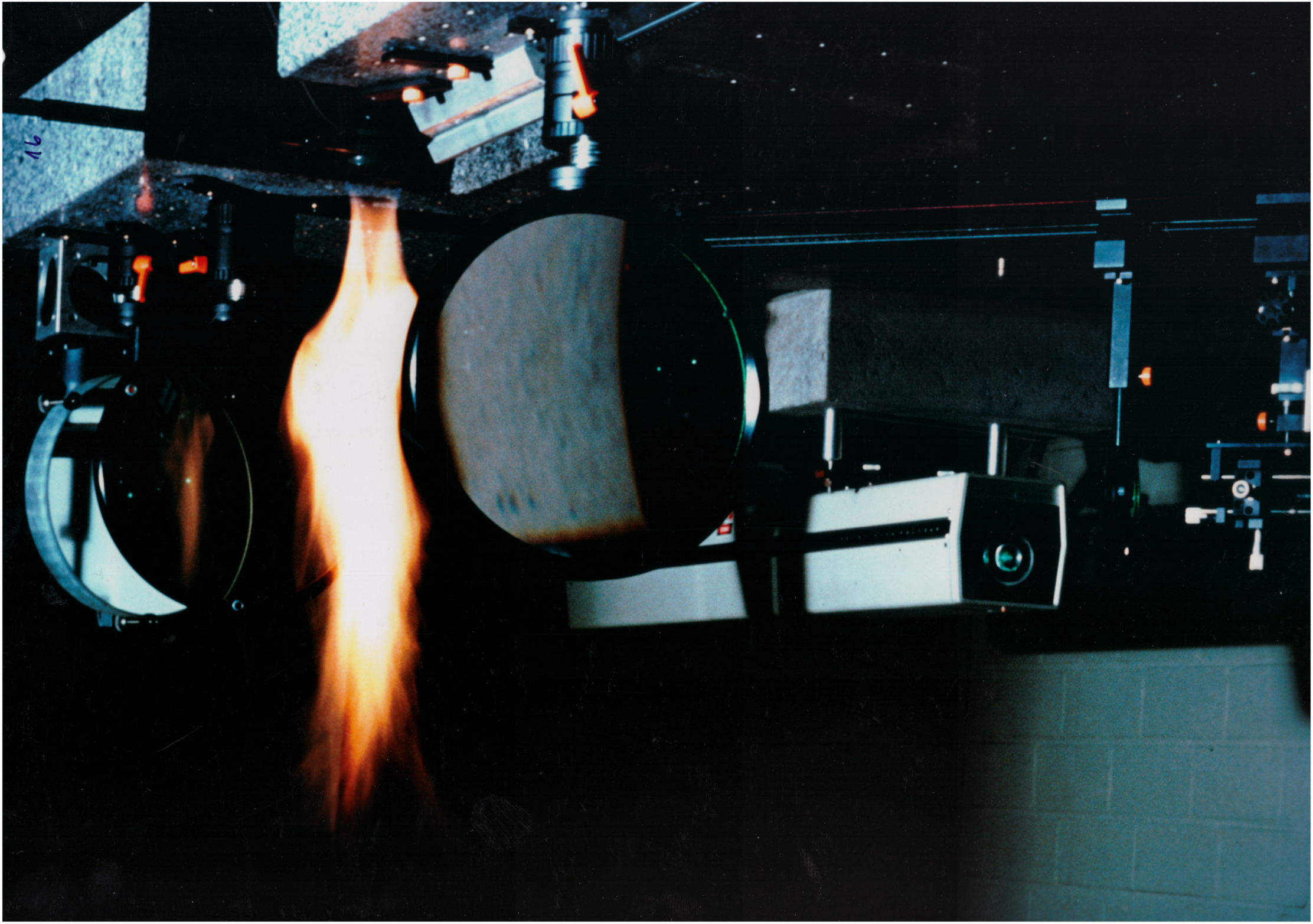
16

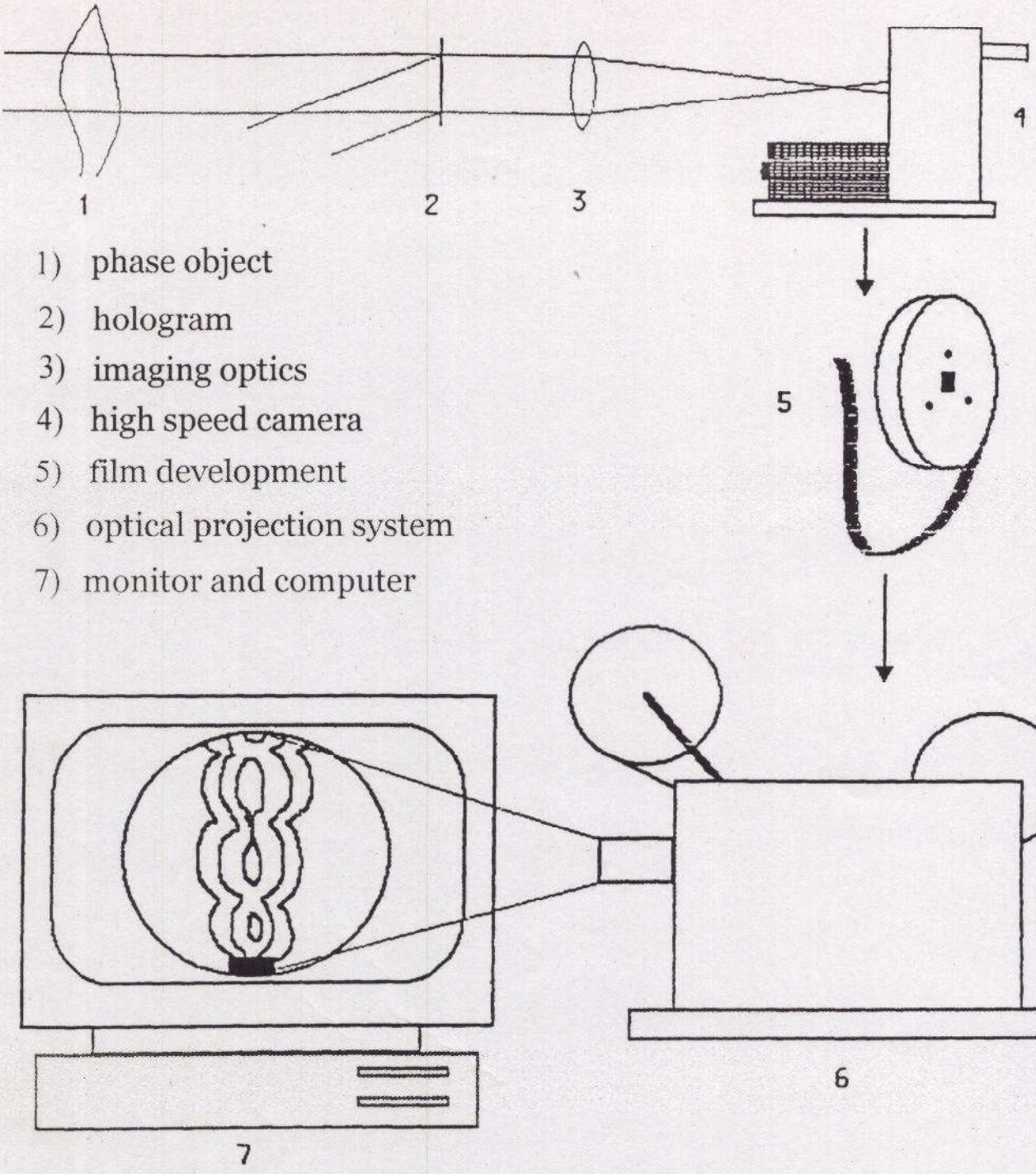

1) phase object
2) hologram
3) imaging optics
4) high speed camera
5) film development
6) optical projection system
7) monitor and computer

Computer aided analyses system for digital data preparation of the interference fringe patterns

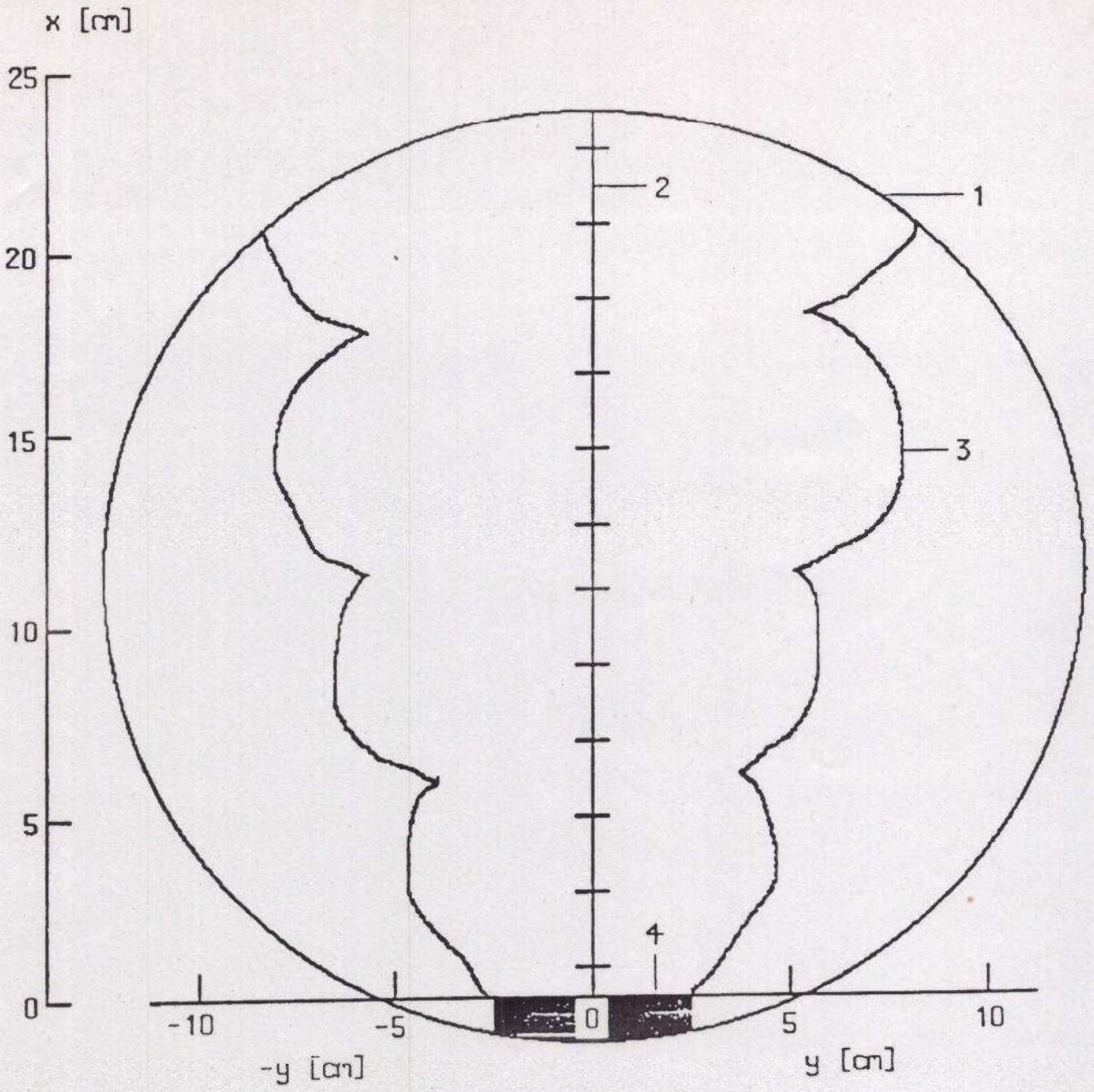

1) contour of the interference fringe pattern
2) reference scale of the phase object
3) contour of the phase object
4) tank rim

Coordinate system of the projected fringe patterns for data preparation via monitor

2.3 Gaseous fluids (non-reacting flows)

Helium

Hot air

Methane (non-ignited)

2.4 Gaseous and liquid fuels (reacting flows)

Methane	Methanol	Acetaldehyde	Acetic acid	Benzene
LNG	Ethanol	Acetone	Acetic ester	
n-Butane	Propanol	Diethyl ether		
n-Pentane	Cyclohexanol			
n-Hexane	Glycerol			
n-Heptane				
Premium gasoline				
Diesel fuel				
JP-4				

Hydrogen

2.4 Gas feed and tanks for non-reacting flows (I)

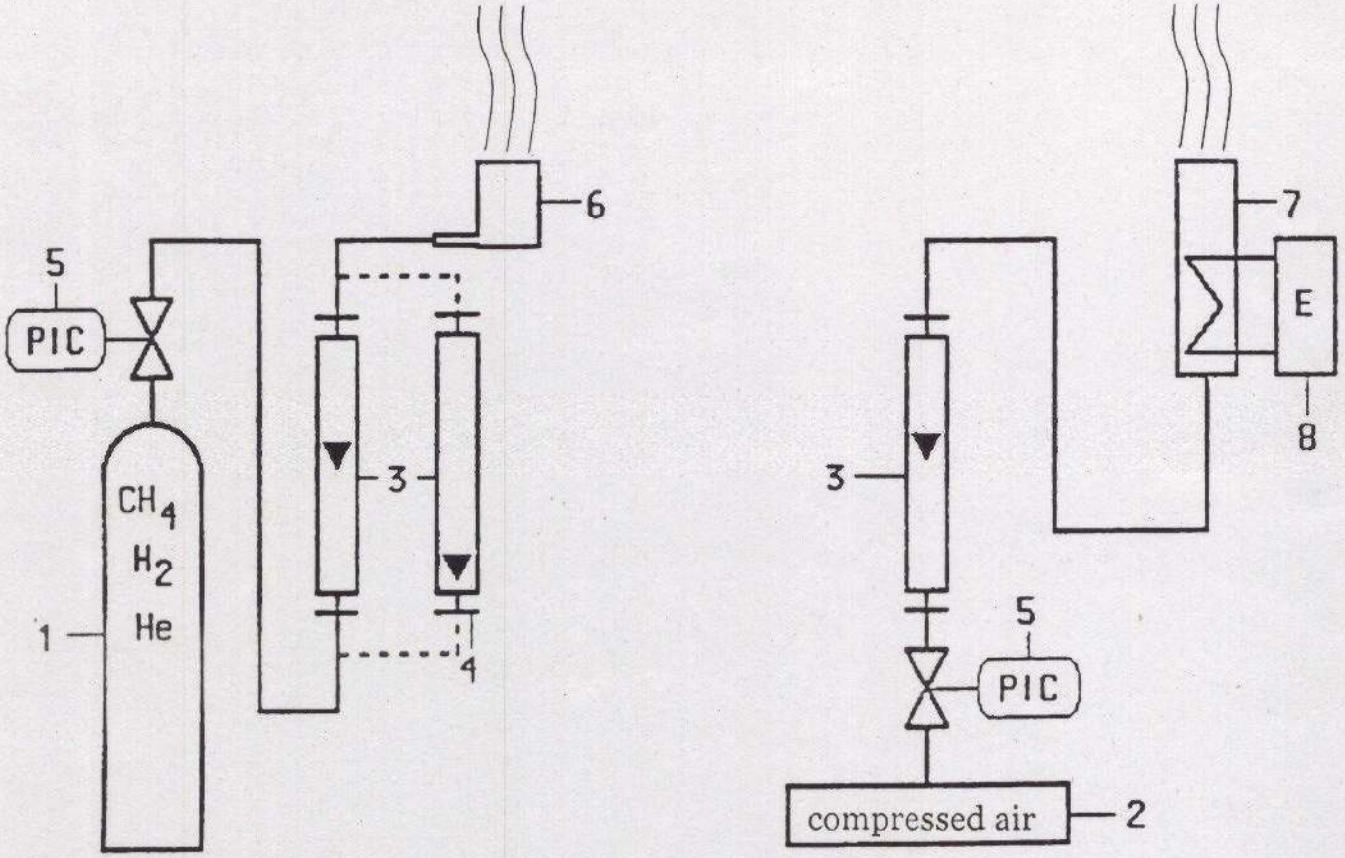

1) pressure cylinder
2) compressed air network
3) rotameter
4) spherical joint
5) pressure control valve
6) steel tank
7) air furnace
8) electrical energy supply

2.4 Fuel supply and tank construction for non-reacting flows (II)

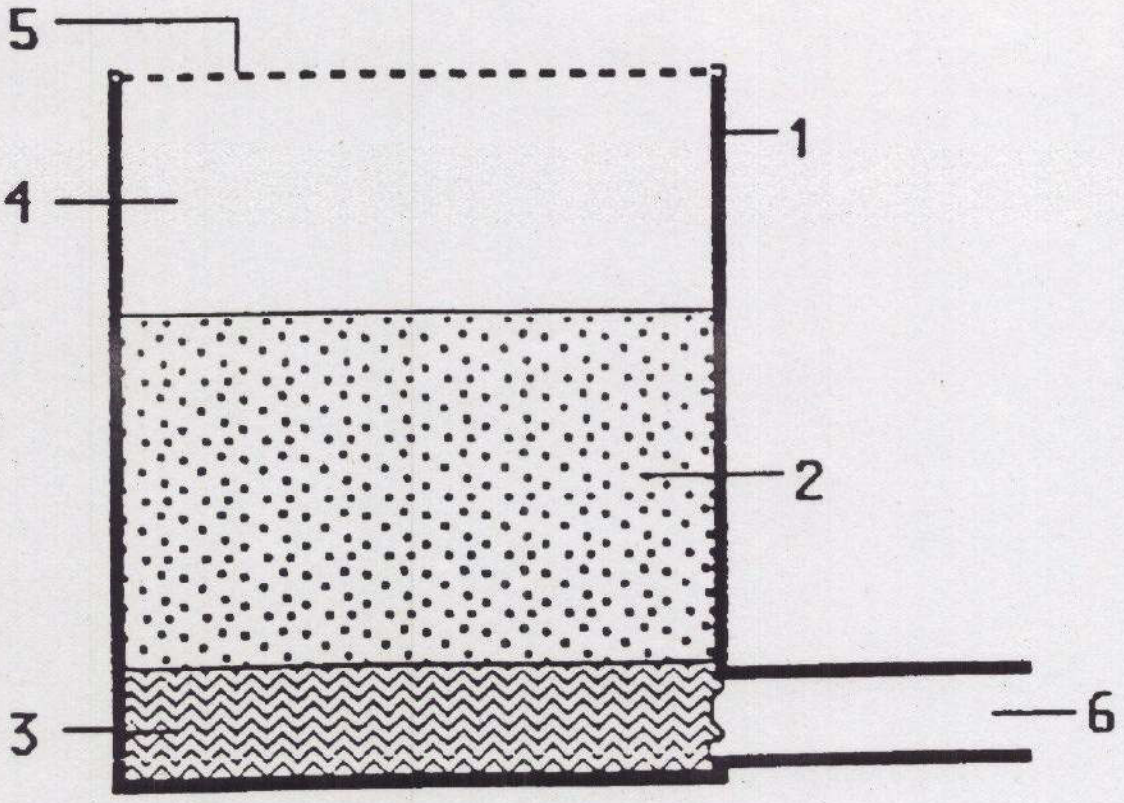

1) Steel pipe (d_{wall} = 2 mm)
2) Sand bed (d_{grain} = 1 - 1.5 mm)
3) Glass wool (h = 1 cm)
4) Expansion release zone
5) Wire mesh (d_{mesh} = 1 mm)
6) Gas supply

Steel tank for He- and CH_4 outflows

2.5 Fuel supply and tanks for gaseous and liquid fuels

(reacting flows) (I)

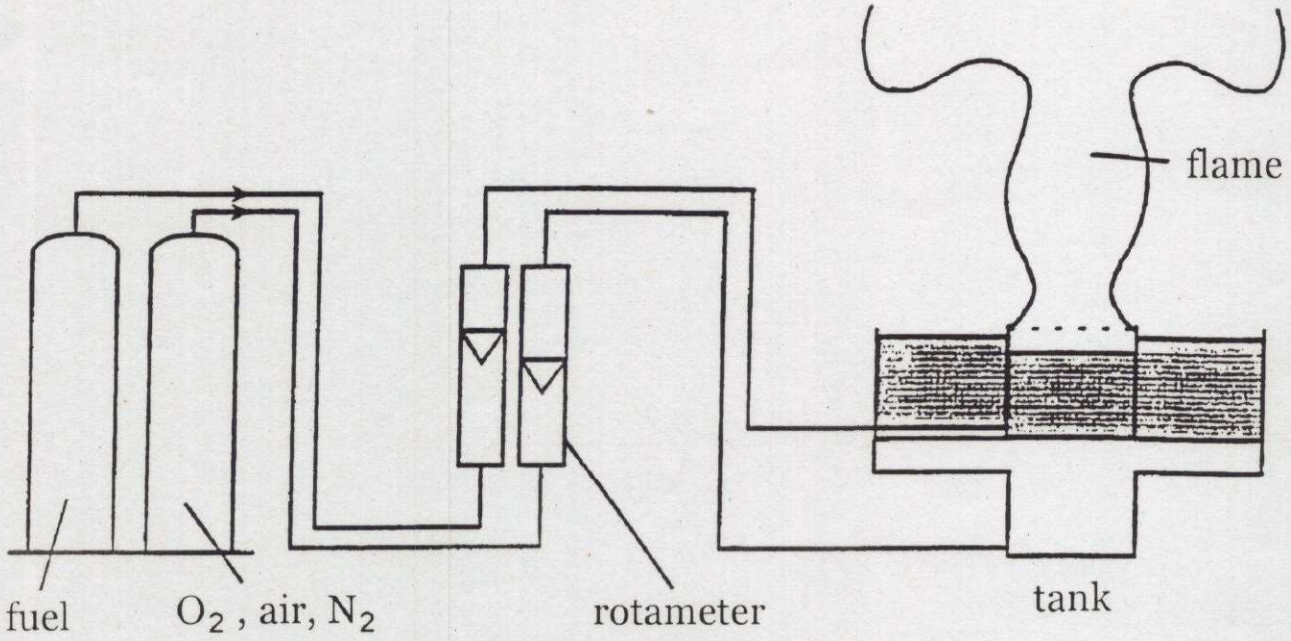

Fuel supply for gaseous fuels and variable ambient atmosphere due to *axial* gas feed

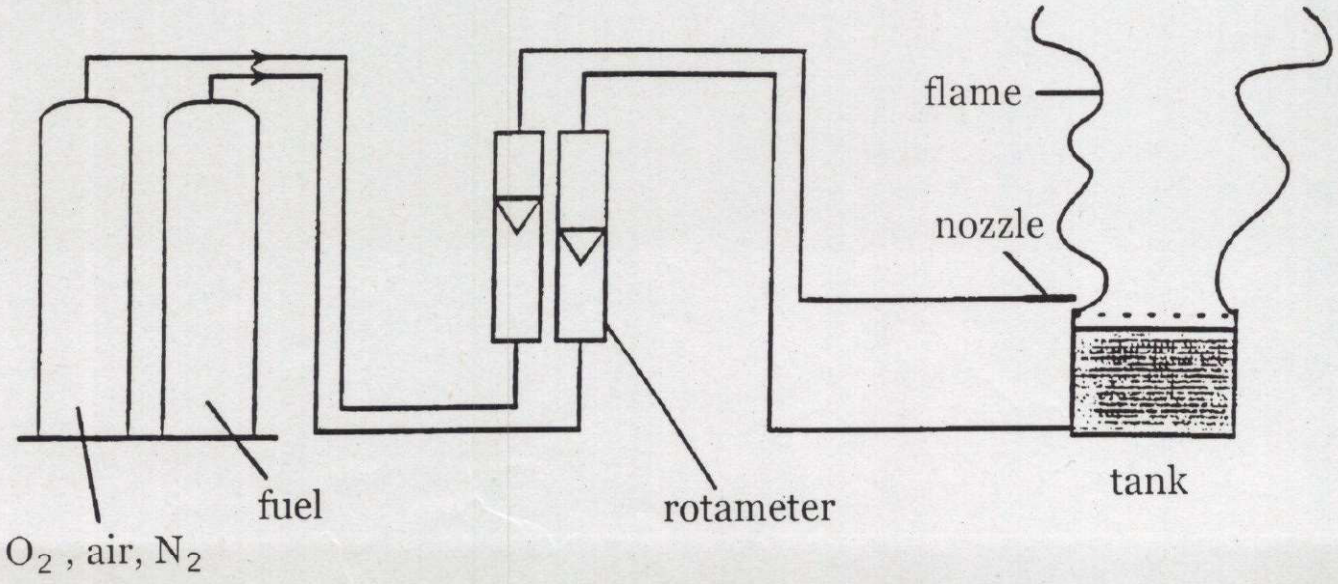

Fuel supply for gaseous fuels and *radial* gas feed

2.5 Fuel supply and tanks for gaseous and liquid fuels

(reacting flows) (II)

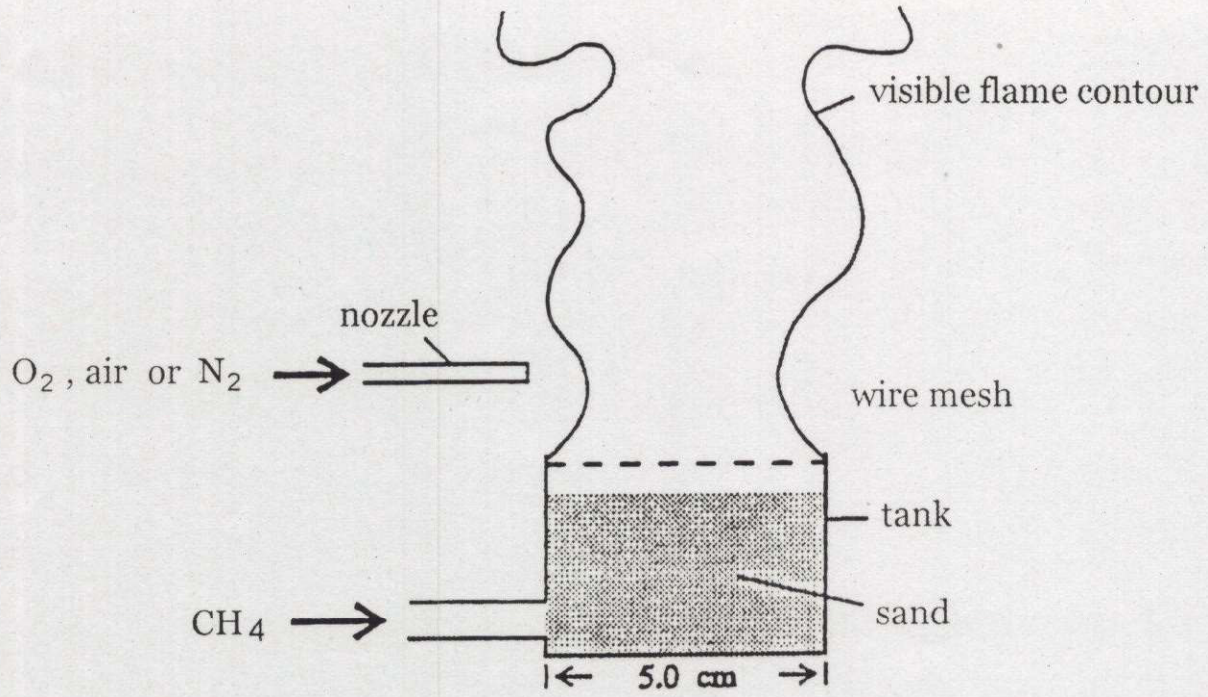

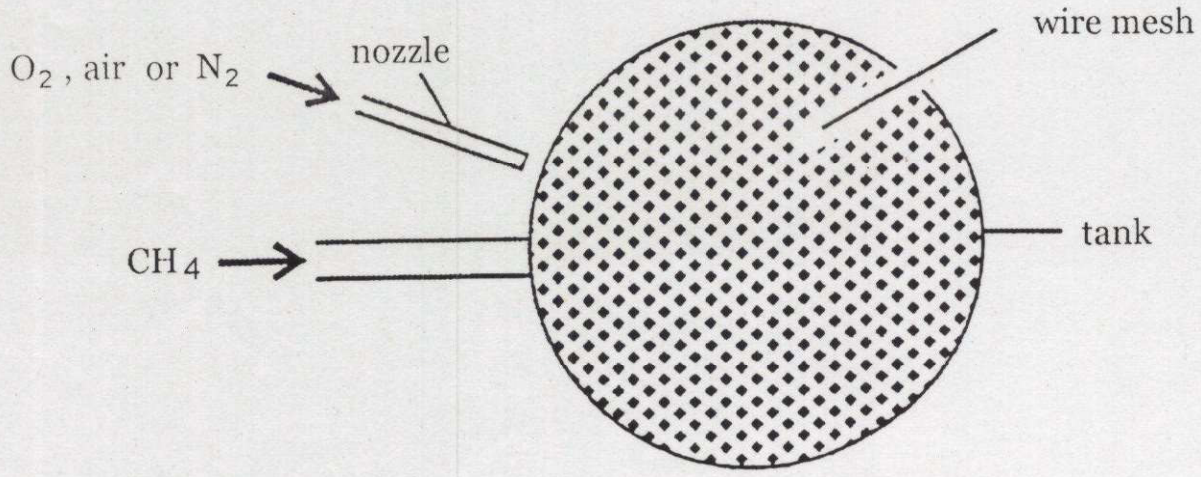

Tank construction for *radial* gas feed near the tank rim

2.5 Fuel supply and tanks for gaseous and liquid fuels *(reacting flows)* (III)

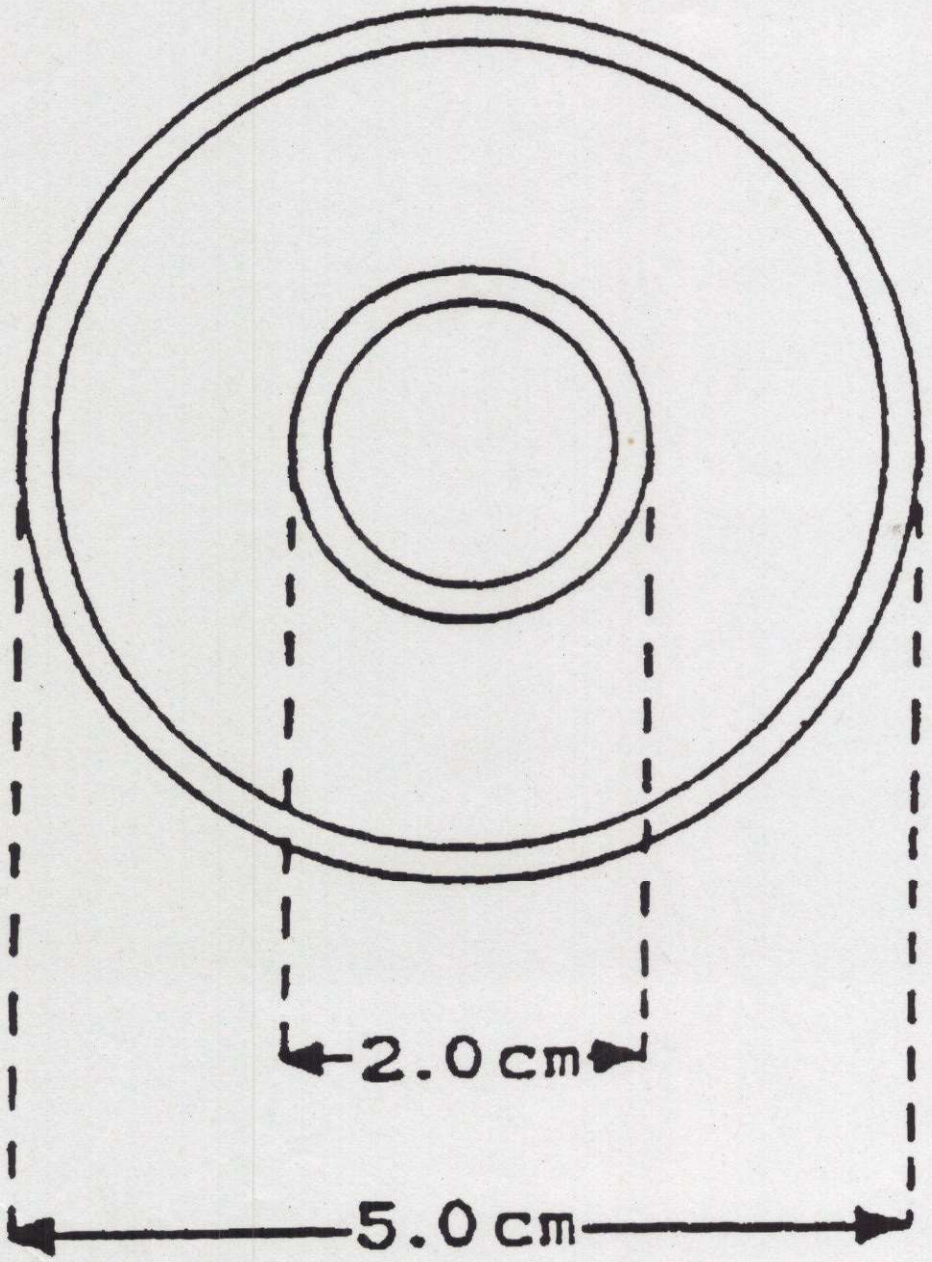

ringlike tank

2.5 Fuel supply and tank construction for gaseous and liquid fuels *(reacting flows)* (IV)

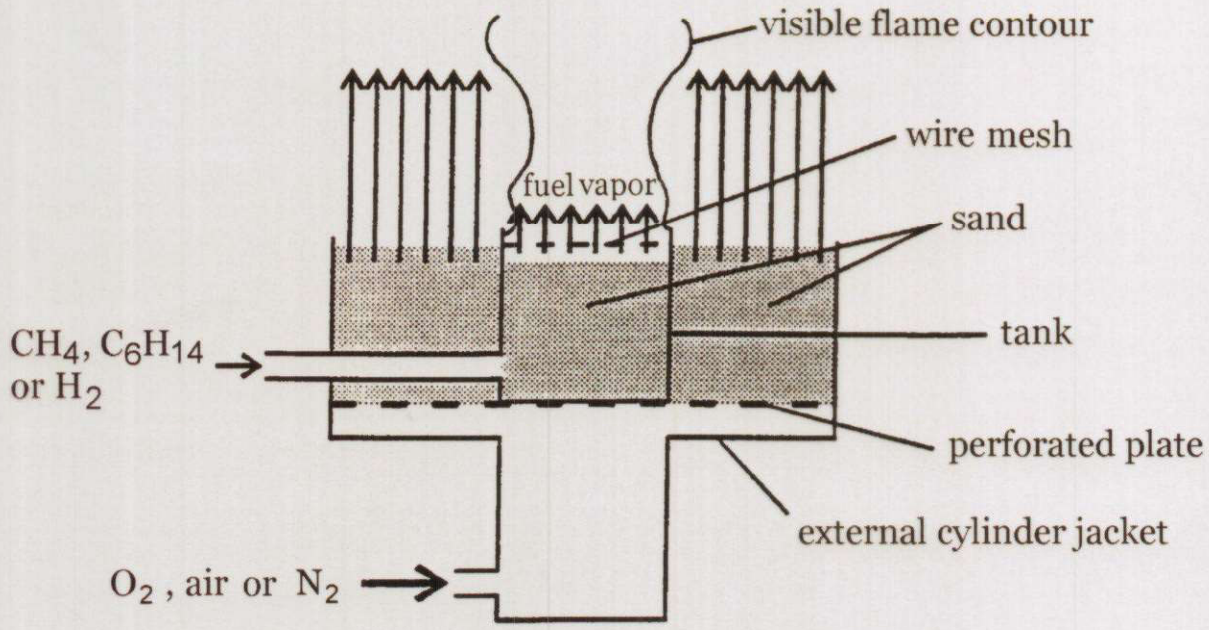

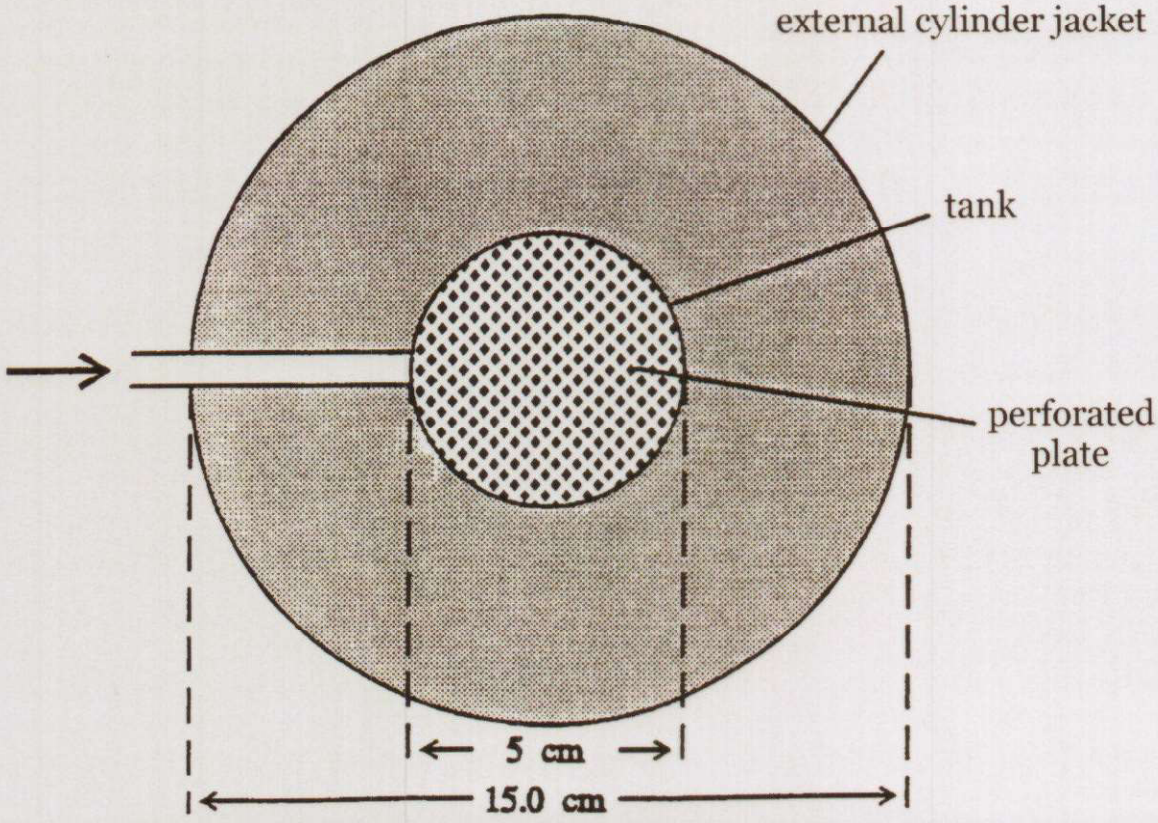

Tank construction for variation of the ambient atmosphere in the case of tank flames

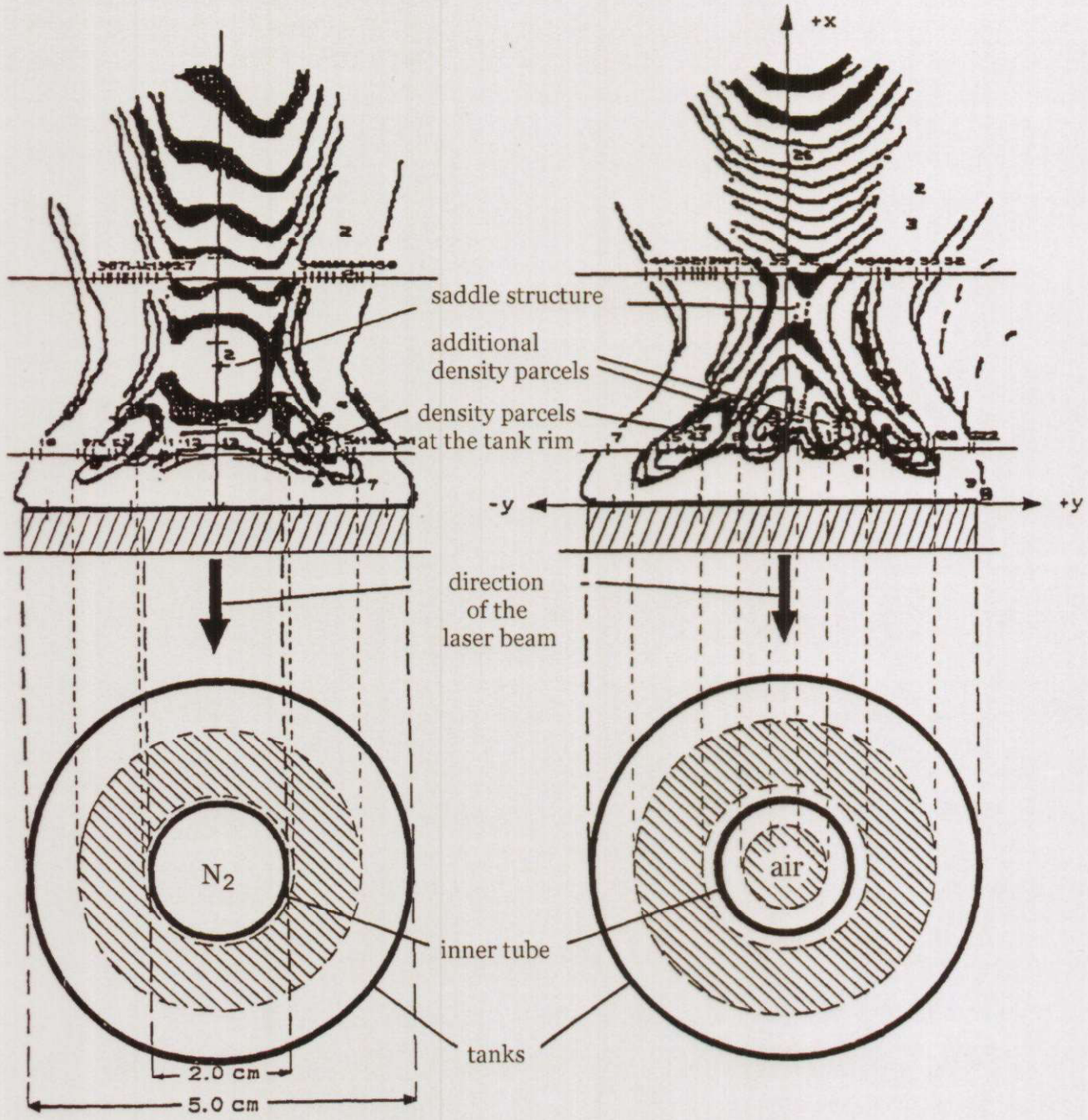

(a) (b)

Density sources at the tank rim of an n-hexane tank flame for axial feed of:

a) N_2 b) air

3.0 Visualisation and interpretation of the dissipative (coherent) structures in space and time

3.1 Interpretation der Interferenzstreifen bei Phasenobjekten

Linien konstanten Eikonals (Linien-Integral):

n_u : Brechzahl der Umgebungsluft

$$S(x,y,t)\ \lambda = \int_{-z_G}^{+z_G} (n_m(x,y,z,t) - n_u)\ dz$$

$n_m(x, y, z)$: Brechzahlfeld des Flammengasgemisches

Abel-Inversion:

$$n_m(r,x,t) - n_u = -\frac{\lambda}{\pi} \int_r^R \frac{\left(\frac{\partial S(y,x,t)}{\partial y}\right)_x}{\sqrt{y^2 - r^2}}\, dy$$

λ : Laserwellenlänge

Gladstone - Dale Gleichung:

$$\rho_m(r,x,t) = \tfrac{2}{3}\,[n_m(r,x,t) - 1]\,\frac{\sum_i \gamma_i(r,x)}{\sum_i \gamma_i(r,x)\ N_i^{\ominus}}$$

$\gamma_i \equiv y_i$: Massenbruch der Gaskomponente i

ideales Gasgesetz:

$N_i^{\ominus}$: spezifische *Standard*-Refraktion

$$T(r,x,t) = \frac{\sum_i \gamma_i(r,x)\ \rho_i^{\ominus}}{\sum_i \gamma_i(r,x)}\ T^{\ominus}\ \frac{1}{\rho_m(r,x,t)}$$

Flammenfahne: Konzentrationseinfluß ($\frac{\gamma}{d_i}$) vernachlässigbar

Interferenzstreifenmuster $\hat{=}$ Dichtestrukturen

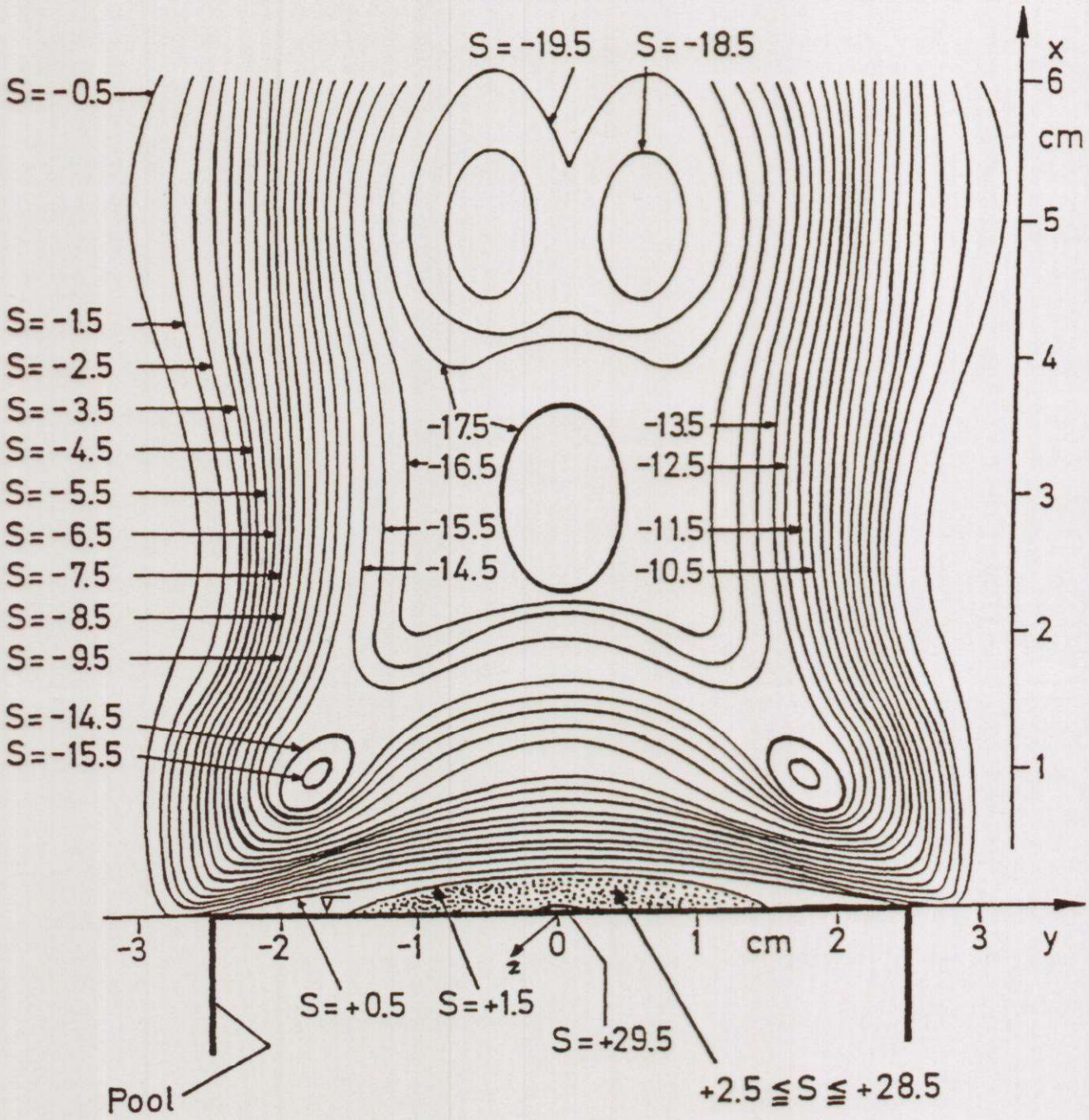

$$S(x,y,t)\,\lambda = \int_{-z_G}^{+z_G} (n_m(x,y,t) - n_u)\, dz$$

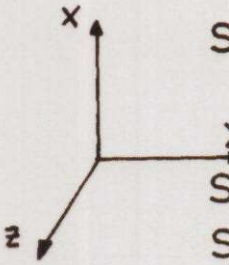

$S < 0 : n_m < n_u$ → flame has a larger optical density

$S > 0 : n_m > n_u$ → flame has a smaller optical density

$$n_m \equiv n_F \sim \frac{1}{c_F} \sim \rho_F \sim \frac{1}{T}$$

Calculated interference fringes pattern of an n-hexane tank flame with d = 4.6 cm

⇨ für $t = t_1 = \text{const}$ (*Momentbilder*) gilt:

Linien mit der Interferenzstreifenordnung $\mathbf{S (y, x, t_1) = const}$ entsprechen näherungsweise Linien mit $\rho_m = \text{const}$ (*Isodichtenfeld*) bzw. Linien mit $\mathbf{T = const}$ (*Isothermenfeld*)

■ Inhomogenitäten

$$\left(\frac{1}{b}\right)_t = \left(\frac{\partial S}{\partial y}\right)_t \sim \left(\frac{\partial \rho}{\partial y}\right)_t \sim \overline{\left(-\frac{\partial T}{\partial y}\right)_t}$$

b [mm]: Linien (Streifen) *abstand*

1/ b $\left[\frac{1}{mm}\right]$: Linien (Streifen) *dichte*

■ Zeitabhängiges Verhalten

$$\left(\frac{\partial S}{\partial t}\right)_{y,x} \sim \left(\frac{\partial \rho}{\partial t}\right)_{y,x} \sim \overline{\left(-\frac{\partial T}{\partial t}\right)_{y,x}}$$

⇨

$\rho' (t), T' (t)$: Dichte-, Temperatur-fluktuationen

$\rho (y, x, t), T (y, x, t)$: periodische, quasiperiodische und chaotische Dichte - bzw. Temperaturänderungen

---

■ *raum-zeitliche* **Strukturen (→ Quellen S und Senken S)**

spontane Entstehung, charakteristische Längen, Translationsgeschwindigkeiten, Aufstiegsfrequenzen und Kommunikation lokaler Strukturen mit S = const als äußere Kontur

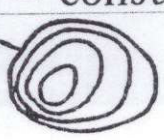

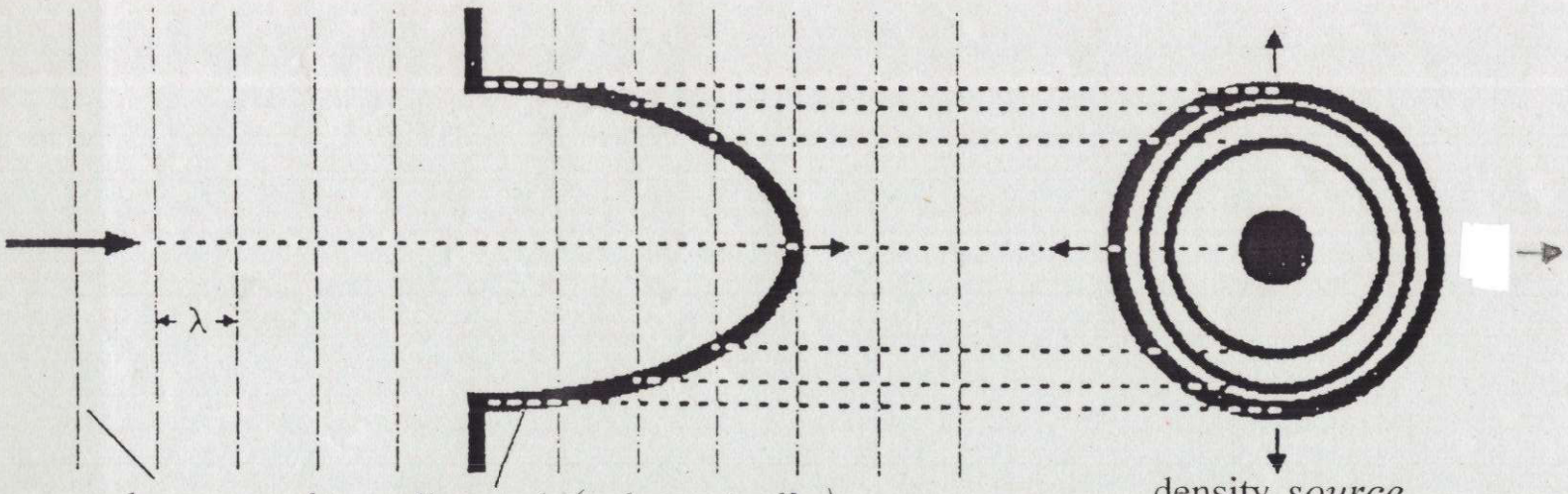

$$n_F \sim \frac{1}{c_F} \sim \rho_F \sim \frac{1}{T}$$

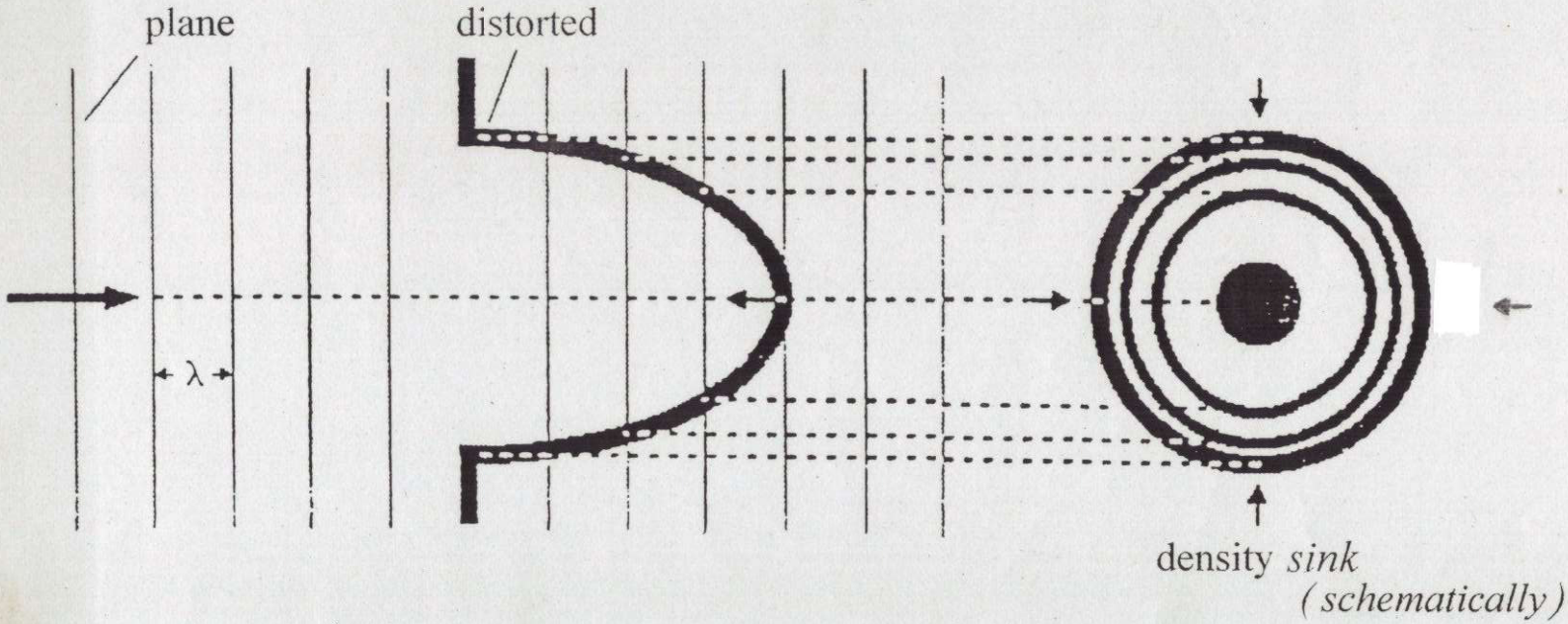

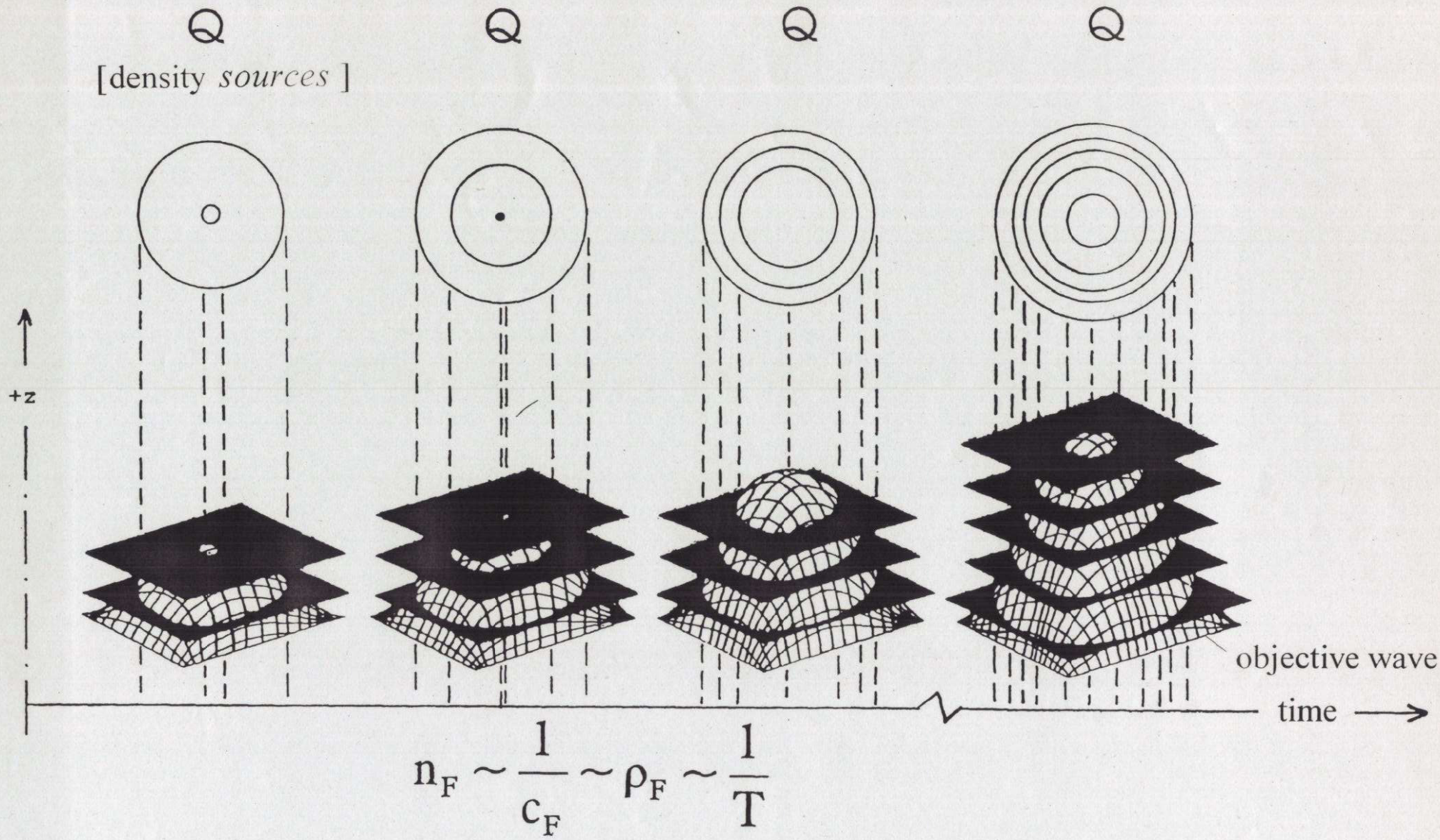

Formation of a density soure (Q) due to a continuously distortion of the objective wave as a function of time

c_F : light velocity in the flame [index F]

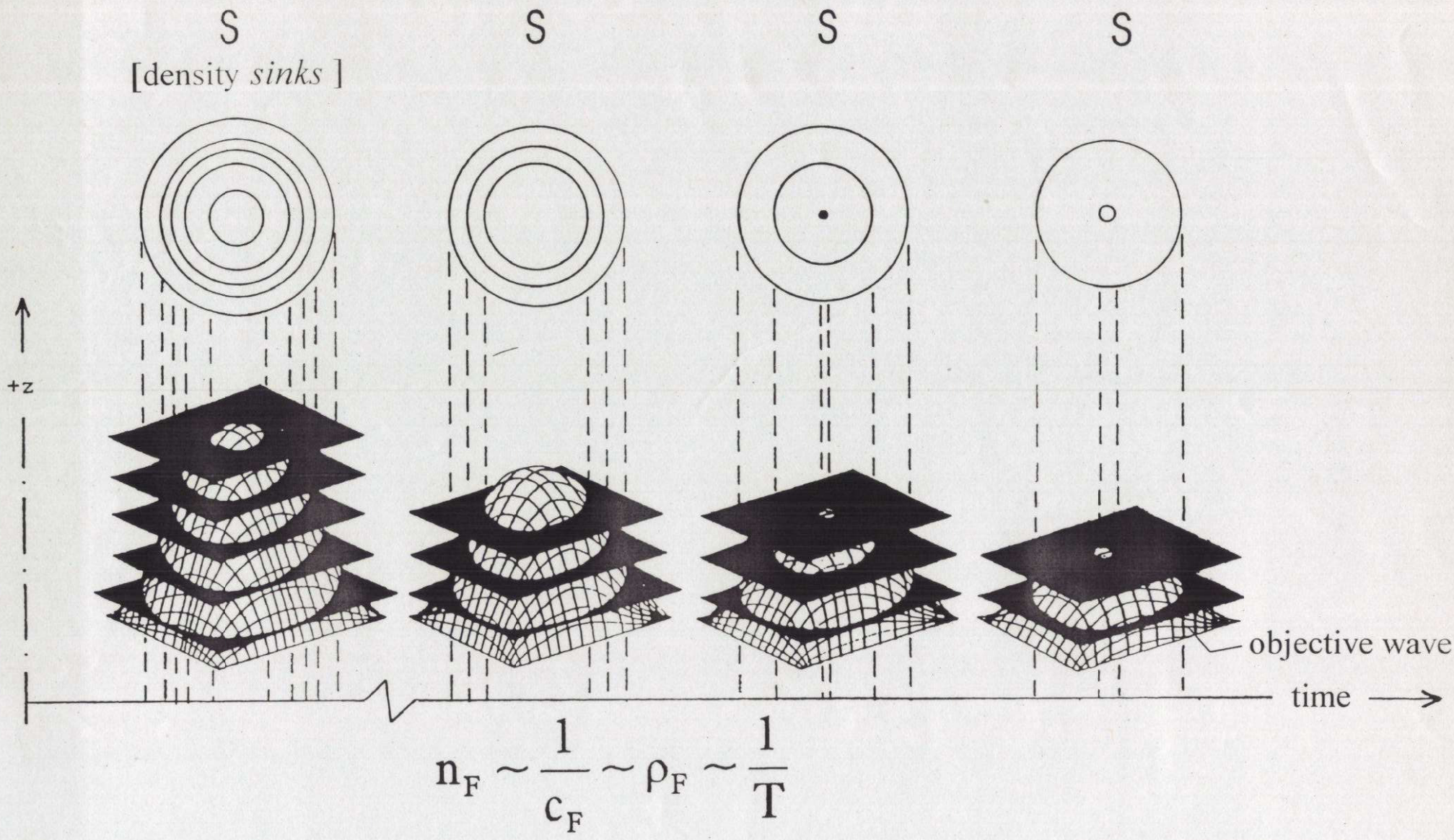

Formation of a density sink (S) due to a decreasing distortion of the objective wave as a function of time

c_F : light velocity in the flame [index F]

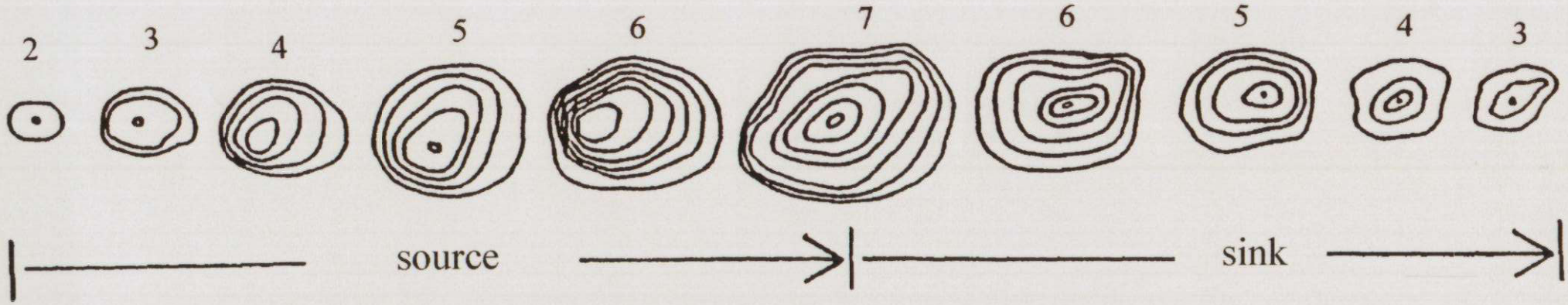

spatial temporal *decrease* in density
resp. a temporal *increase* in temperature

$$\frac{d\rho}{dt} < 0 \quad \text{resp.} \quad \frac{dT}{dt} > 0$$

spatial temporal *decrease* in density
resp. a temporal *increase* in temperature

$$\frac{d\rho}{dt} > 0 \quad \text{resp.} \quad \frac{dT}{dt} < 0$$

⇨ real sources (Q) and sinks : *asymmetric* phenomena (symmetry breaking)

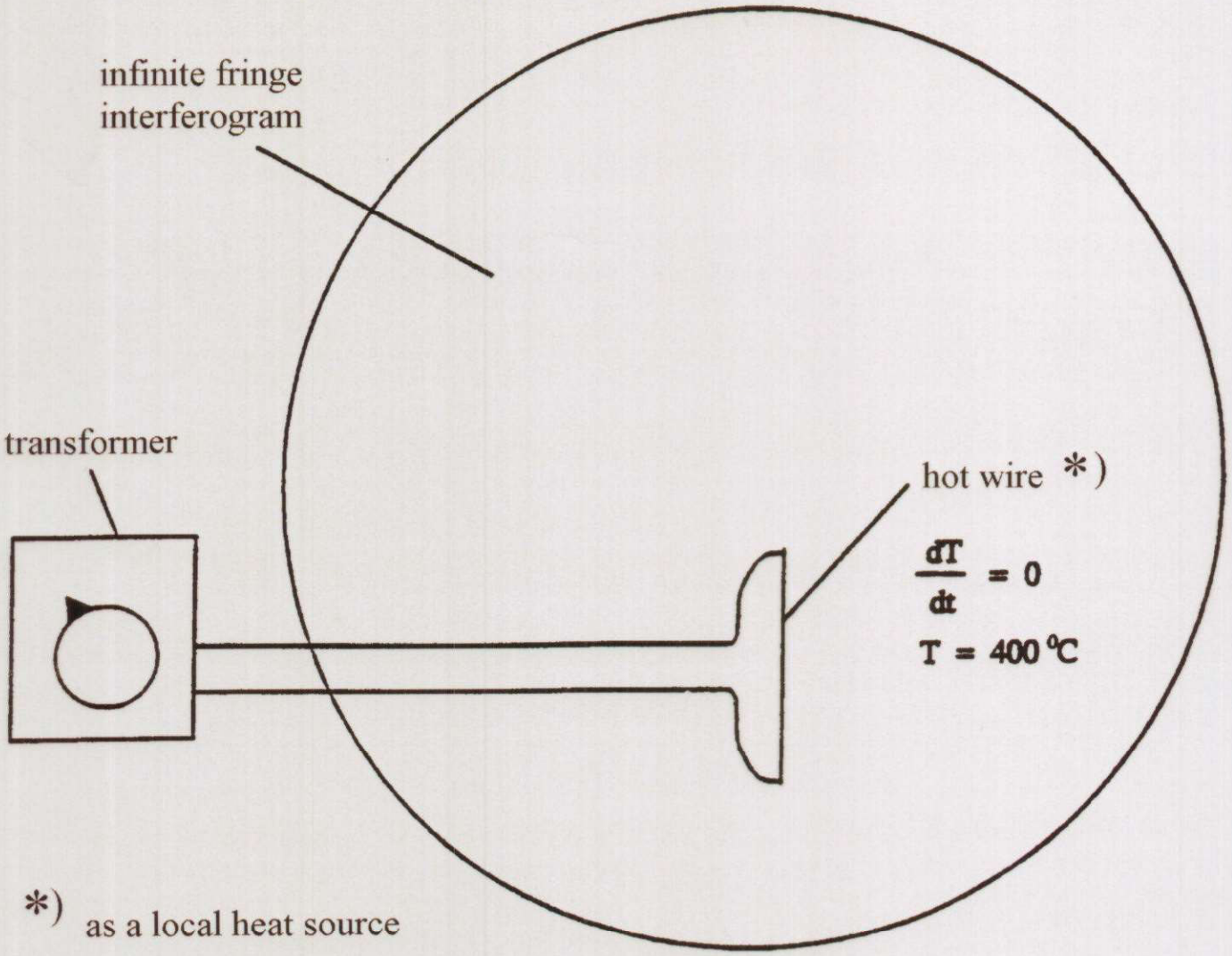

Simulation of density *sources* (Q) using a vertical hot wire at a constant temperature. The hot wire can be considered as a local increase in temperature of an air volume element near the heated wire

after the *detachment* of the density *sources* (Q) from the hot wire:

buoyant rise of density *sinks* (S)

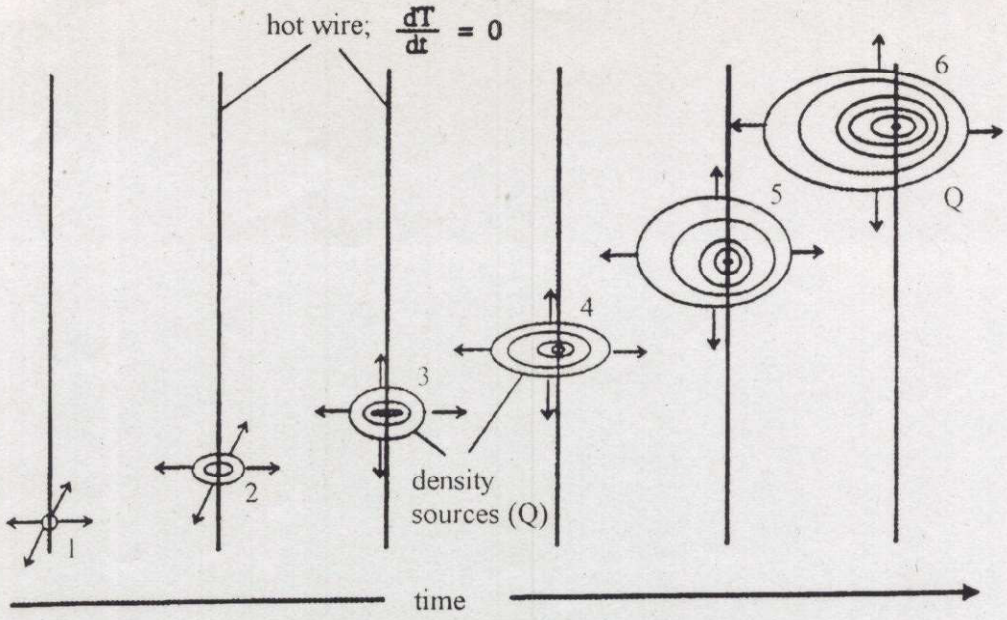

this is a schematical presentation of the observations as a function of time t. At first we observe only density sources.

Formation of density *sources* Q at a vertical hot wire with an *elevated* temperature T = const. (schematically)

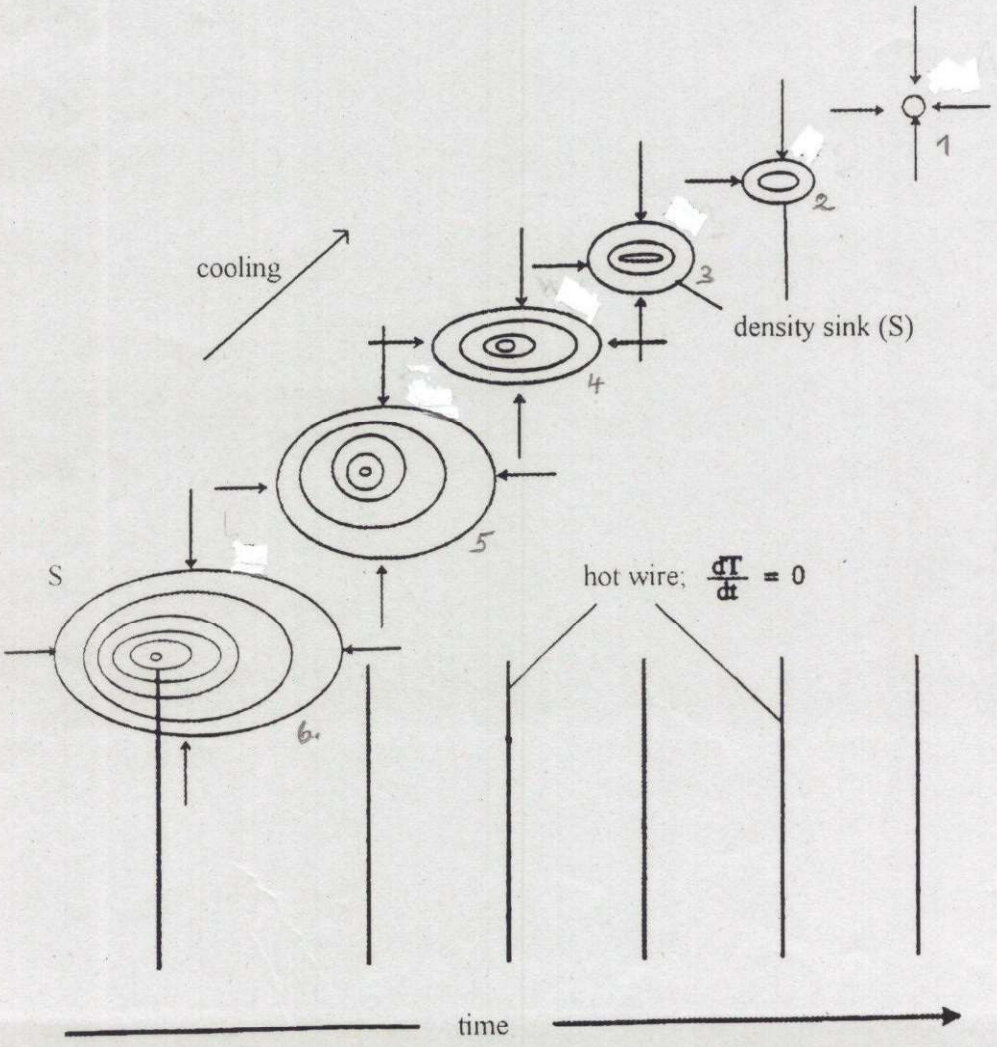

after a certain time t we observe a detachment of the density source from the hot wire, and due to cooling effekts we observe density sinks phenomena.

Formation of density *sinks* (S) *above* the hot wire (schematically)

3.2 Types of dissipative structures

- Types of dissipative structures in *non-reacting* flows
  - Waves and oscillations of the (thermal) boundary layer
  - Axial ring-shaped density parcels

- *Continuous flame zone*
  - Wave of the (thermal) boundary layer
  - Oscillation of the boundary layer between fuel surface (≈ tank rim) and the flame
  - Density *sources* (Q) at the tank rim
  - Density *sources* (Q) near the flame axis
  - VIS-radiance structures

- *Transition flame zone*
  - Wave of the (thermal) boundary
  - Sources (Q) and sinks (S)
  - Multiple combinations of Q and S
  - Ribbon-shaped structures
  - Isolated structures
  - VIS-radiance structures

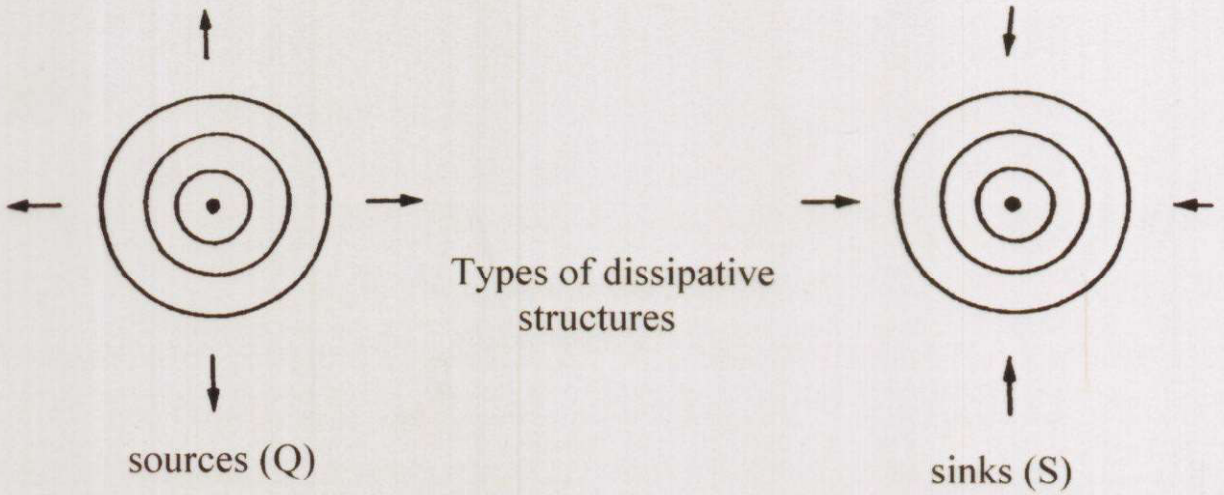
Types of dissipative structures
sources (Q)
sinks (S)

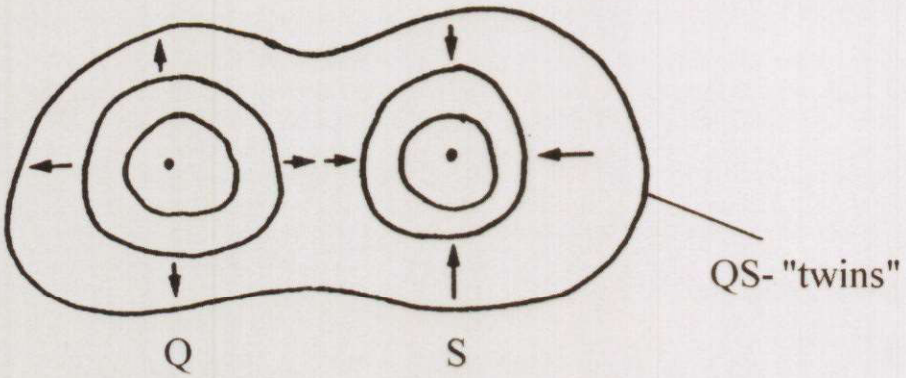
QS- "twins"
Q
S

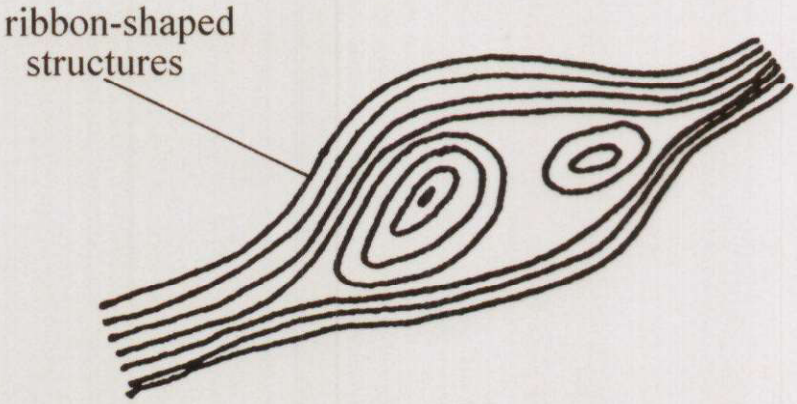
ribbon-shaped structures

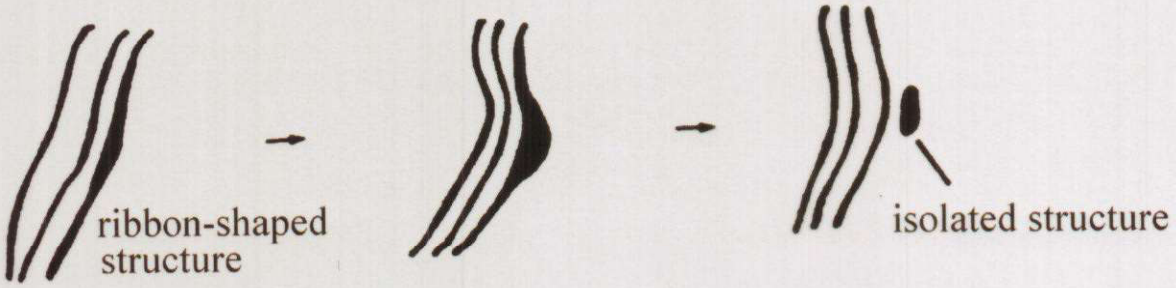
ribbon-shaped structure
isolated structure

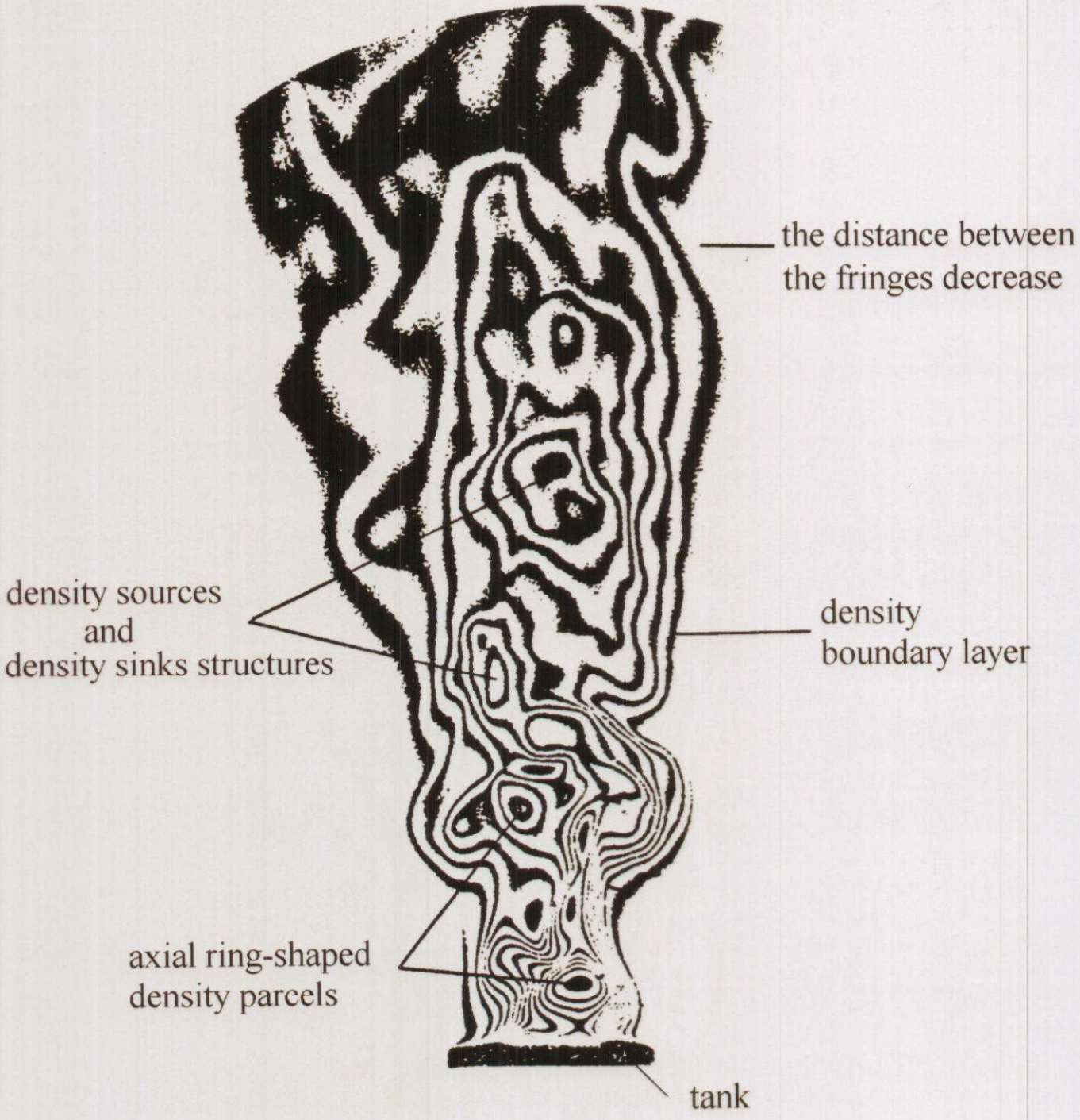

Dissipative density structures in an He-flow above a tank

($d = 4.6$, $\dot{V} = 2.25 * 10^{-4}$ m^3/s)

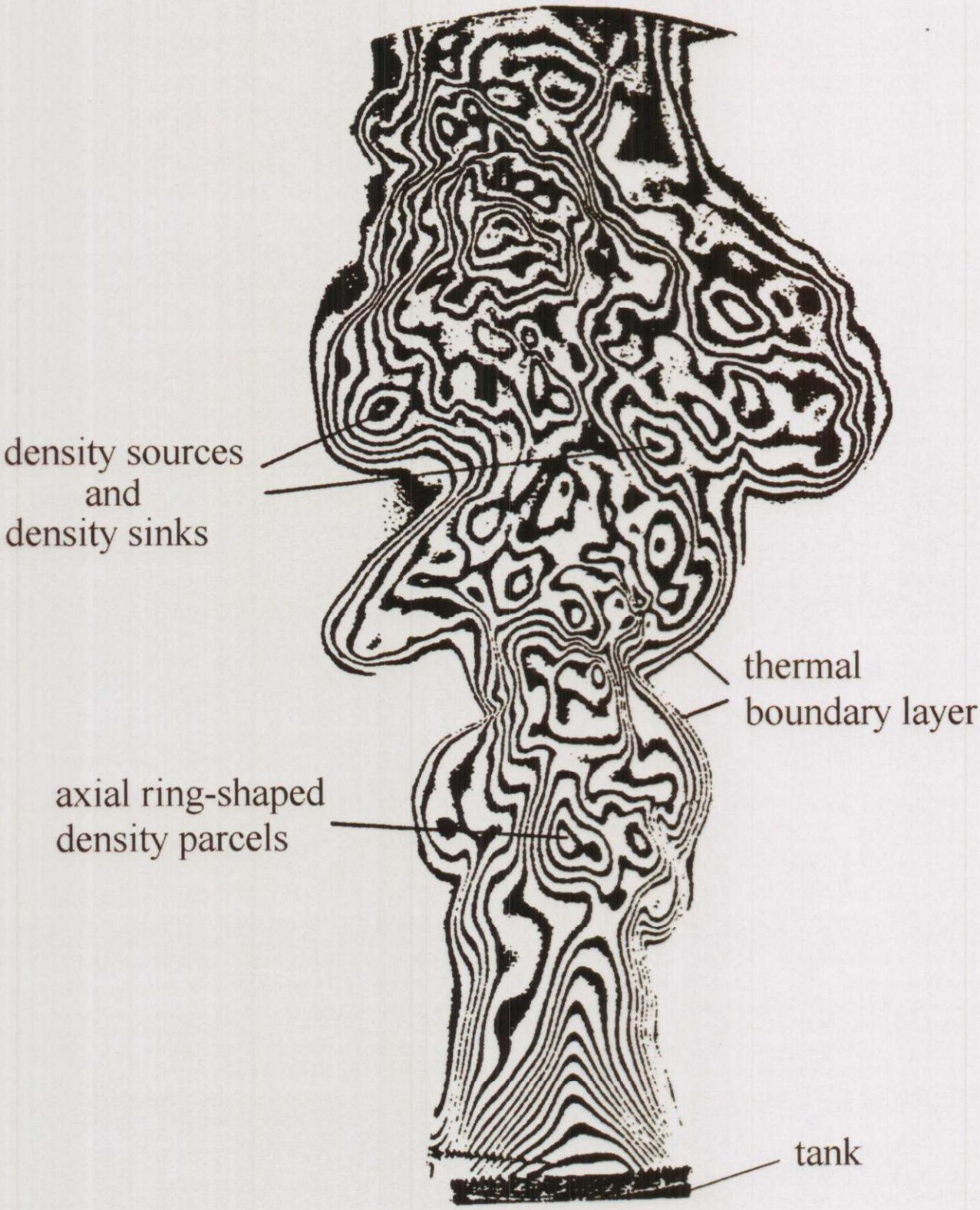

Dissipative density structures in a *hot air flow* above the tank

($d = 4.6$, $\dot{V} = 1.8 * 10^{-4}$ m³/s, $T = 950°K$)

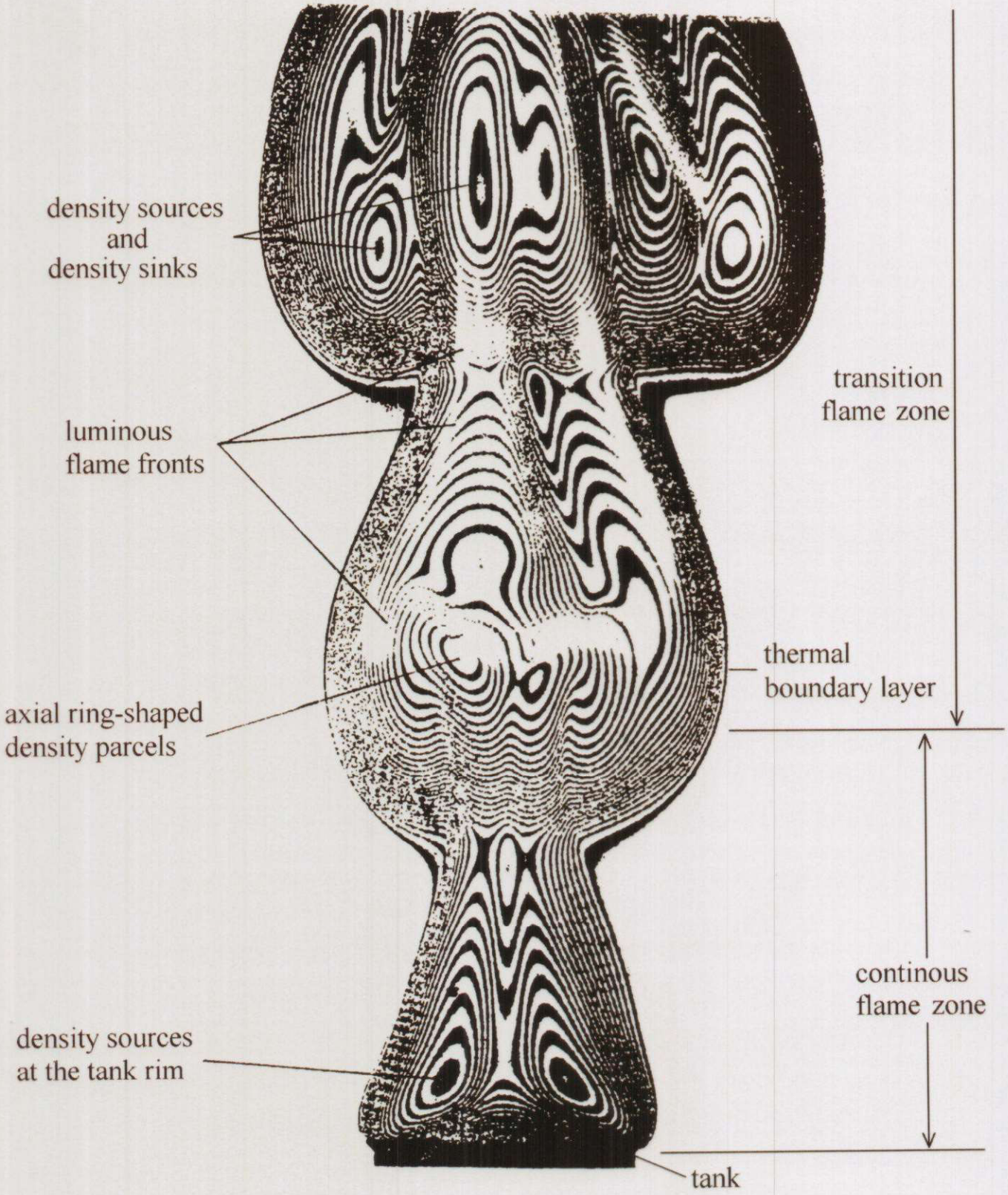

Dissipative density structures and VIS - radiance structures

in a nonpremixed CH_4 - tank flame

($d = 4.6$, $\dot{V} = 2.5 * 10^{-4}$ m^3/s)

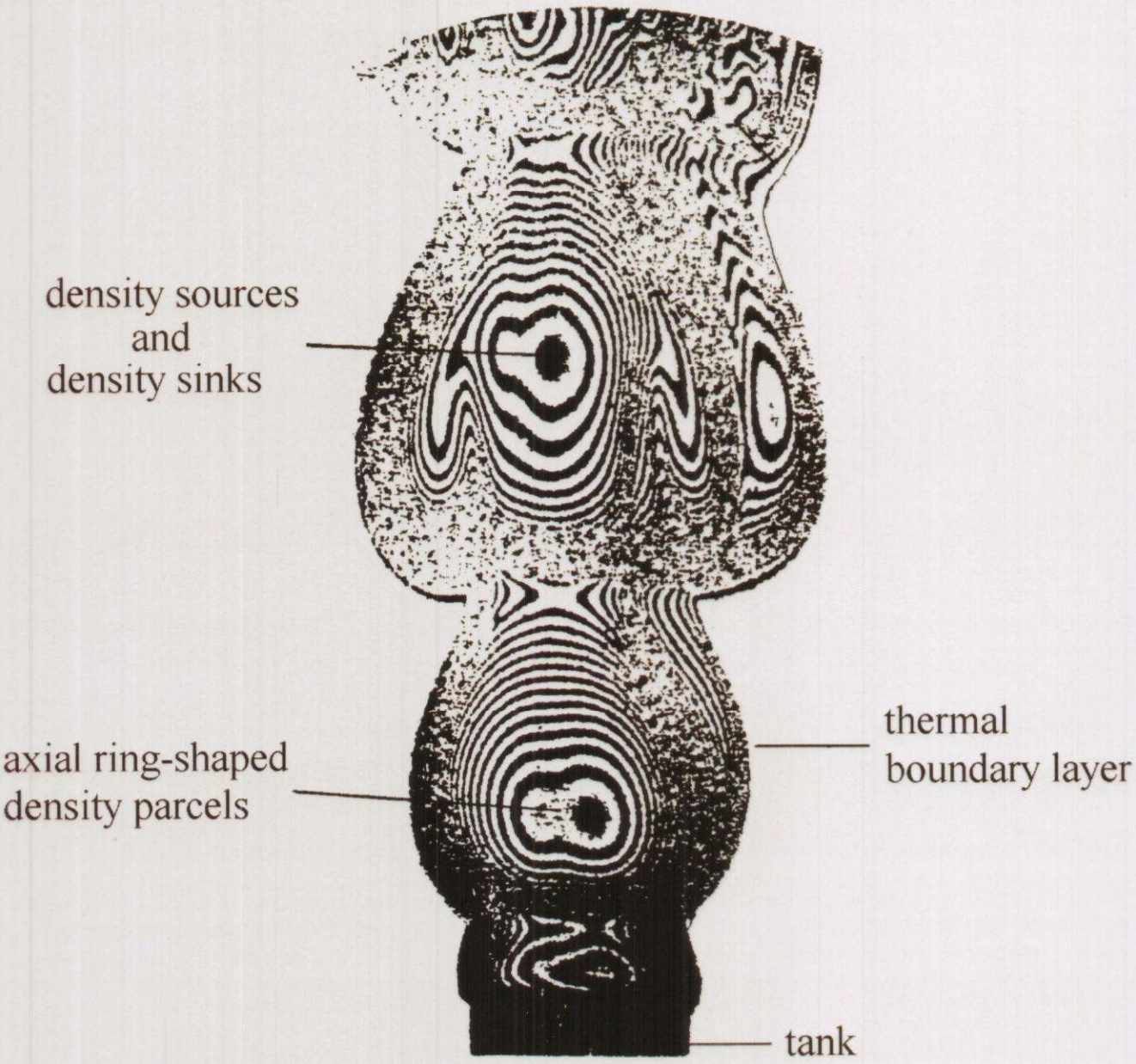

Dissipative density structures in a nonpremixed H_2- tank flame

$(d = 4.6,\ \dot{V} = 3.5 * 10^{-4}\ m^3/s)$

3.3 DVD-Video:

"Tank Flames, Dynamics of Dissipative Structures"

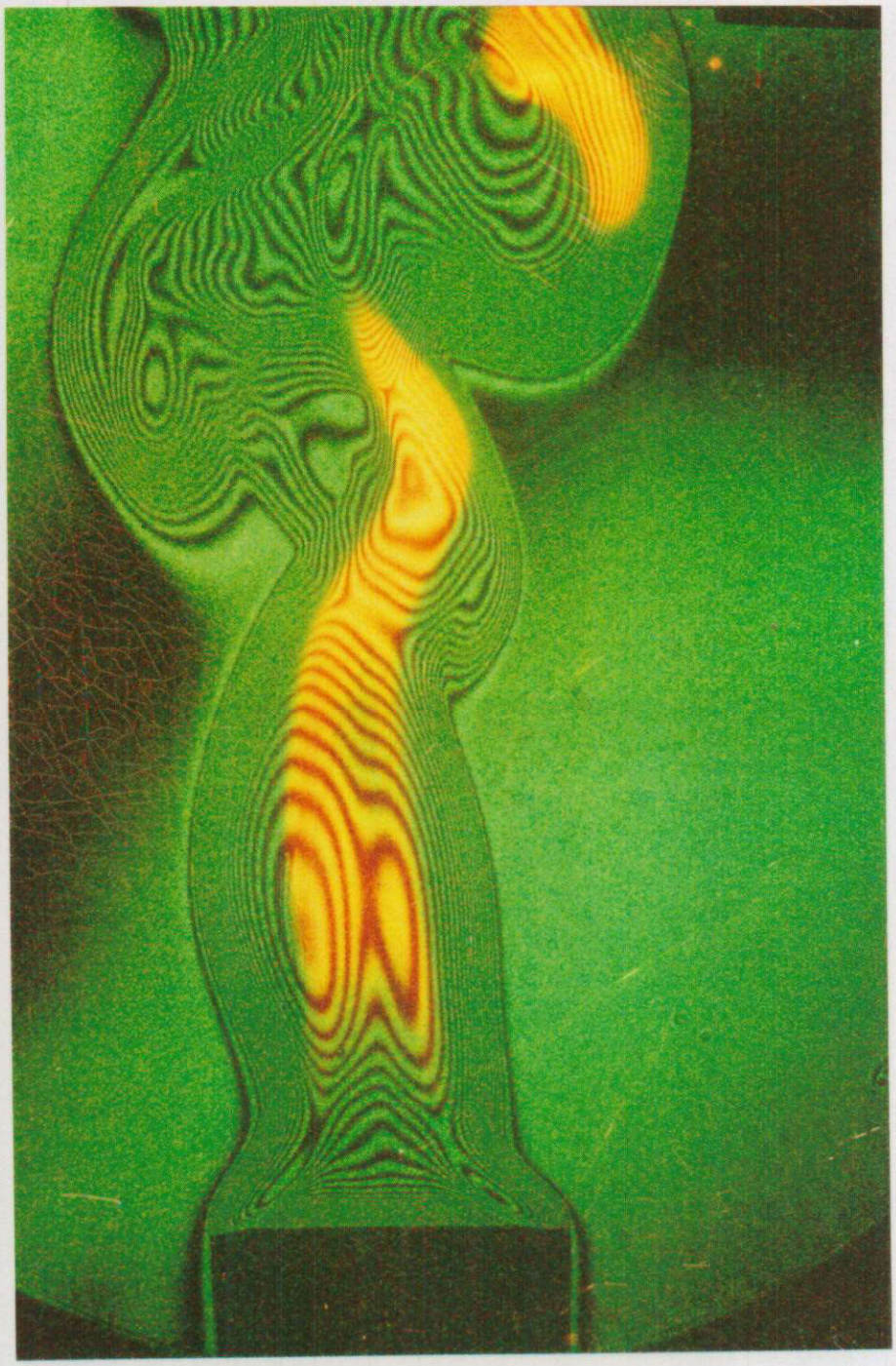

n-hexane tank flame (d = 4.6 cm) : 0 < x < 25 cm

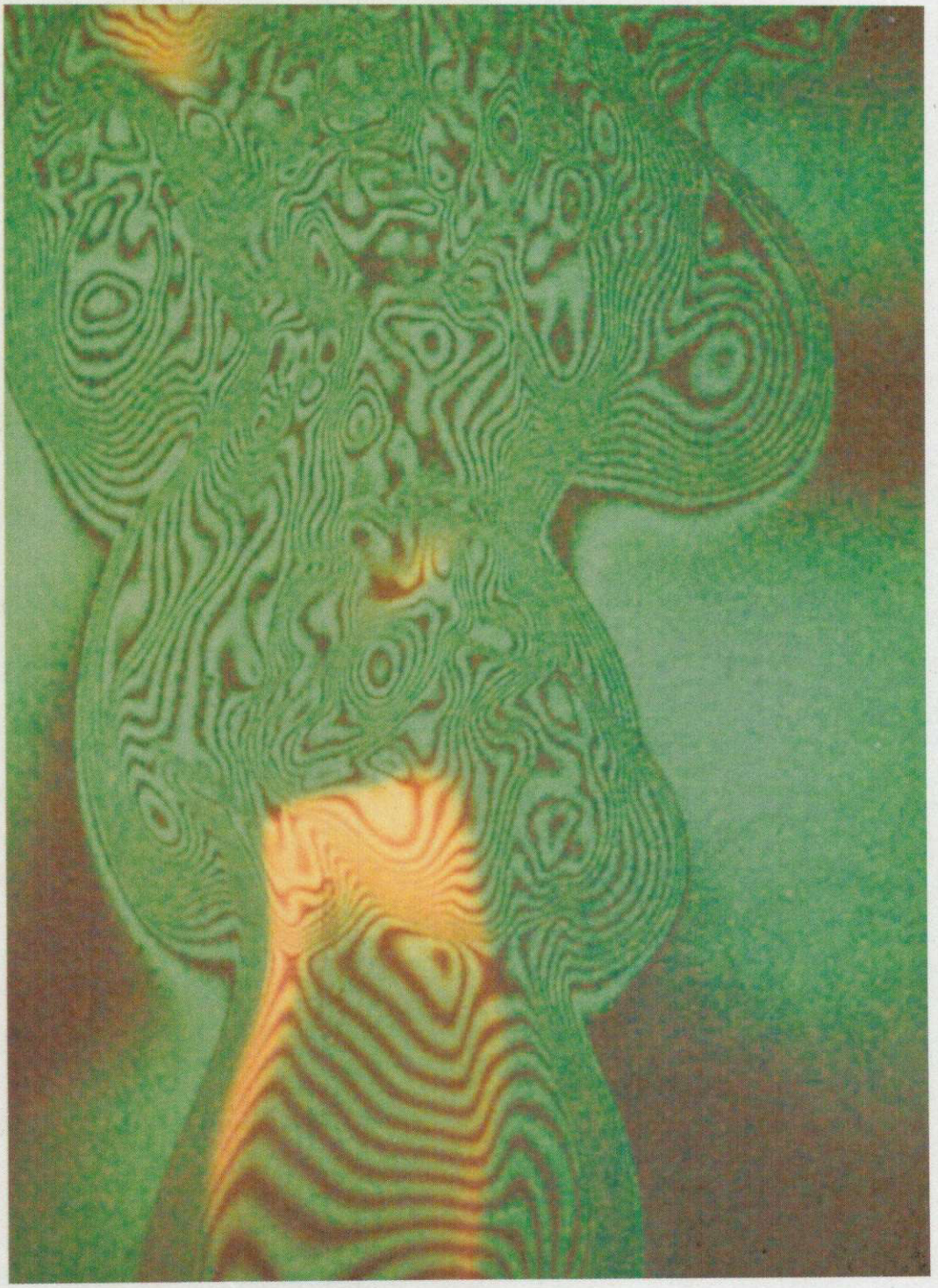

n-hexane tank flame (d = 4.6 cm) : 25 < x < 50 cm

Axel Schönbucher

Institute of Chemical Engineering

UNIVERSITÄT DUISBURG ESSEN

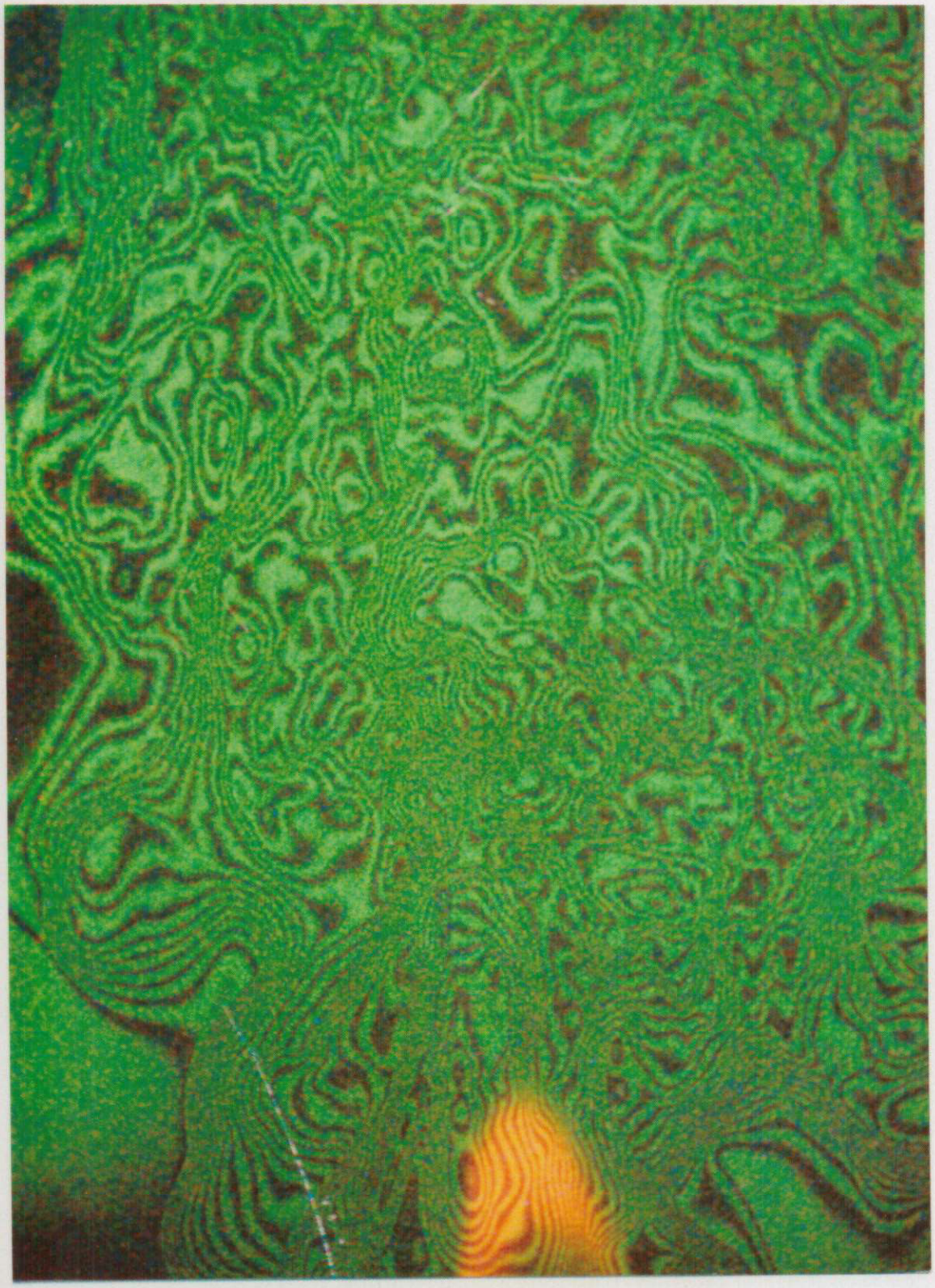

n-hexane tank flame (d = 4.6 cm) : 50 < x < 75 cm

4.0 Concepts for modeling dissipative (coherent) structures

4.1 Present flame models: *modeling of local structures (dissipative structures) is not possible*

- *Fast-chemistry* ($r_R \rightarrow \infty$) [H. *Rummel,* 1930] for nonpremixed flames; [*Shvab*, 1948; *Zeldovich*, 1949]

- *DNS* [*Reynolds*, 1989] for turbulent reacting flows

- *PDFs* [*Williams*, 1980; Libby, 1994] for turbulence modeling + PDF-transport equations [e.g. *Dopazo, O'Brien* 1974; *Pope*, 1986; *Chen*, 1989]

- *Turbulence models*
  * Zero-Equation Models [*Prandtl*, 1925]
  * One-Equation Models, e.g. for turbulent kinetic energy (TKE)

* Two-Equation Models, e.g. k-ε-turbulence model [*Launder, Spalding*, 1972; *Jones, Whitelaw*, 1985]

- Eddy-Break-Up Models [e.g. *Peters*, 2000]
- Large-Eddy-Simulations (LES) [*Reynolds*, 1989 ; *Pope*, 2000] and Linear Eddy Model LES-LE [Kerste*in*, 1992]
- *Equilibrium chemistry* for nonpremixed flames
- *Finite-Rate Chemistry* for nonpremixed flames and *Flamelet* Models [*Bilger*, 1980; *Peters*, 1987]
- *PDF*-Simulations of turbulent nonpremixed flames

Additional (special) problems in the case of tank/pool flames :

- Modeling of the buoyant term (*slow flows*)
- Modeling of the heat radiation
- Modeling of the phenomena within the liquid phase and at the liquid/gaseous interface for liquid fuels
- Modeling of air entrainment
- Turbulent exchange coefficients in the conservation equations are different
- Scale-up of tank/pool flames
- Influence of chemical reaction kinetics on dissipative structures
- Formation of pollutants: unburned hydrocarbons, PAHs and soot particles

4.2 Some aspects of nonlinear science: *modeling of local structures should be possible*

Flames should be considered as *dissipative* systems [contrary to *conservative* systems] with typical *irreversible* behaviour:

- Nonequilibrium states
  - Thermodynamic *open* systems with continuous exchange of momentum-, mass- and energy flows with the ambient atmosphere and with the fuel vapour above the liquid fuel surface
  - *Far away* from the chemical equilibrium state
    In general *no detailed* chemical equilibrium state exists in a nonpremixed flame ;
    For stationary burning flames there exist *stationary none*quilibrium states.

- Nonlinearities and feedback
  - Nonlinear reaction kinetics, e.g. due to
    - Chemical reactions with $n > 1$ (or $n \neq 1$)
    - Catalytic reactions, chain branching reactions:
      → chemical instabilities
    - *Arrhenius* temperature dependence of the reaction rate r_R, e.g. in the case of strong exothermic reactions (*thermal* feedback)
  - Consideration of (molecular) transport terms, e.g. the diffusion term in the species mass conservation equation
    - *Fast* but *diffusion-controlled* reactions
      ($r_R >> r_D$) : → *reaction-diffusion* equations
      r_R : reaction rate r_D : diffusion rate

- Periodic and quasi-periodic oscillations

  - thermal boundary layer
  - source and sinks structures

- Bifurcation and symmetry breaking

  Coexistence of two simultaneously stable states:
  Source and *sinks* structures

- Asymptotic stability

  As soon as the influence of a *disturbance* (e.g. due to injection of air) has stopped, the system (e.g. a flame) will reach exactly the same state as before the disturbance has occurred.

- Selection of preferred *asymmetric* structures (*chiral* structures)
  → e.g. definitely *more sinks* than source structures

- Order and long-range correlations

  Formation of new order states (in general of higher order), e.g. due to energy input:

  Molecular ensembles of 10^{10} to 10^{20} molecules, which are *long-range* correlated:

  - *Spatial* structures
  - *Temporal* rhythms
    - *Periodic* oscillations: periodic attractor of the dimension D = 1
    - *Quasi-periodic* oscillations: quasi-periodic attractor of the dimension D = 2
    - Chaotic oscillation behaviour: non-periodic attractor of the dimension D > 2 or non-integer fractal objects.

      Such systems show a very *sensitive dependence on the initial conditions* (e.g. external air flows, geometry of the tank rim)

- *Spatial-temporal* structures (e.g. source-, sink structures)

- *Macroscopic* length-scales: ≈ cm

- *Macroscopic* time-scales: ≈ ms

5.0 Properties of dissipative (coherent) structures

5.1 Turbulent length-, time- and velocity scales

1. from frequency spectra of p'_{dyn}

2. from frequency spectra of $L'_{\Delta\lambda}$

3. from bimodal frequency distributions $H(l_{DB})$

Turbulent length-, time- and velocity scales (I)

Determination from interference fringes pattern

$[H(l_{DB})]; H(b_{DB})$; f(fuel)

(a) L_E : 2.maximum of $H(b_{DB})$: $\Delta\hat{y}_{DB}$
also from density sources at the tank rim

(b) l_E : 1.maximum of $H(b_{DB})$: Δy_{DB}

(c) l_K : $\lim_{x \to \overline{H}_F} \Delta y_{DB}(x) = \Delta y_{DB,min} \equiv l_K$: $\Delta y_{DB,min}$

(d) v' : from $v_{DB}(t)$: $\langle v'_{DB} \rangle$

(e) S_F : $\bar{u}_{rel}$ of axial density parcels : $\bar{u}_{DB} - u_{f,o}$

(f) $\gamma_F(r,x)$: from $\langle v'_{DB} \rangle$, Δy_{DB} : $K_I(r,x)$

Bimodal frequency distributions $H(\ell_{DB})$, $H(b_{DB})$ of the length scales of Q and S

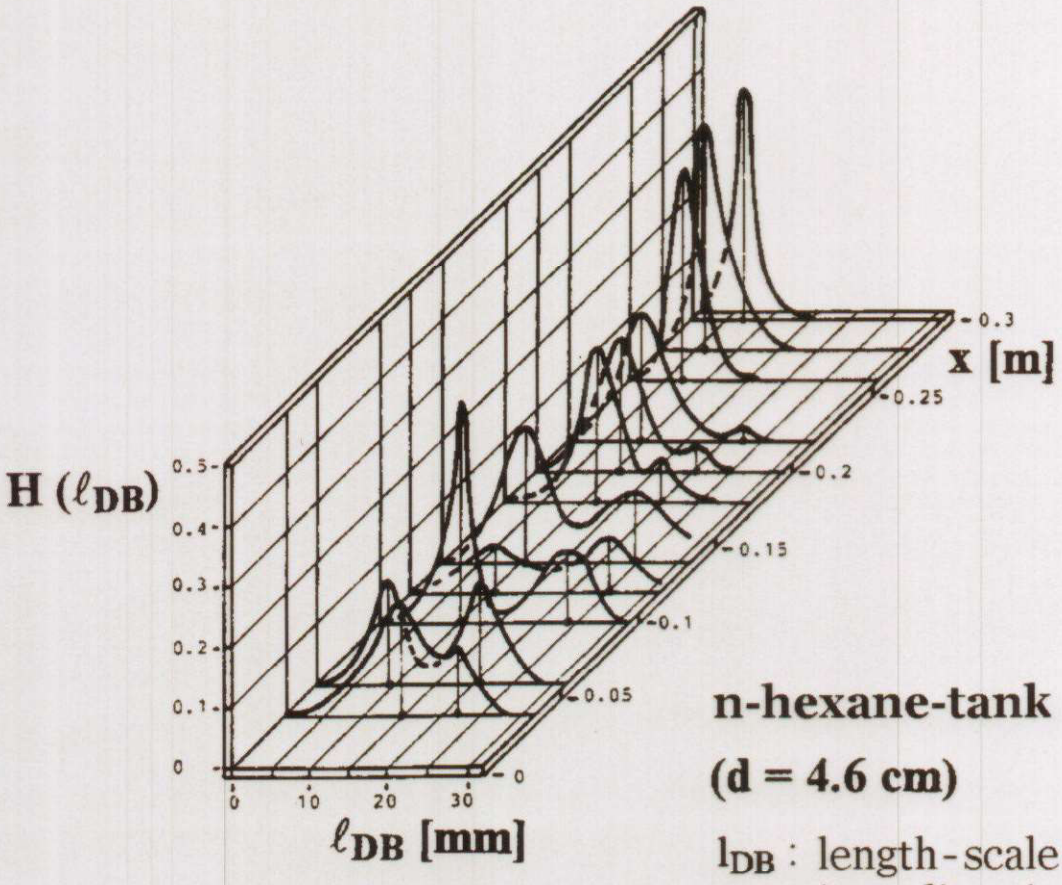

n-hexane-tank flame

(d = 4.6 cm)

l_{DB} : length-scale of Q and S in x-direction

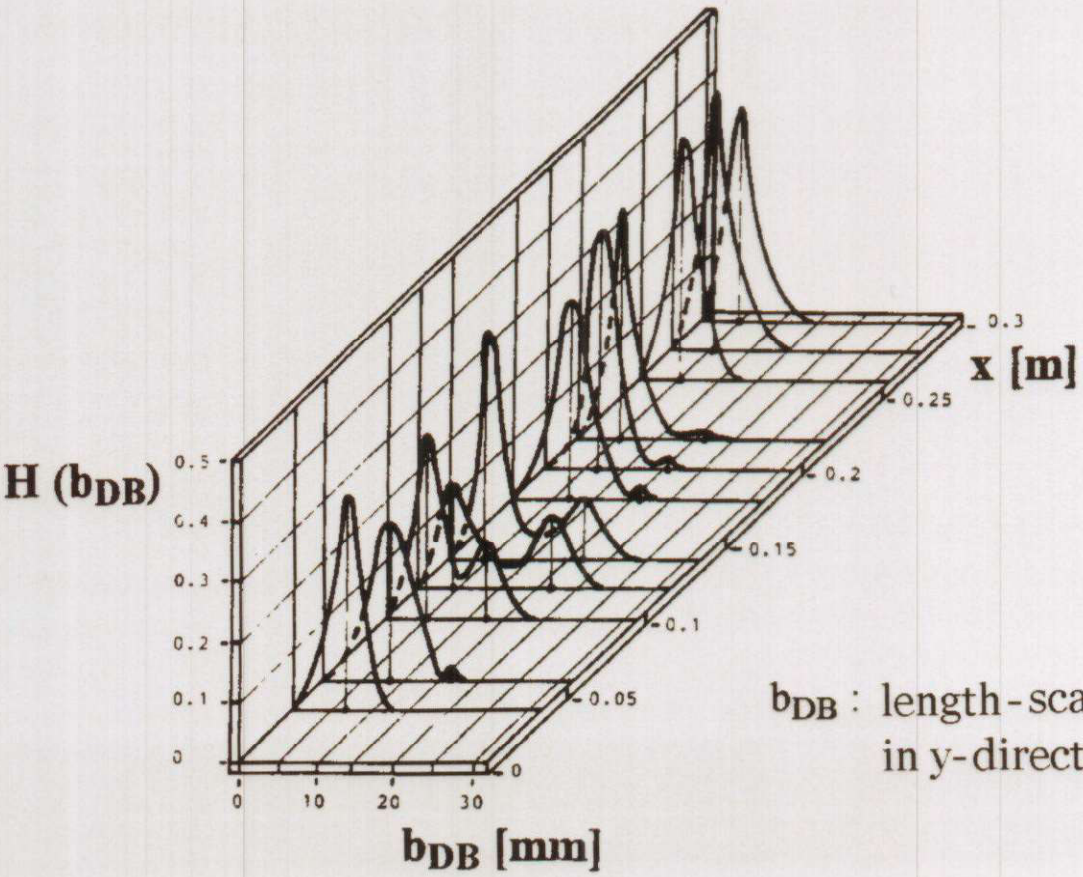

b_{DB} : length-scale of Q and S in y-direction

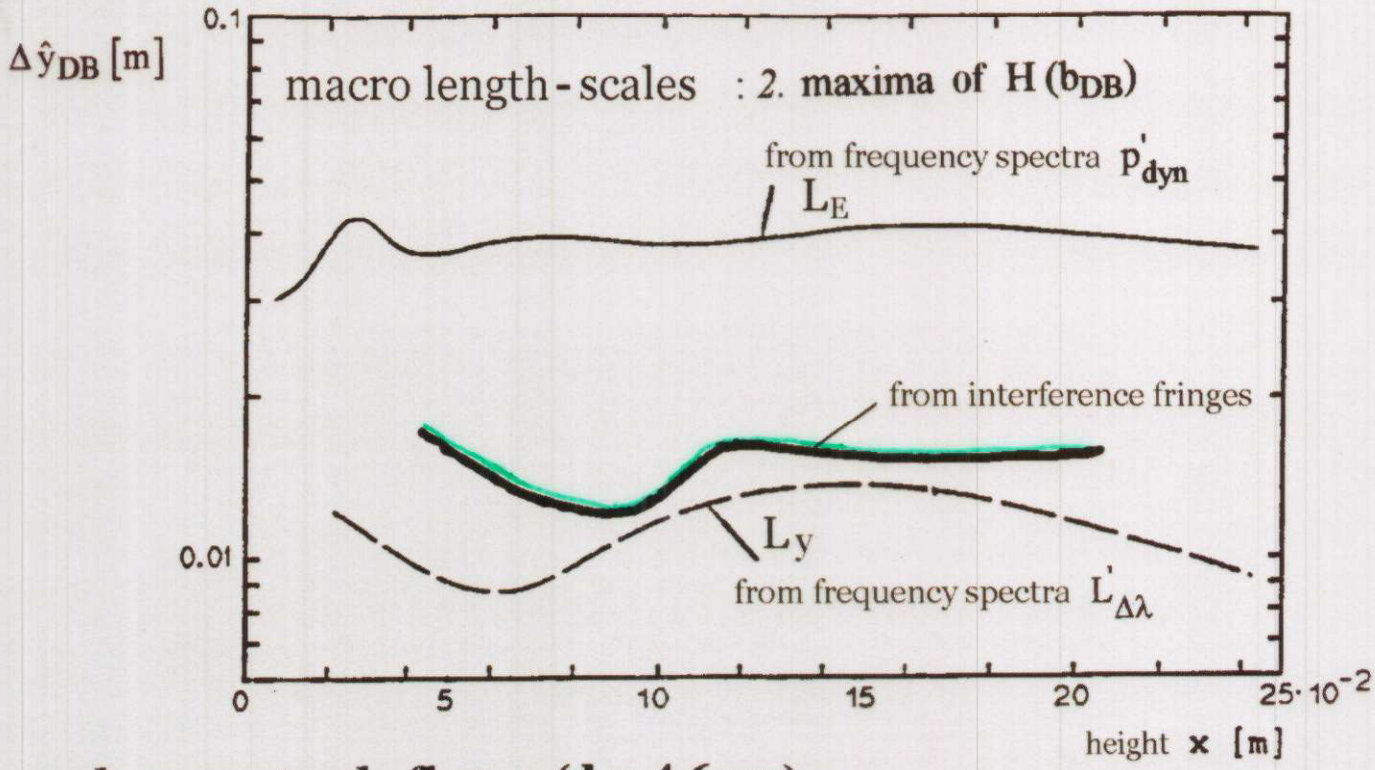

n-hexane-tank flame (d = 4.6 cm)

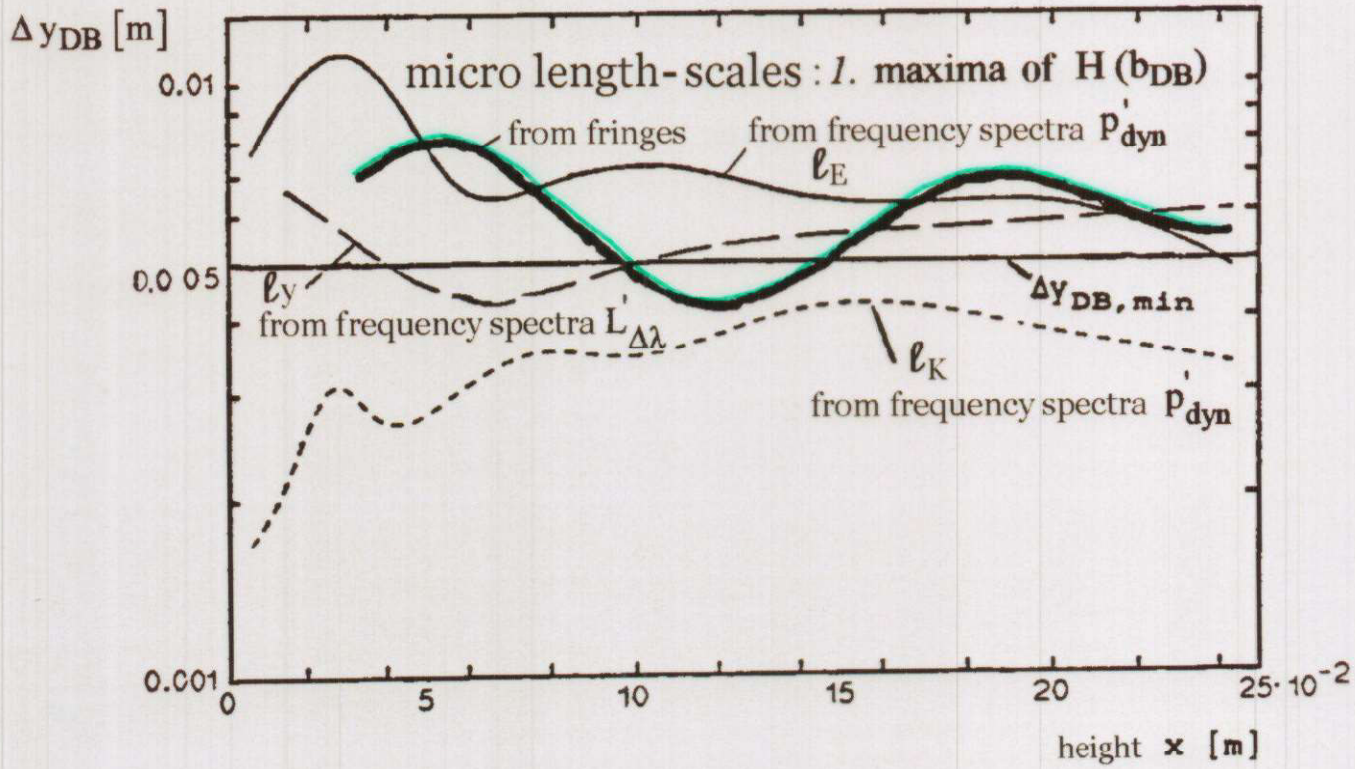

p'_{dyn} (t) : oscillations of the dynam ic pressure in the flame

$L'_{\Delta\lambda}$ (t) : oscillations of the radiance of the flame

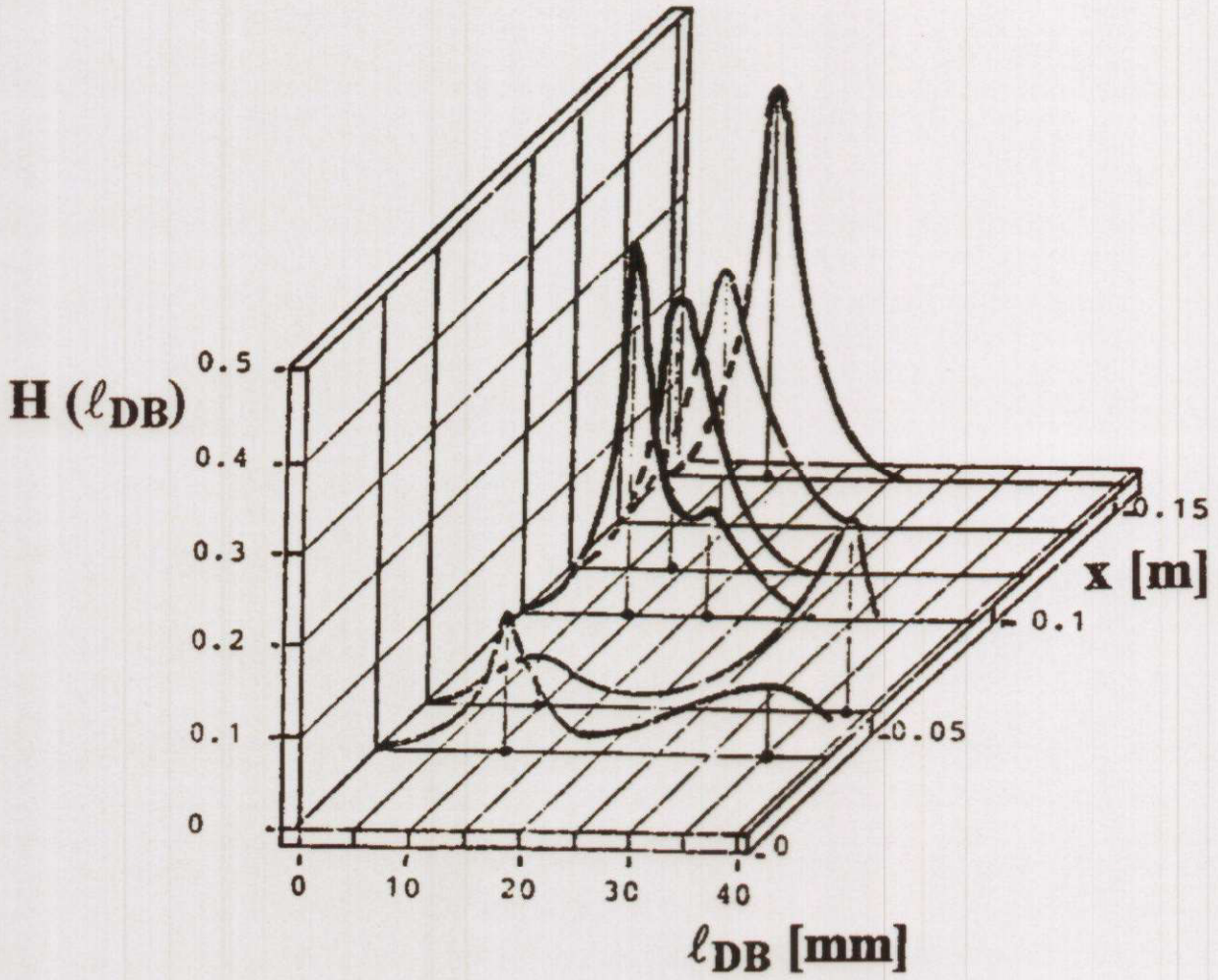

methanol- tank flame

(d = 4.6 cm)

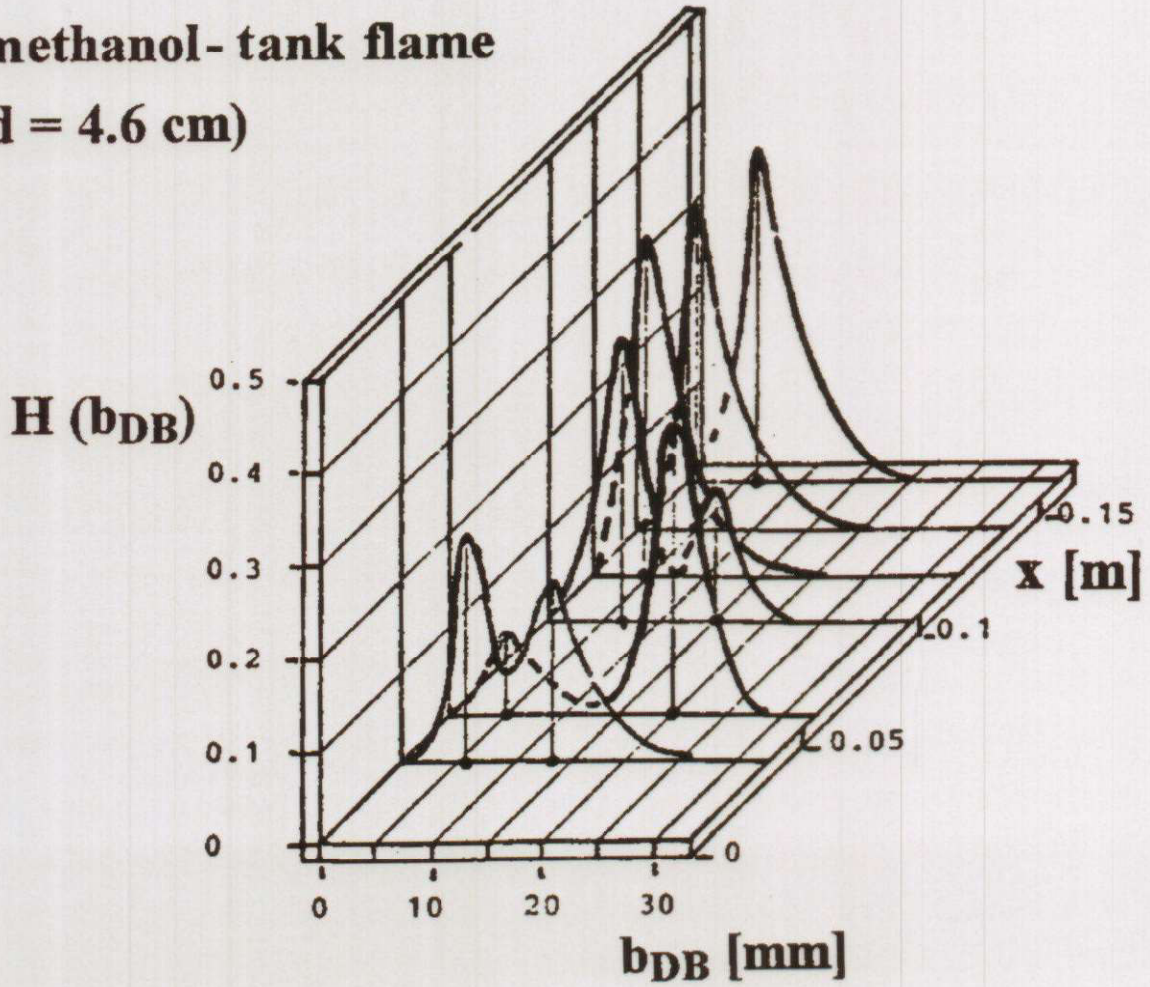

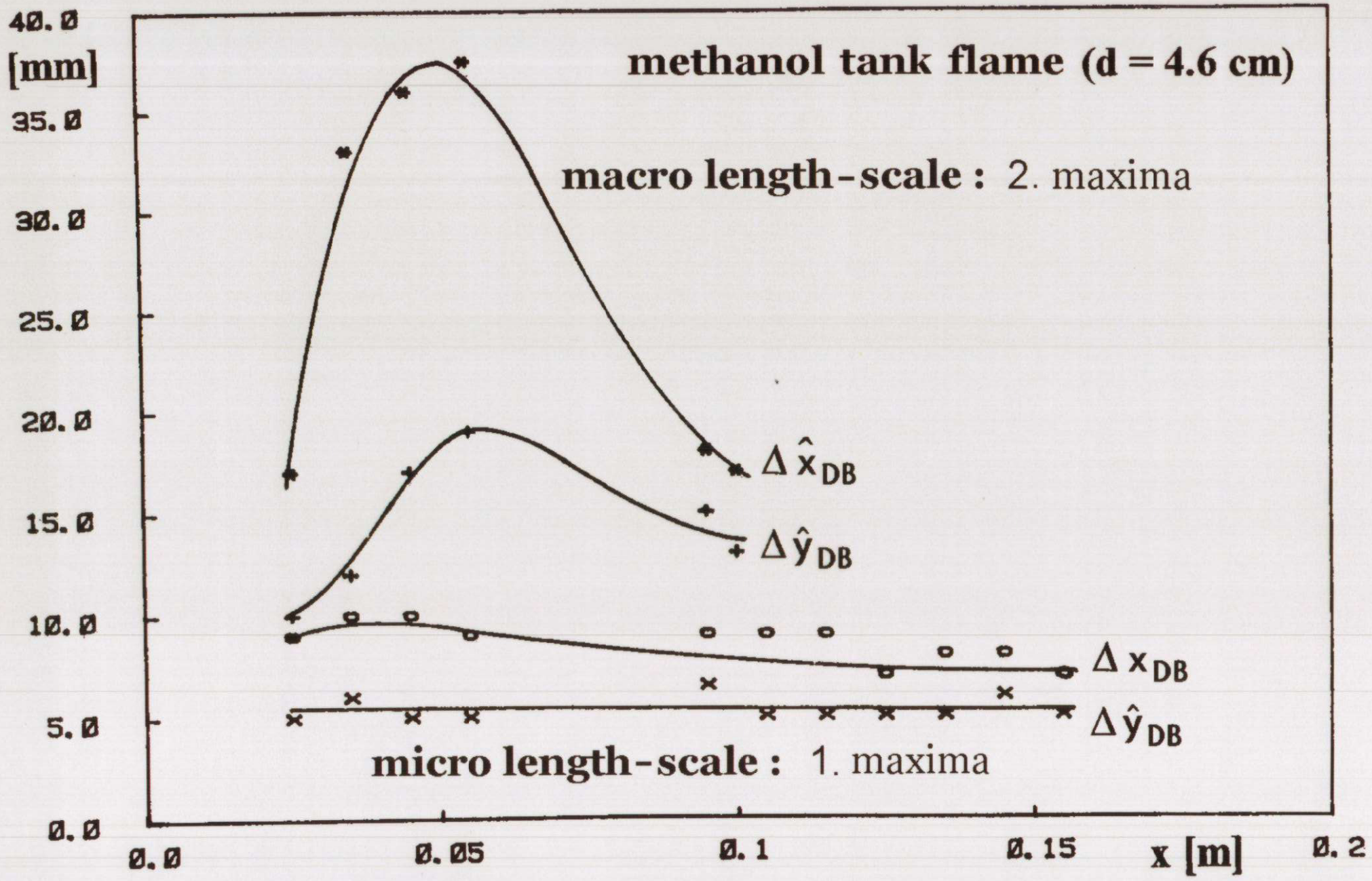
methanol tank flame (d = 4.6 cm)
macro length-scale : 2. maxima
micro length-scale : 1. maxima
$\Delta \hat{x}_{DB}$
$\Delta \hat{y}_{DB}$
Δx_{DB}
$\Delta \hat{y}_{DB}$
40.0
[mm]
35.0
30.0
25.0
20.0
15.0
10.0
5.0
0.0
0.0
0.05
0.1
0.15
x [m]
0.2

Length-, time- and velocity scales (II)

T_E macro time-scale by Euler

L_E macro length-scale

t_E micro time-scale (measure for the disspation time)

l_E micro length-scale (dissipation length)

l_K Kolmogoroff-length

Normalized autocorrelation funktion $R(\tau)$:

$$R(\tau) = \frac{\overline{p'_{dyn}(t)\; p'_{dyn}(t+\tau)}}{\overline{p'^2_{dyn}(t)}}$$

frequency spectrum $F(f)$: measured

$$F(f) = 4 \int_0^\infty R(\tau) \cos(2\pi f \tau)\, d\tau \qquad \text{and}$$

$$R(\tau) = \int_0^\infty F(f) \cos(2\pi f \tau)\, df$$

Length- , time- and velocity scales (III)

$$T_E = \int_0^\infty R_E(\tau)\, d\tau \qquad \left(\lim_{f \to 0} F(f) = 4\, T_E \right)$$

$$\frac{1}{t_E^2} = 4\pi^2 \int_0^\infty f^2\, F(f)\, df$$

$$L_E = \sqrt{\overline{u'^2}}\; T_E \qquad \left(\lim_{k \to 0} F(k) = 4\, L_E \right)$$

$$l_E = \sqrt{\overline{u'^2}}\; t_E \qquad \left(\frac{1}{l_E^2} = 4\pi^2 \int_0^\infty k^2\, F(k)\, dk \right)$$

$$l_K = \left(\frac{\eta_F^3 T_E}{2\, p'_{dyn}\, \varrho^2} \right)^{0.25} \qquad \eta_F = \frac{\sum_i \eta_i \overline{\gamma}_i \sqrt{M_i}}{\sum_i \overline{\gamma}_i \sqrt{M_i}}$$

$$\varrho_F = \overline{\varrho}_F(y,x)$$

$$\eta_i = \eta_i\,(T(y,x))$$

Length-, time- and velocity scales (IV)

$$S_F = \sqrt{\frac{\lambda_F}{\rho c_P t_R}}$$

$$\frac{\lambda_F}{\rho c_P} \equiv a_F \approx \nu_F$$

$$\delta_F = \frac{(\lambda_F/c_P)\, T_{ref}}{\rho_u S_F} \left(\frac{i}{\Theta}\right)$$

$$\Theta \equiv \frac{E_A}{RT}$$

$$E_A \to \infty \; : \; \delta_F \to 0$$

$$1600 < T_{ref} < 2000\,K$$

$$t_F = \frac{\delta_F}{S_F}$$

$$t_F \equiv t_R$$

Length-, time- and velocity scales (V)

$$L_E = \frac{u'^3}{\varepsilon}$$

$$u' = \sqrt{\frac{u'^2}{3}} = \sqrt{\frac{2}{3} E_t}$$

$$T_E = \frac{L_E}{u'} = \frac{2}{3} \frac{E_t}{\varepsilon}$$

$$l_K = \left(\frac{\nu_E^3}{\varepsilon} \right)^{1/4}$$

$$l_c = \left(\frac{D_M^3}{\varepsilon} \right)^{1/4}$$

5.1.1 *Borghi* diagram

Borghi diagram **(1984)** :

$$\frac{u'}{S_F} = Re_t \left(\frac{L_E}{\delta_F}\right)^{-1}$$

$$\frac{u'}{S_F} = Da_t^{-1} \left(\frac{L_E}{\delta_F}\right)$$

$$\frac{u'}{S_F} = Ka_t^{2/3} \left(\frac{L_E}{\delta_F}\right)^{1/3}$$

$Re_t = 1$, $Da_t = 1$, $Ka_t = 1$: limits of the regimes

$\frac{u'}{S_F} = 1$: line between slowly wavy and folded flame fronts

$$Re_t = Da_t^2 \, Ka_t^2$$

$$\frac{L_E}{l_K} = Re_t^{3/4}$$

$$\delta_F = \frac{(\lambda_F / c_P) \; Tref}{\rho_u S_F}$$

$$Re_t \equiv \frac{u' L_E}{\nu_F}$$

$Re_t > 1$: turbulent
$Re_t < 1$: laminar

$$Da_t \equiv \frac{T_E}{t_R} = \frac{L_E / u'}{t_R}$$

$Da_t > 1$: fast chemistry
$Da_t < 1$: slow chemistry

$$Ka_t \equiv \frac{t_R}{t_K} = t_R \sqrt{\frac{\varepsilon}{\nu_F}}$$

$$t_K = l_K / u_K$$

$$u_K = (\nu_F \varepsilon)^{1/4}$$

$Ka_t > 1$: large flame stretch
$Ka_t < 1$: small flame stretch

	Da_t	Re_t	Ka_t
CH_4 / air : $\Phi = 1$	11	0.2	0.1
CH_4 / air			
d = 4.6 cm	58	2	0.1
d = 10 cm	73	3	0.2
$n\text{-}C_6H_{14}$ / air			
d = 4.6 cm	143	4	0.1
d = 10 cm	171	5	0.2
CH_3OH / air			
d = 4.6 cm	432	6	0.04
d = 10 cm	659	11	0.1
H_2 / air			
d = 4.6 cm	1890	28	0.01

Borghi diagram

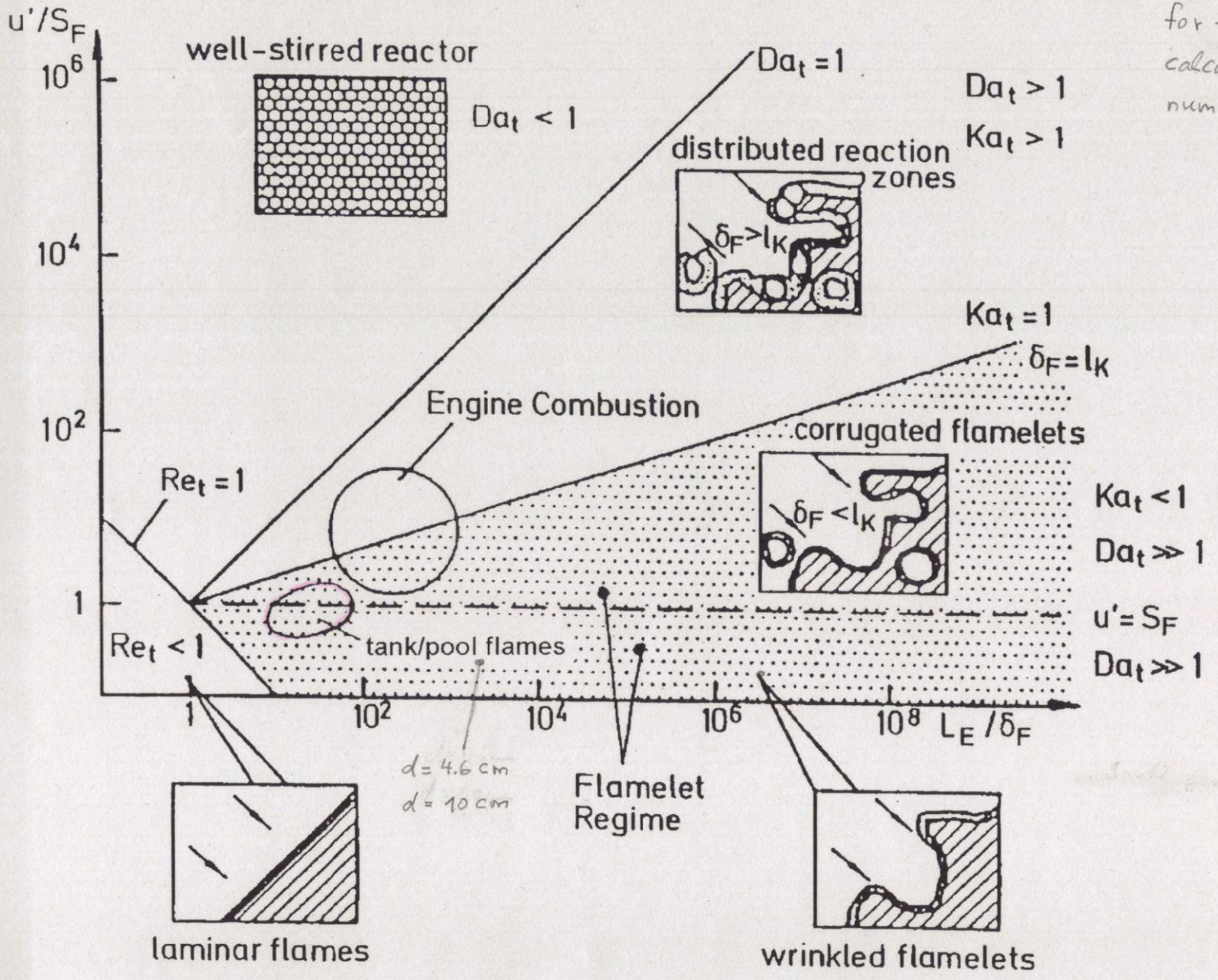

for this diagram we have calculated the turbulent numbers of Da_t, Re_t, Le_t

small pool flames: in the region between wrinkled flamelets and corrugated flamelets

Turbulent Pr_t-, Sc_t- and Le_t- numbers

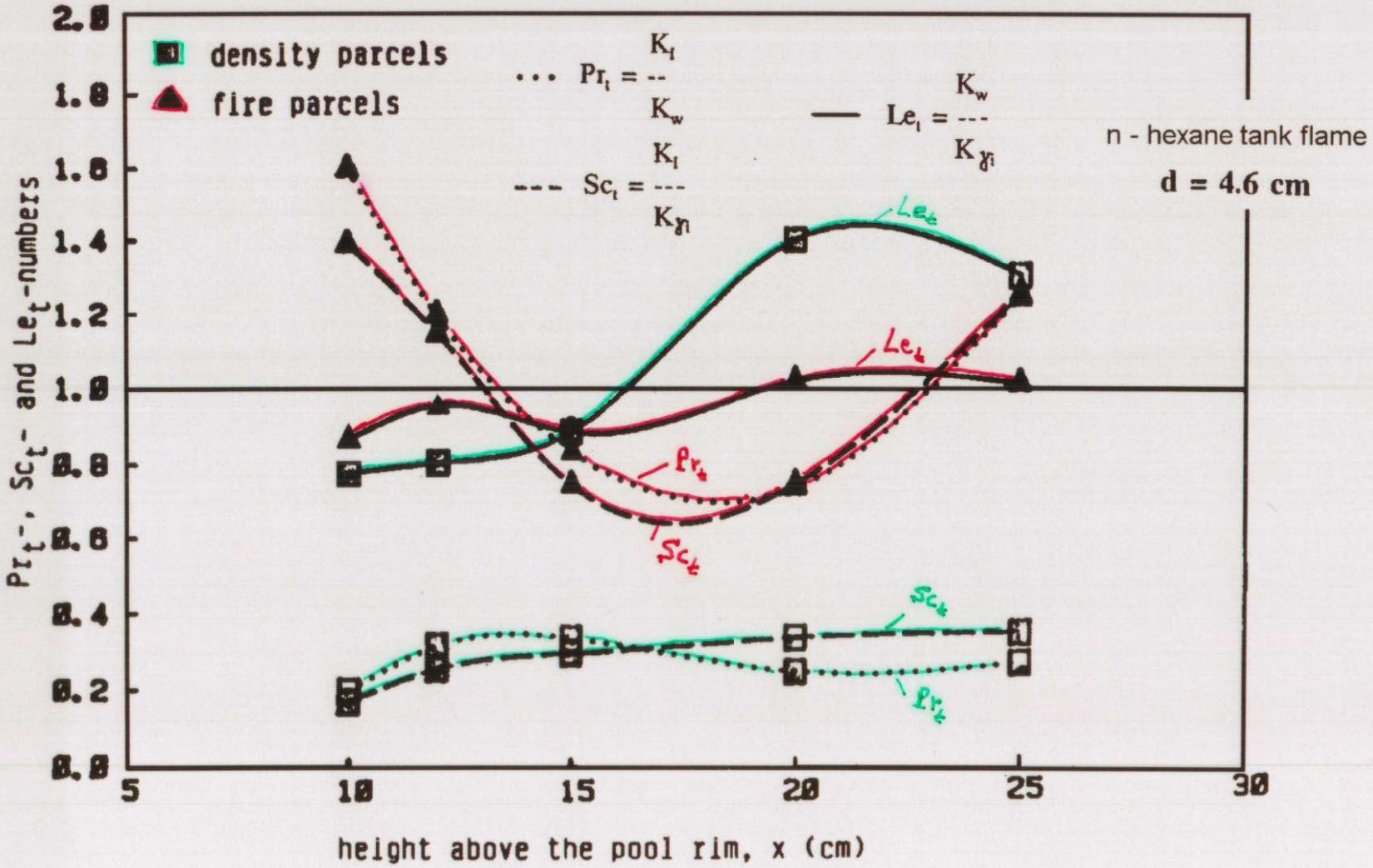

density parcels: transport of mass > transport of heat → transport of mass < transport of heat

transport of momentum < transport of heat / transport of mass

---

flame parcels: transport of mass ≈ transport of heat

transport of momentum < transport of mass / transport of heat → transport of momentum > transport of mass / transport of heat

5.2 Turbulent Pr_t-, Sc_t- and Le_t- numbers

Momentum, mass and heat exchange coefficients

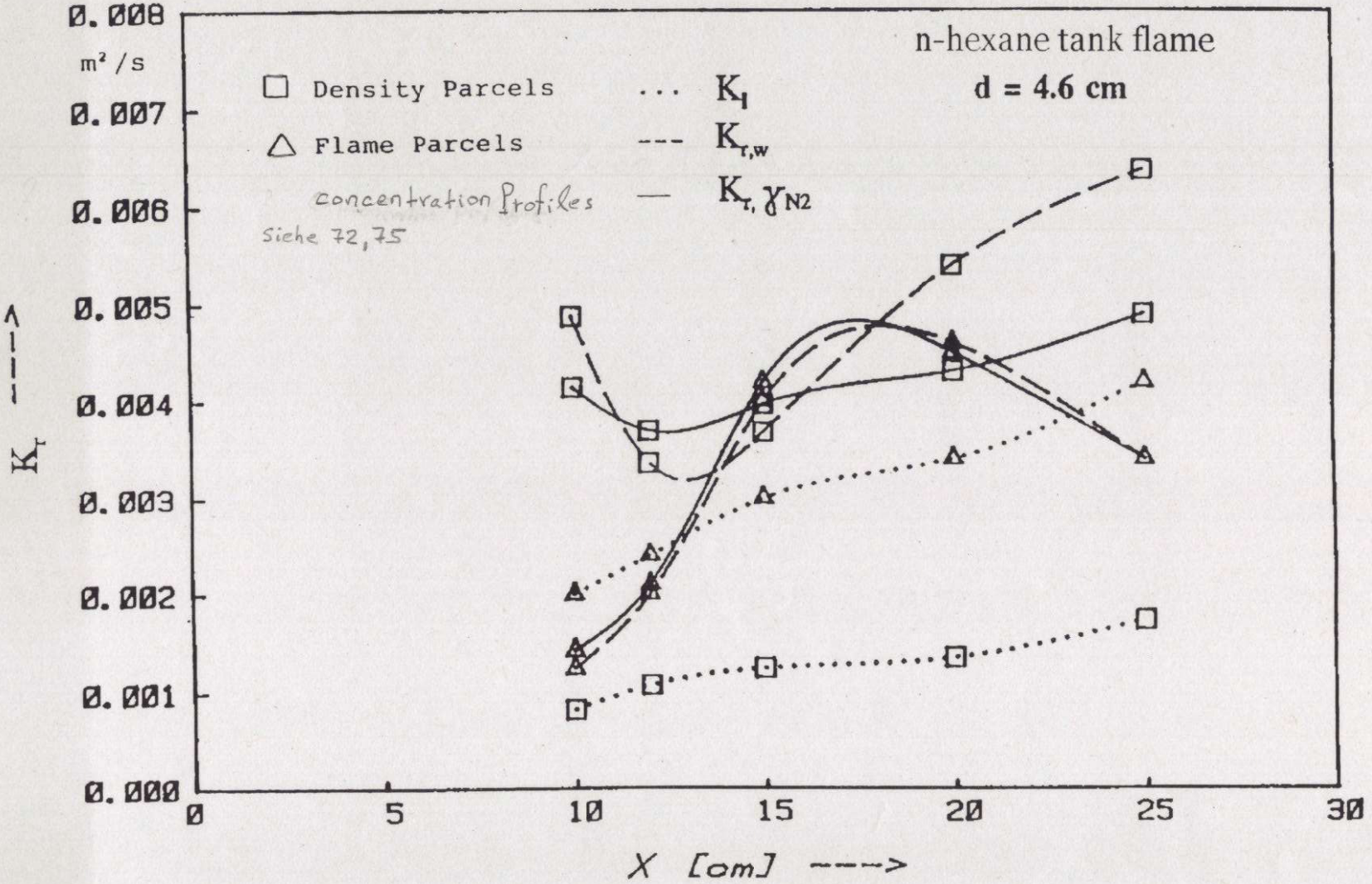

Turbulent momentum exchange coefficients

$$K_I(x) = \sqrt{\overline{u'^2}(x)}\; l_E(x)$$

$$K_{I,K}(x) = \sqrt{\overline{u'^2}(x)}\; l_K(x)$$

$$K_{I,DB}(x) = \sqrt{\overline{v'^2_{DB}}(x)}\; \Delta y_{DB}(x)$$

(a) $K_I(x)$, $K_{I,K}(x)$ and $K_{I,DB}(x)$

$$K_{I,K} < K_{I,DB} < K_I$$

⇒ density parcels are also connected with the exchange of momentum

(b) $(K_I)_{C_6H_{14}} > (K_I)_{CH_3OH}$

Momentum exchange coefficients

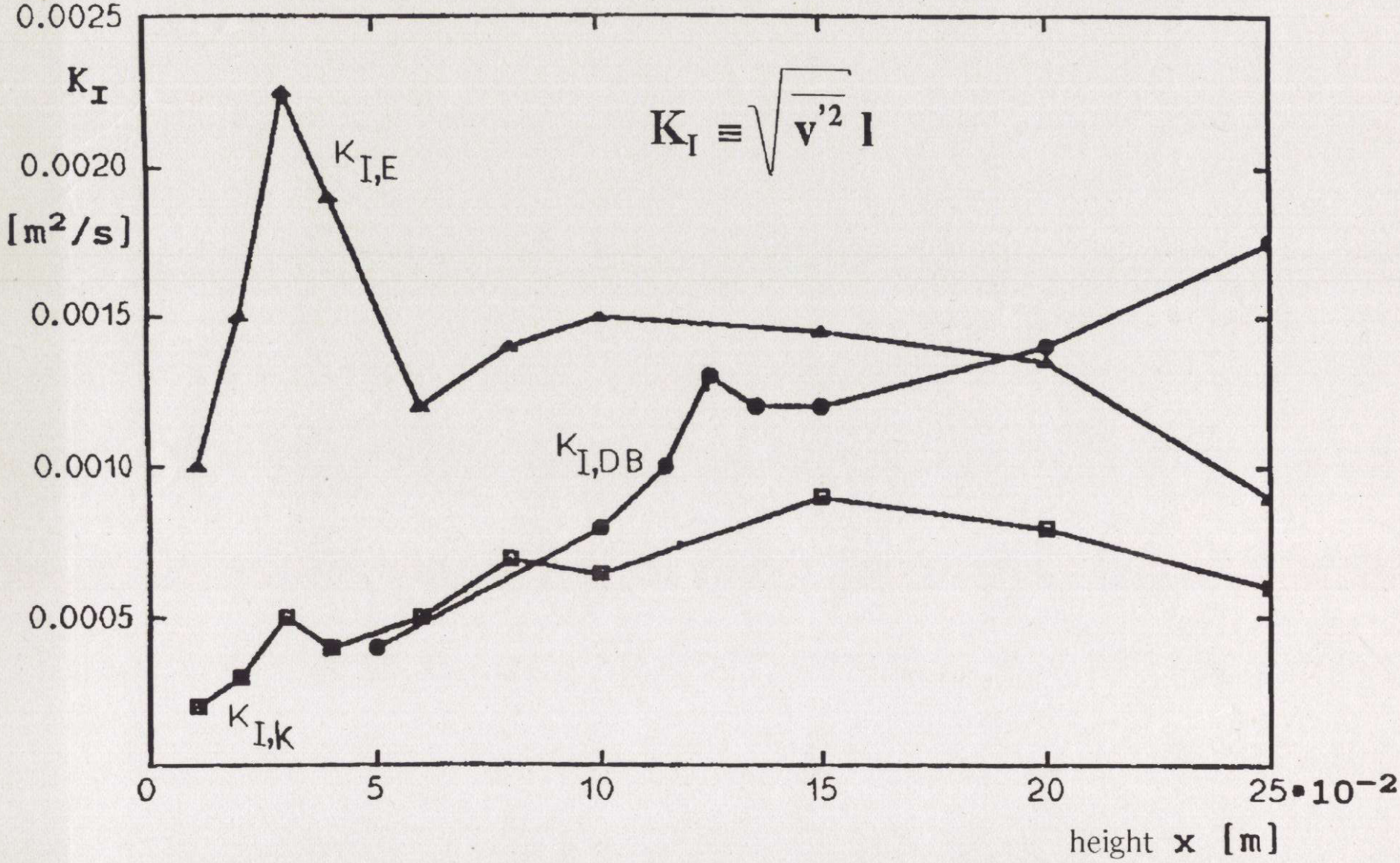

Calculation of mass exchange coefficients

Species mass conservation

$$-\frac{\partial}{\partial x}(u\rho\gamma_i) - \frac{1}{r}\frac{\partial}{\partial r}(rv\rho\gamma_i) + \frac{1}{r}\frac{\partial}{\partial r}\left(rK_{r,\gamma_i}\frac{\partial}{\partial r}(\rho\gamma_i)\right) = 0$$

overall mass conservation

$$\frac{\partial}{\partial x}(\rho u) + \frac{1}{r}\frac{\partial}{\partial r}(rv\rho) = \frac{1}{\pi r^2}\alpha_E\left(\frac{\pi}{4}\rho\dot{I}\right)^P \equiv A \quad ; \quad \dot{I} = \pi\int_0^\infty \rho u^2\, dr^2$$

turbulent mass exchange coefficient

$$K_{r,\gamma_i}(r,x) = \frac{\int_0^r \frac{\partial}{\partial x}(u\rho\gamma_i)\, r\, dr + \int_0^r \left[\frac{\partial\gamma_i}{\partial x}\int_0^r \left(A - \frac{\partial}{\partial x}(u\rho)\right) r\, dr\right] dr + \int_0^r \gamma_i\left(A - \frac{\partial}{\partial x}(u\rho)\right) r\, dr}{r\frac{\partial}{\partial r}(\rho\gamma_i)}$$

Radial concentration profiles of stable molecules

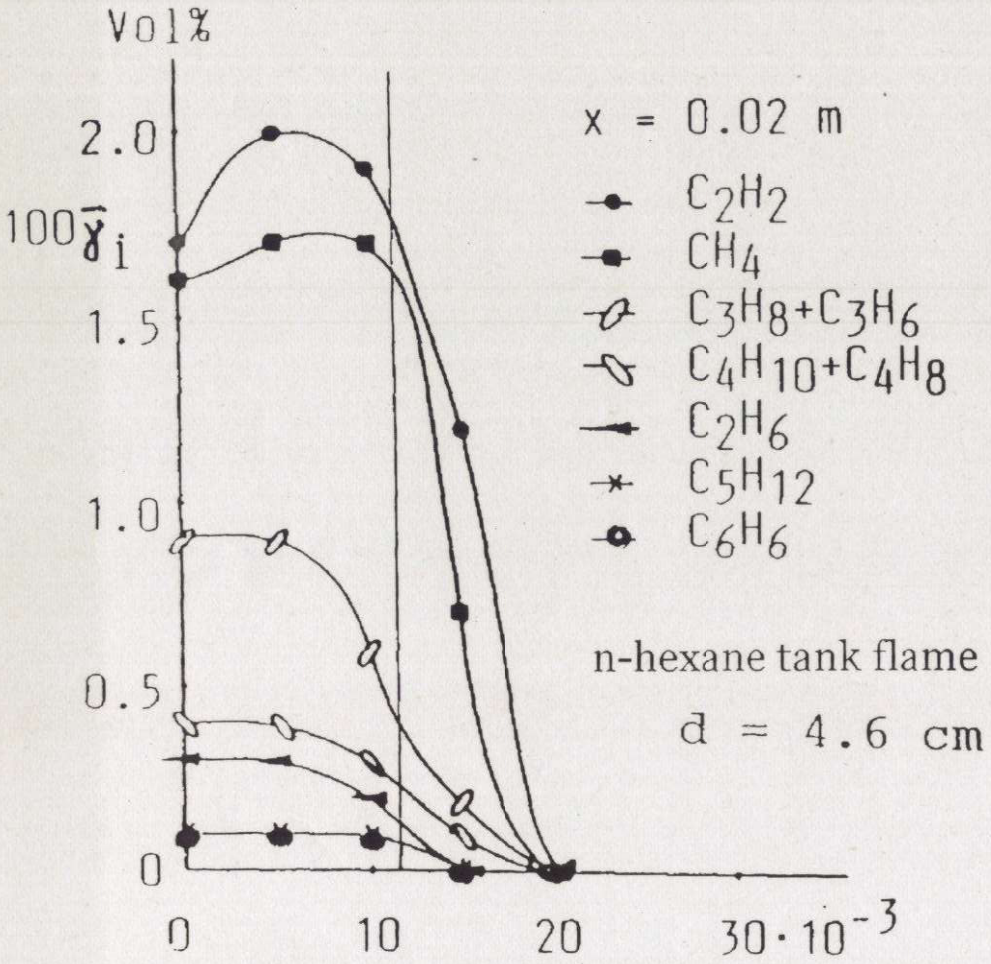

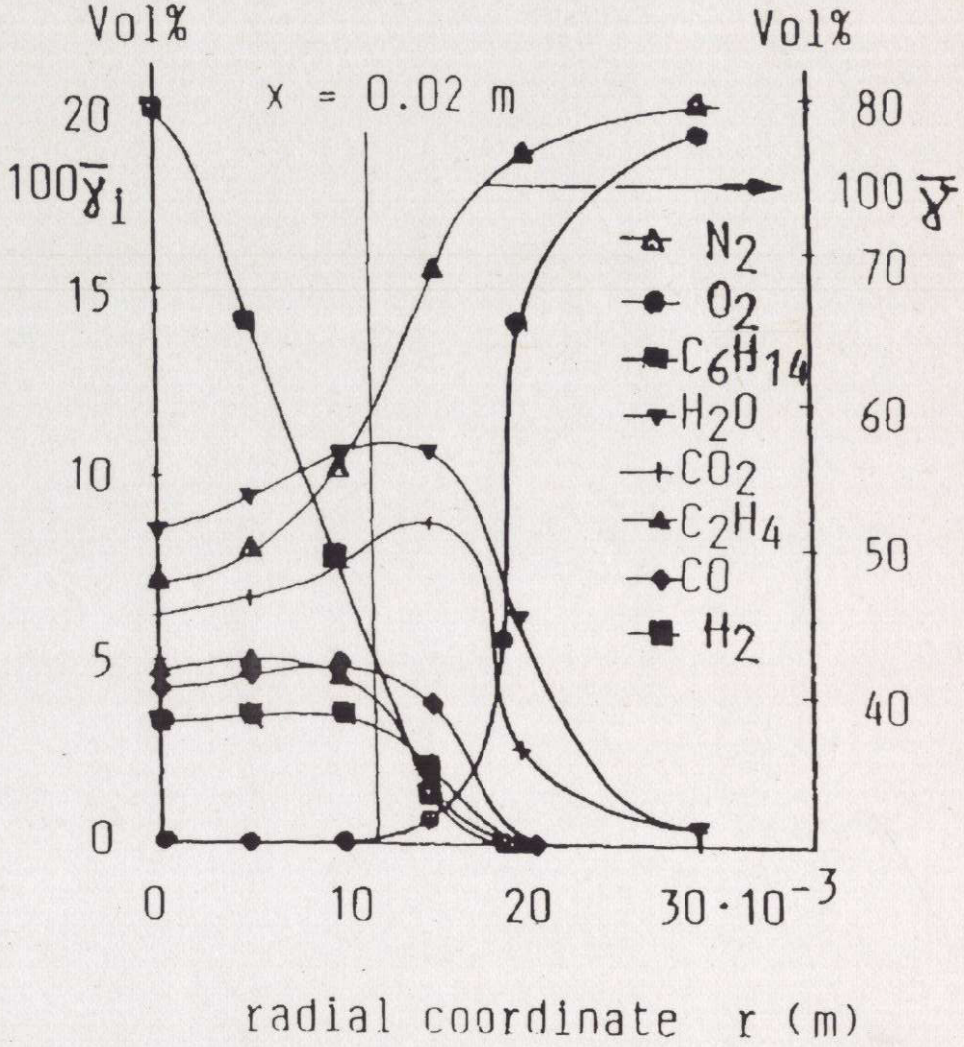

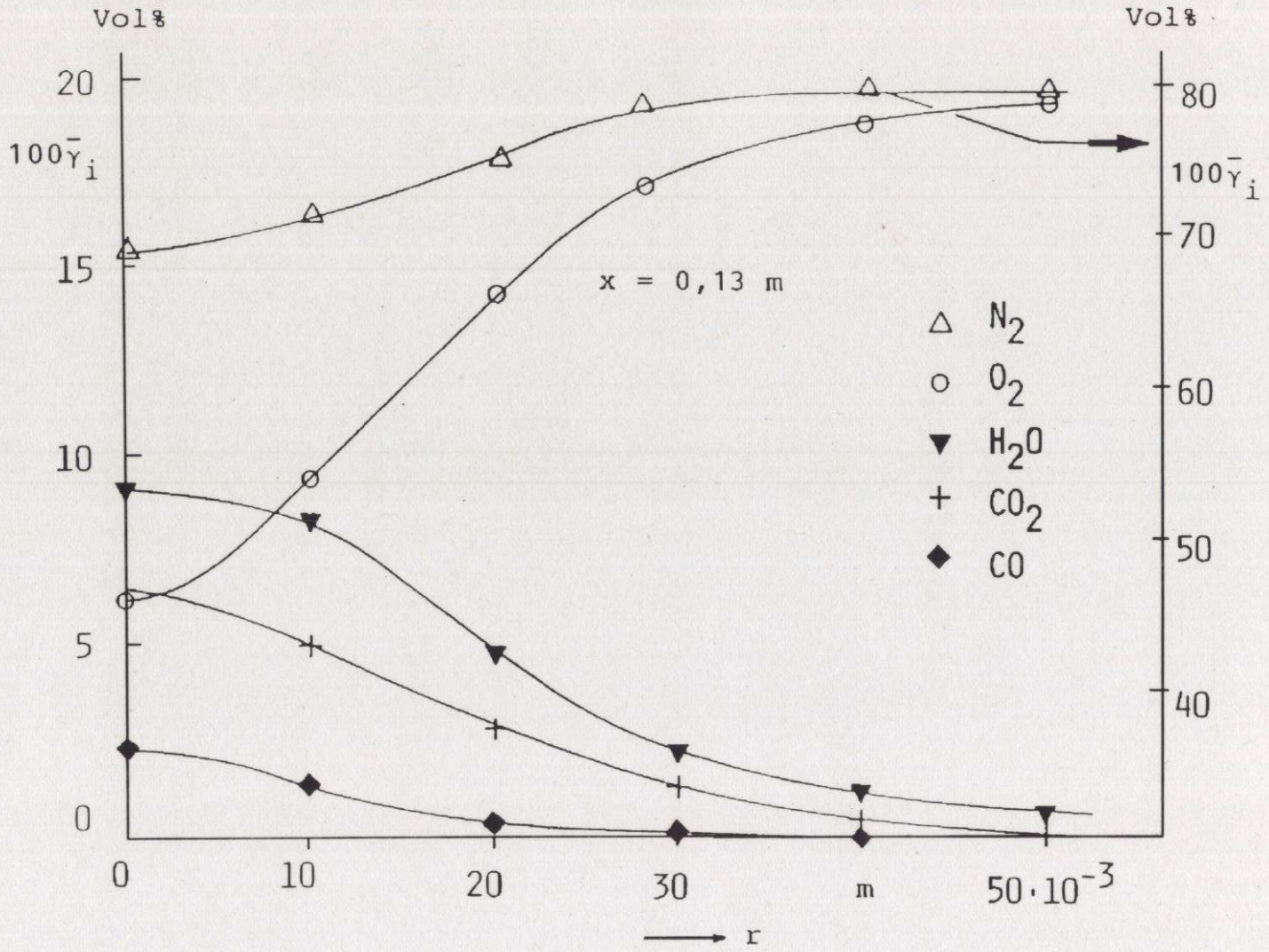

Radial concentration profiles of stable molecules

(a) in the continuous flame zone

(b) in the transition flame zone

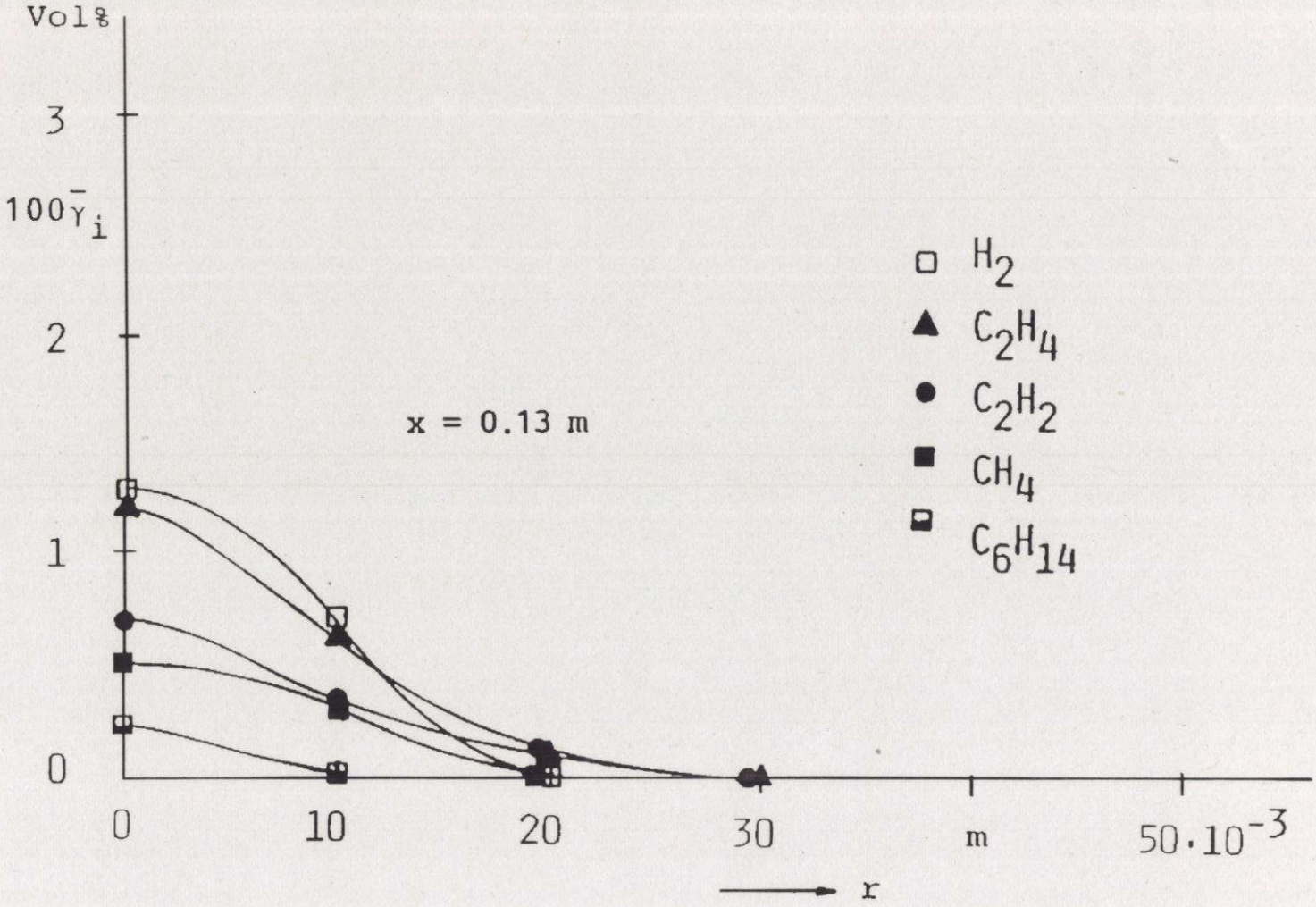

Radial concentration profiles of stable molecules

(a) in the continuous flame zone

(b) in the transition flame zone

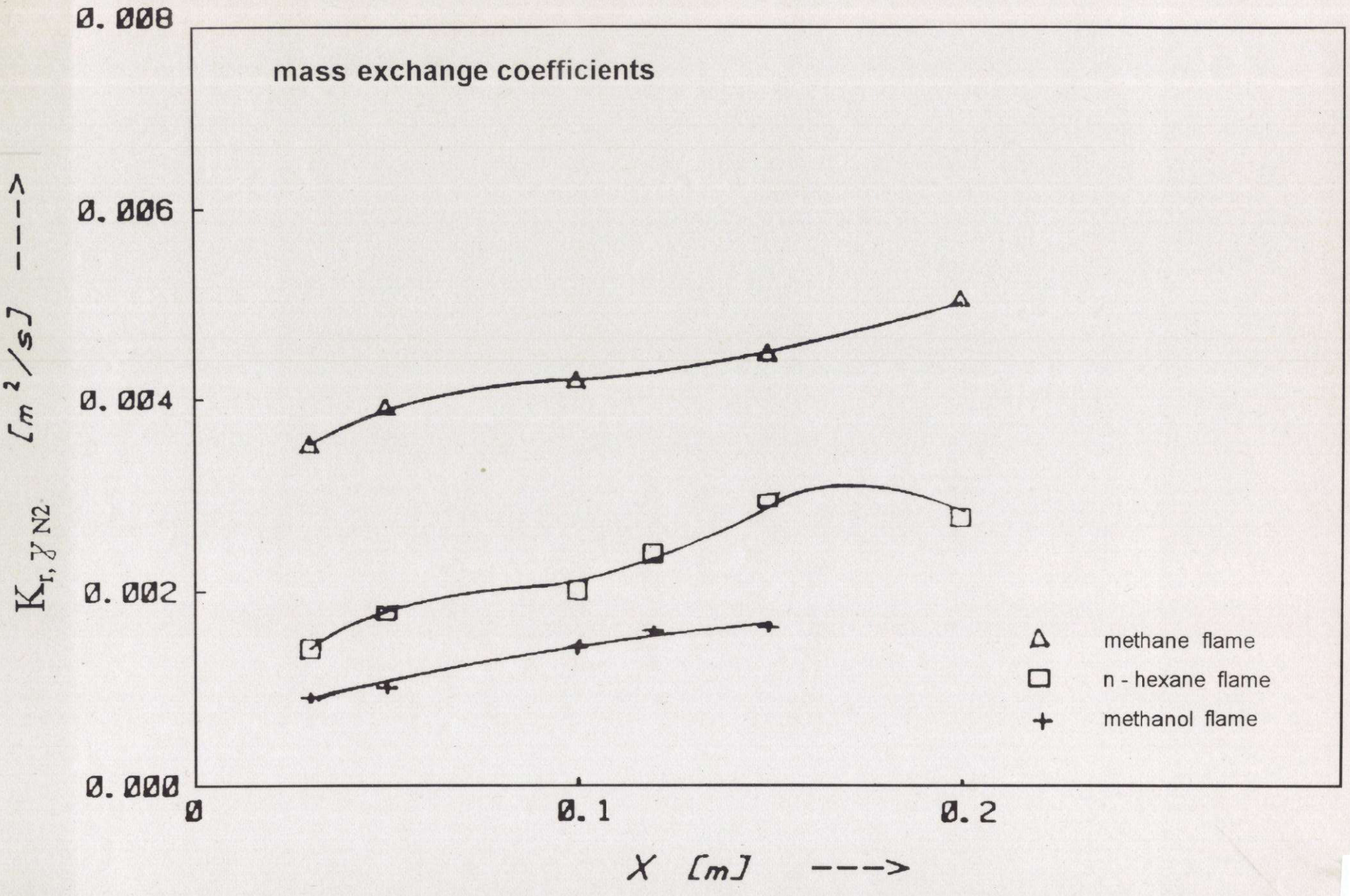
mass exchange coefficients
0.008
0.006
0.004
0.002
0.000
0
0.1
0.2
$K_{r,\gamma N2}$ [m²/s] --->
X [m] --->
methane flame
n - hexane flame
methanol flame

Calculation of heat exchange coefficients

energy conservation

$$-\frac{\partial}{\partial x}\left(u\rho c_p T\right) - \frac{1}{r}\frac{\partial}{\partial r}\left(r v \rho c_p T\right) + \frac{1}{r}\frac{\partial}{\partial r}\left(r K_{r,w}\frac{\partial}{\partial r}\left(\rho c_p T\right)\right) = 0$$

turbulent heat exchange coefficient

$$K_{r,w}(r,x) = \frac{\int_0^r \frac{\partial}{\partial x}\left(u\rho c_p T\right) r\,dr + \int_0^r \left[\frac{\partial(\rho c_p)}{\partial x}\int_0^r \left(A - \frac{\partial}{\partial x}\left(u\rho\right)\right) r\,dr\right] dr + \int_0^r c_p T\left(A - \frac{\partial}{\partial x}\left(u\rho\right)\right) r\,d}{r\frac{\partial}{\partial r}\left(\rho c_p T\right)}$$

Radial temperature profiles

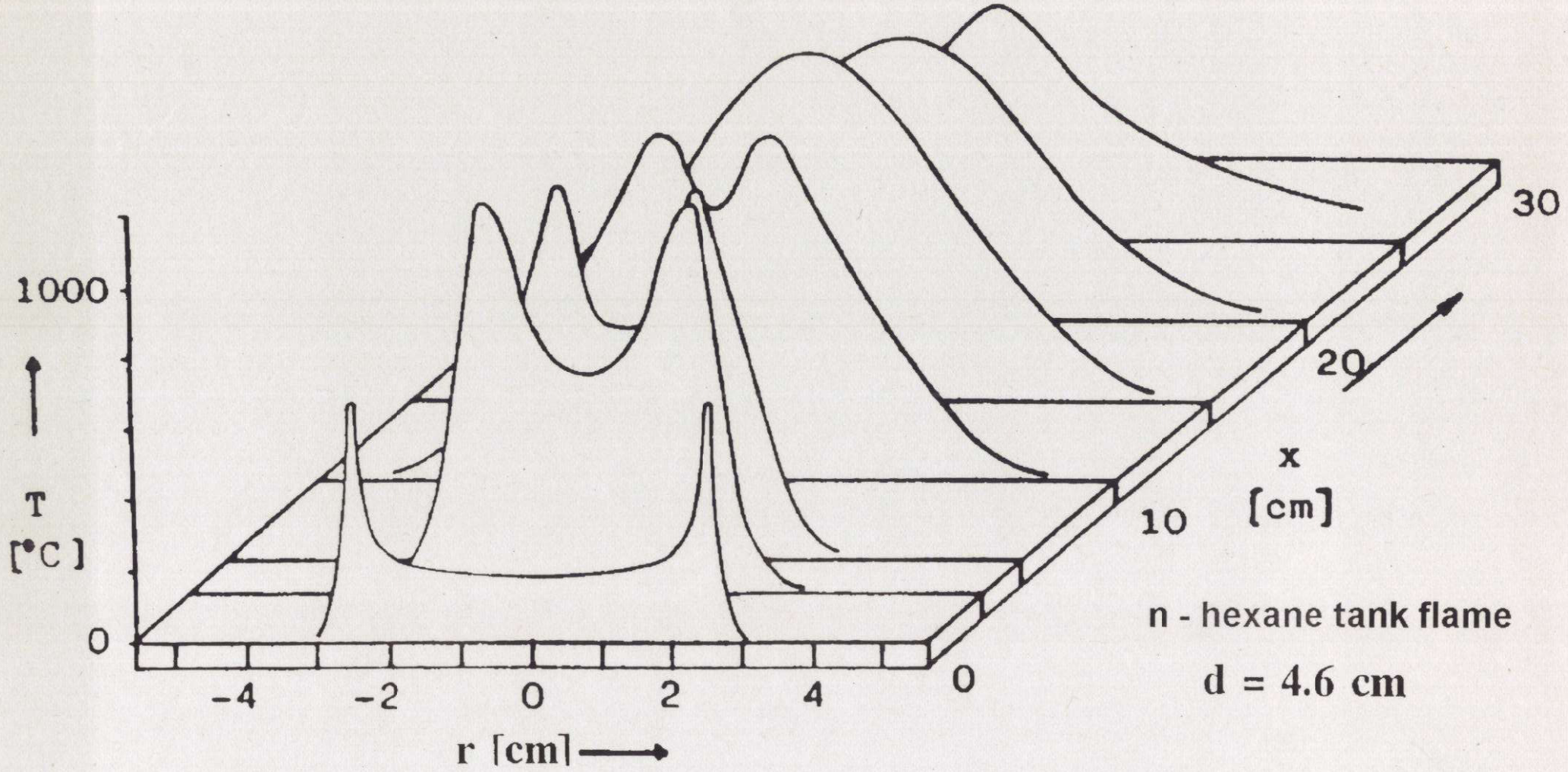

Radial density profiles

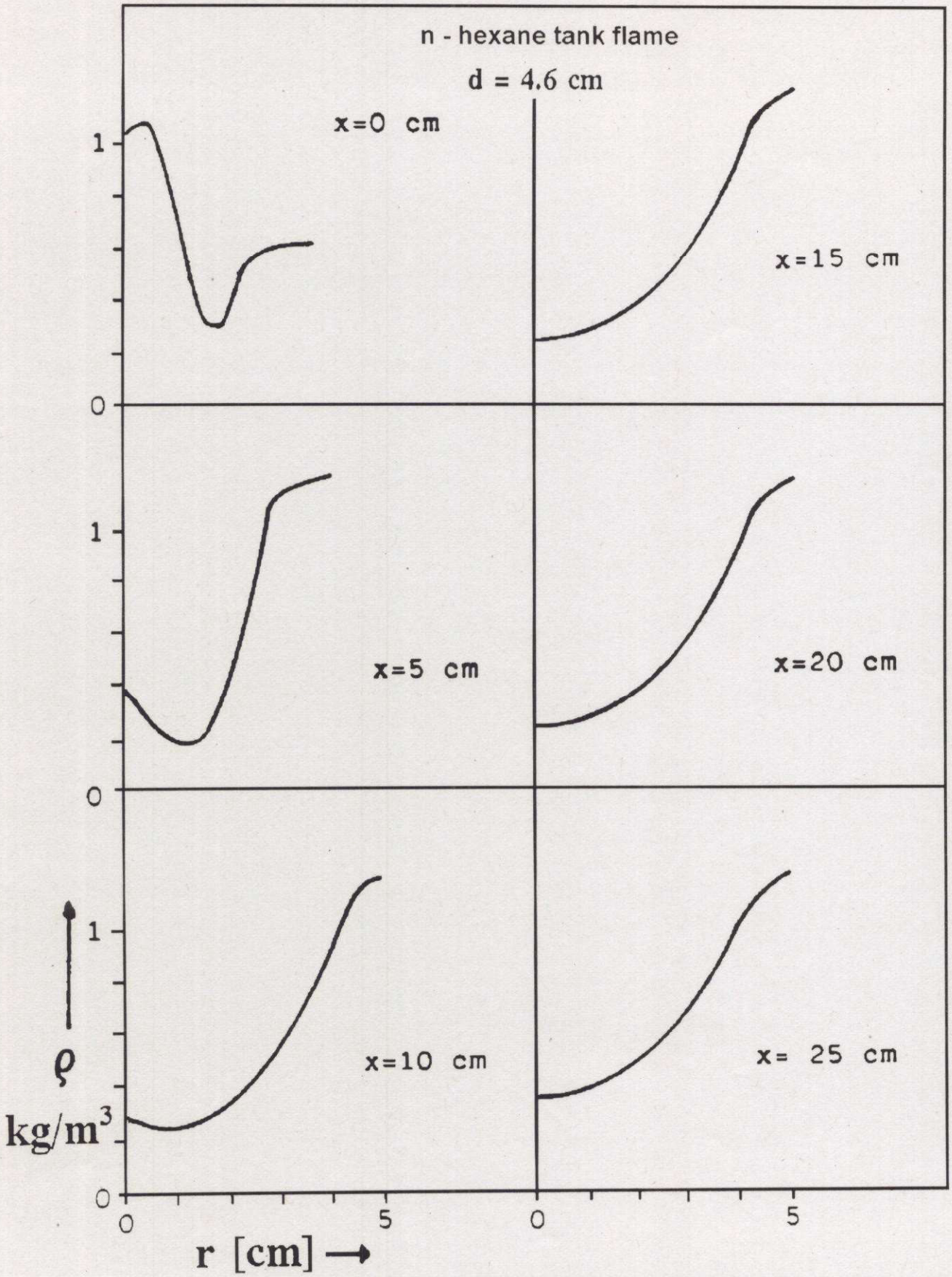

Turbulent Pr_t-, Sc_t- and Le_t- numbers

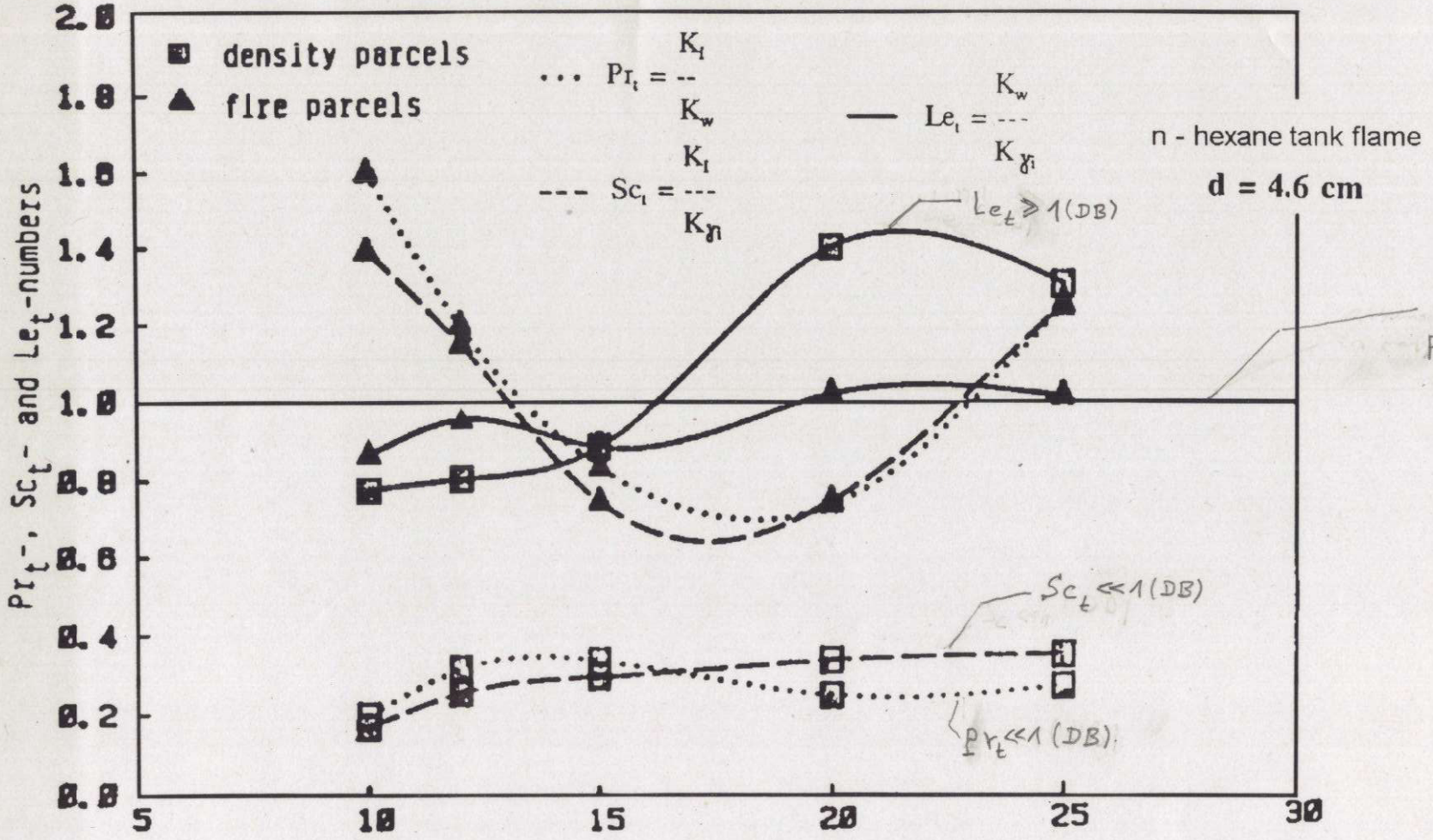

density parcels: transport of mass > transport of heat → transport of mass < transport of heat

transport of momentum < transport of heat / transport of mass (as usual)

flame parcels: transport of mass ≈ transport of heat

transport of momentum < transport of mass / transport of heat → transport of momentum > transport of mass / transport of heat (as unusual)

5.3 Dynamic properties of density sources (Q) and density sinks (S)

5.3.1 Physical meaning of Q and S

1. Q: local *decrease* of density (e.g. *increase* of *temperature*)

   S: local *increase* of density (e.g. *decrease* of *temperature*)

2. n-hexane $25 < \Delta x < 50$ cm

   d = 4.6 and 10 cm

   Methanol $0 < \Delta x < 25$ cm

3. Influencing quantities

   Height region Δx

   type of fuel

   Tank diameter d

5.3.2 Number of Q and S

w_Q Number of density sources Q

w_S Number of density sinks S

(a) $\boxed{w_S > w_Q}$ resp. $\boxed{\frac{w_Q}{w_S} < 1}$

$\rightarrow$ flames cool down

(b) $\Delta x \uparrow \quad w_S \uparrow$

(c) $d \uparrow \quad w_S \uparrow$

(d) $(w_S)_{CH_3OH} > (w_S)_{C_6H_{14}}$

5.3.3 Growth and decay of Q and S

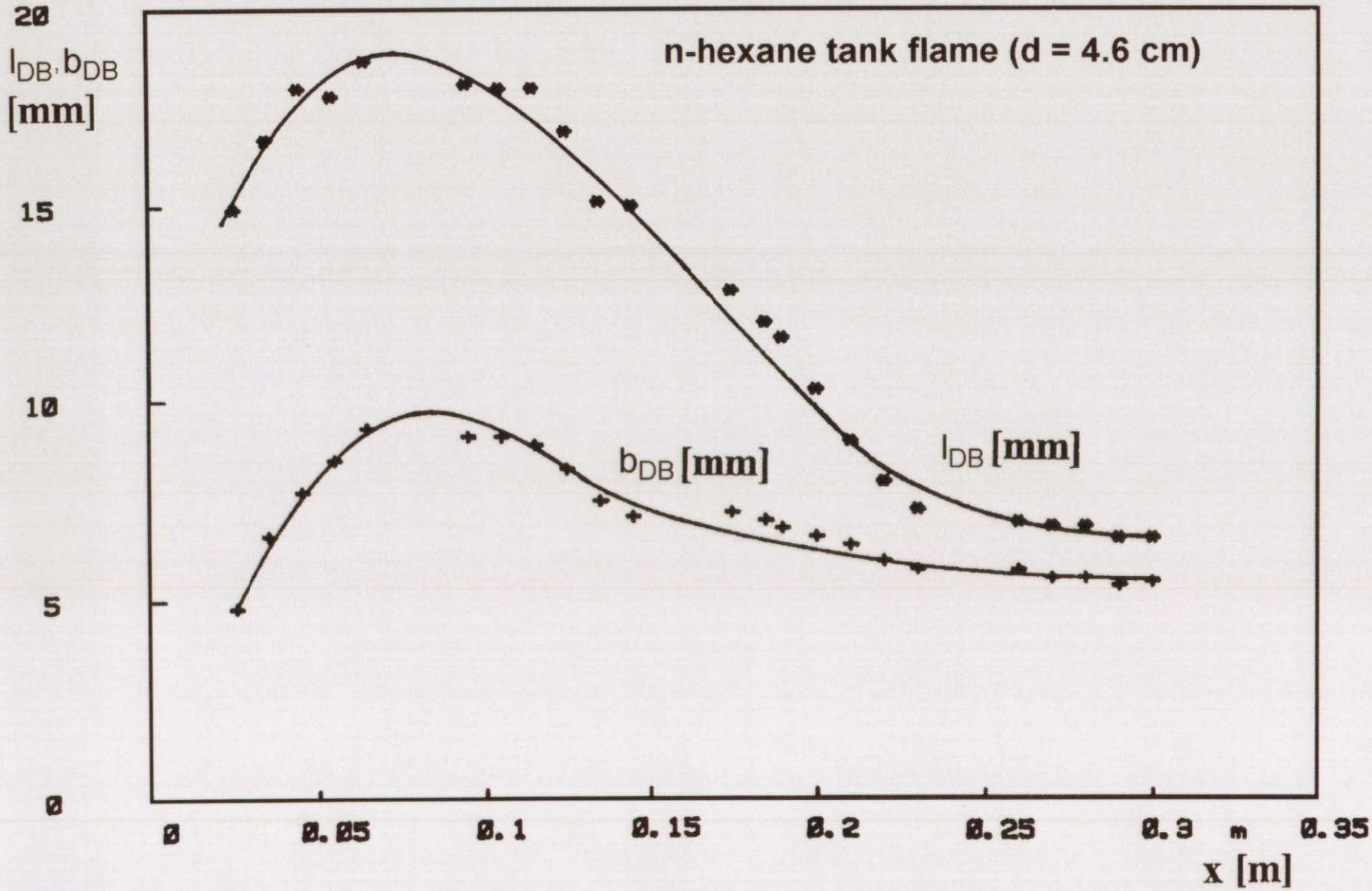

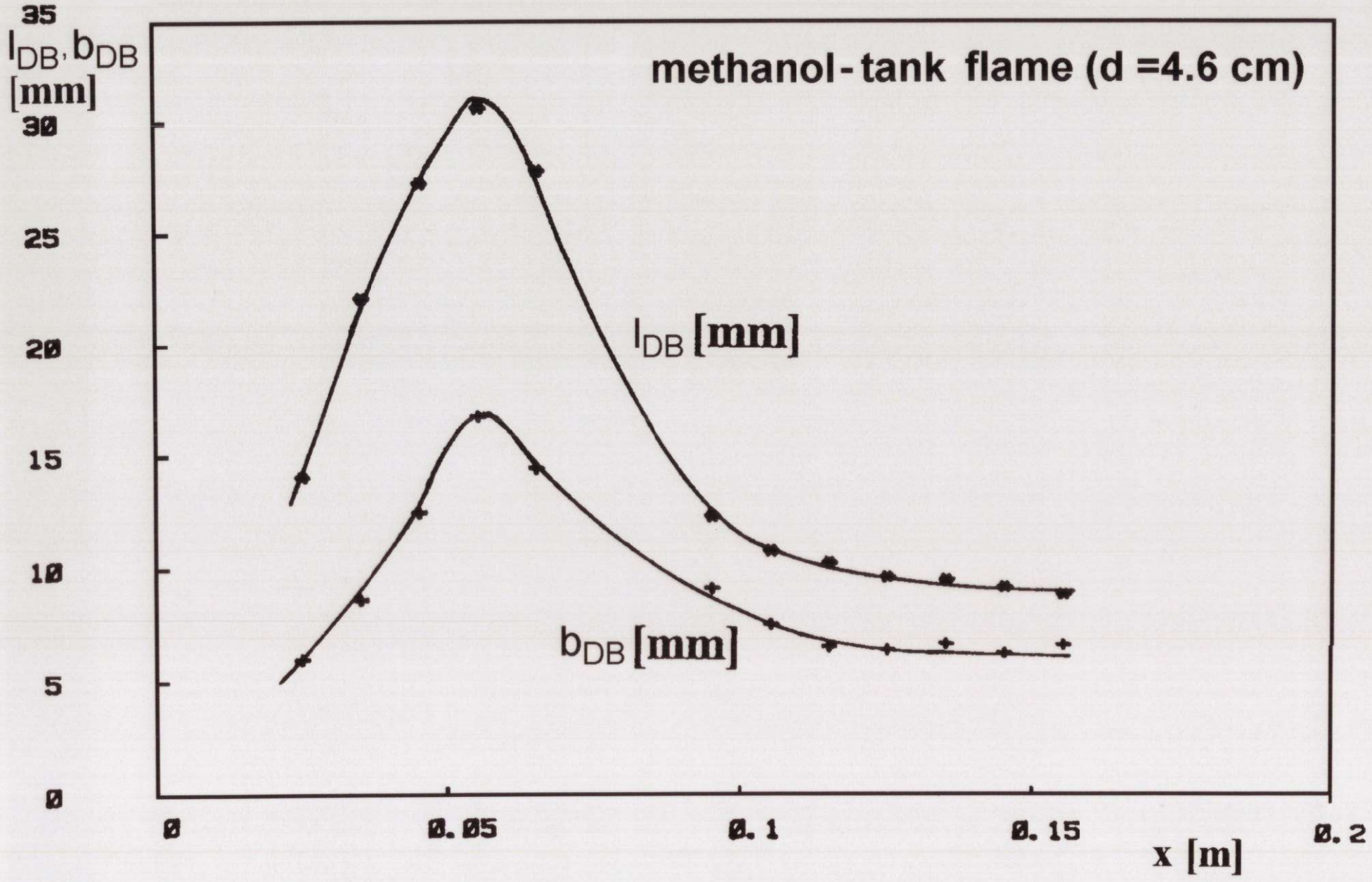
methanol-tank flame (d =4.6 cm)
l_{DB}, b_{DB} [mm]
35
30
25
20
15
10
5
0
l_{DB} [mm]
b_{DB} [mm]
0
0.05
0.1
0.15
0.2
x [m]

fuel	d (mm)	Δy (mm)	Δx (mm)	kind of measurement
n-pentane	46	5	6	1
n-hexane	46	5	5	1, 2
	46	4		3
n-heptane	46	5	5	1
methanol	46	6	7	1, 2
propanol	46	6	6	1
cyclohexanol	46	5	7	1
acetone	46	6	5	1
diethylether	46	5	6	1
benzene	46	5	7	1
LNG	46	5	6	1
	78	6	7	1
	120	5	5	1
	150	5	7	1
	200	6	6	1
	300	6	6	1
	500	5	5	1

kind of measurement:

1 Equidensitometry

2 Interferometry

3 heat radiation

Minimal micro length scales Δy, Δx for different fuels and tank diameters d

5.3.4 Lifetimes τ of Q and S

P(τ) PDF: logarithmic normal distribution

$$P(\tau) = P(\tau_{max}) \exp\left[-\frac{1}{2}\left(\frac{\ln\frac{\tau}{\tau_{max}}}{\sigma}\right)^2\right]$$

with σ = const.

(a) $\bar{\tau}_S > \bar{\tau}_Q$: up to 60% larger

(b) $\Delta x \uparrow$: $\bar{\tau} \downarrow$

(c) $d \uparrow$: $\bar{\tau} \downarrow$

(d) $\tau_{CH_3OH} > \bar{\tau}_{C_6H_{14}}$: up to 80% larger

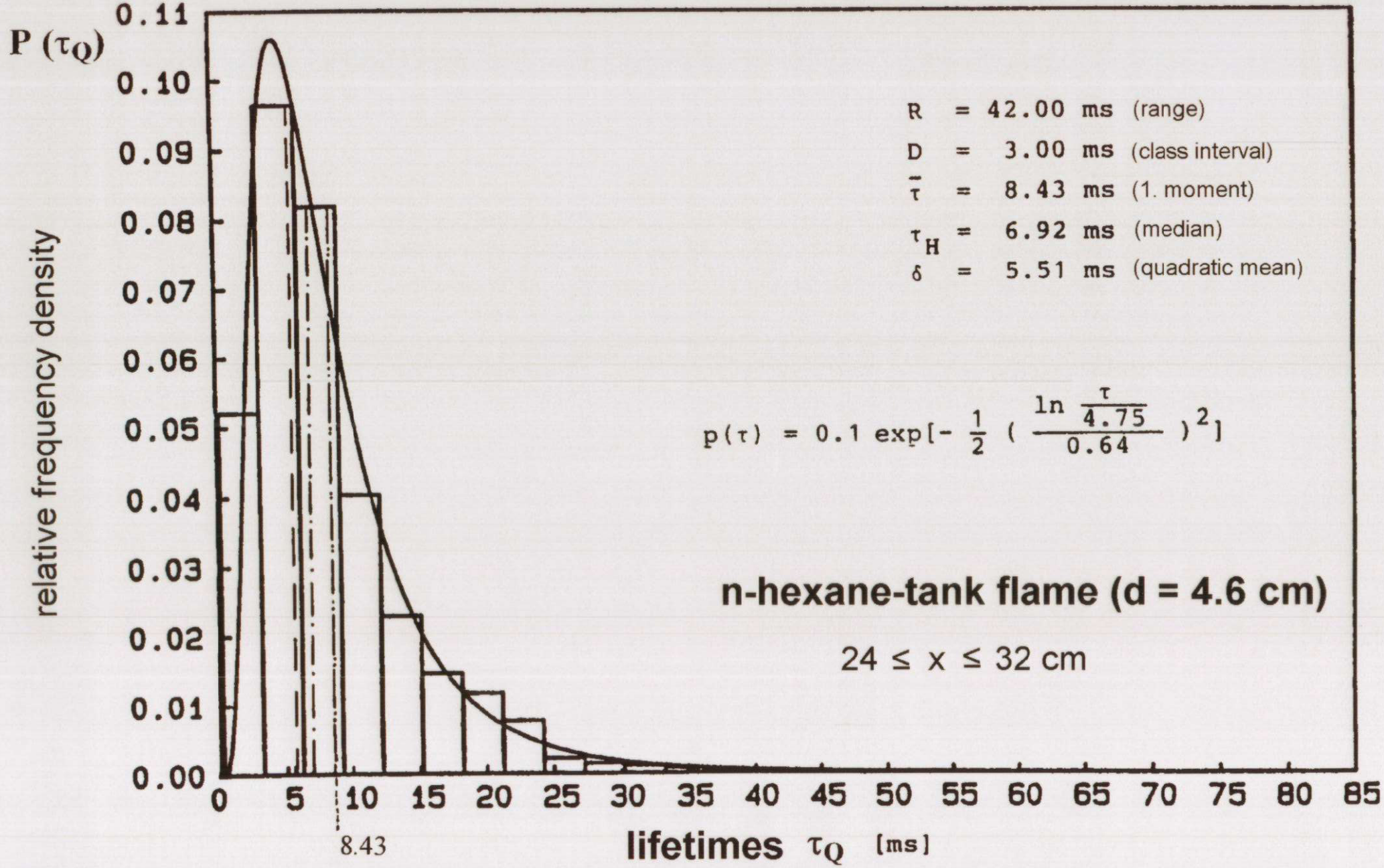
P (τQ)
relative frequency density
0.11
0.10
0.09
0.08
0.07
0.06
0.05
0.04
0.03
0.02
0.01
0.00
0 5 10 15 20 25 30 35 40 45 50 55 60 65 70 75 80 85
8.43
lifetimes τQ [ms]
R = 42.00 ms (range)
D = 3.00 ms (class interval)
τ̄ = 8.43 ms (1. moment)
τH = 6.92 ms (median)
δ = 5.51 ms (quadratic mean)
p(τ) = 0.1 exp[- 1/2 (ln τ/4.75 / 0.64)2]
n-hexane-tank flame (d = 4.6 cm)
24 ≤ x ≤ 32 cm

5.3.5 Transitions between Q and S

communicative Phenomena

$Q \rightarrow S$ (local cool-down)

$S \rightarrow Q$ (local heating)

$Q \rightarrow S \rightarrow Q$ and $S \rightarrow Q \rightarrow S$: relatively rare

$Q \rightarrow S \rightarrow Q \rightarrow S$ and $S \rightarrow Q \rightarrow S \rightarrow Q \rightarrow S$

$n_{Q \leftrightarrow S}$: fraction of Q and S, participating in a transition (relative frequency)

$\overline{\Delta t}_{Q \leftrightarrow S}$: averaged time difference between 2 transitions

(a) $n_{Q \leftrightarrow S} \gg n_{S \rightarrow Q}$

(b) $15\ \% < n_{Q \leftrightarrow S} < 35\%$

(c) $\overline{\Delta x} \uparrow$: $n_{Q \leftrightarrow S} \downarrow$ $\overline{\Delta t}_{Q \leftrightarrow S} \downarrow$

(d) $d \uparrow$: $n_{Q \leftrightarrow S} \downarrow$ $\overline{\Delta t}_{Q \leftrightarrow S} \downarrow$

(e) $(\overline{\Delta t}_{Q \leftrightarrow S})_{CH_3OH} > (\overline{\Delta t}_{Q \leftrightarrow S})_{C_6H_{14}}$

5.3.6 Temporal sequences of Q and S

Tupel formation: Temporal succession of a definite sequence of Q, S

1-tupel: Q, S

2-tupel: QQ, QS, SQ, SS

3-tupel: QQQ, QQS, SQS, SSQ, QSS, SSS, SQQ, QSQ

j-tupel: 2^j configurations

- Each configuration of a j-tupel exists at least once:

  $2^j + j \leq w_Q + w_S + 1 \quad \Rightarrow \quad j_{max} \leq 9$

  Experimental: $j \leq 5 \Rightarrow$ *selection*

  Not all possible configurations actually occur

  $\Rightarrow$ *partial order* or *selection*, respectively

$\overline{n}_{Q/S}$ Averaged relative frequency of the j-tupel

$\overline{\Delta t *}$ Sequence duration of the j-tupel:

Time difference between the first and last Q/S within a definite sequence

$\overline{\Delta t}_{Q/S}$ Formation time of the j-tupel:

Time difference between two following sequences of a definite configuration

Temporal sequences of Q and S (II)

(a) $\bar{n}\ldots_S \ldots \gg \bar{n}\ldots_Q \ldots$

(b) $\Delta x \uparrow$: $\overline{\Delta t}^* \downarrow$ $\overline{\Delta t}_{Q/S} \downarrow$

(c) $d \uparrow$: $\overline{\Delta t}^* \downarrow$ $\overline{\Delta t}_{Q/S} \downarrow$

(d) $\left(\overline{\Delta t}^*\right)_{CH_3OH} > \left(\overline{\Delta t}^*\right)_{C_6H_{14}}$

$\left(\overline{\Delta t}_{Q/S}\right)_{CH_3OH} > \left(\overline{\Delta t}_{Q/S}\right) C_6H_{14}$

(e) most probably configuration: tuple, which consists only of S_n

(f) most probably composition

Q_2S_3 d = 4.6 cm

QS_3 d = 10 cm

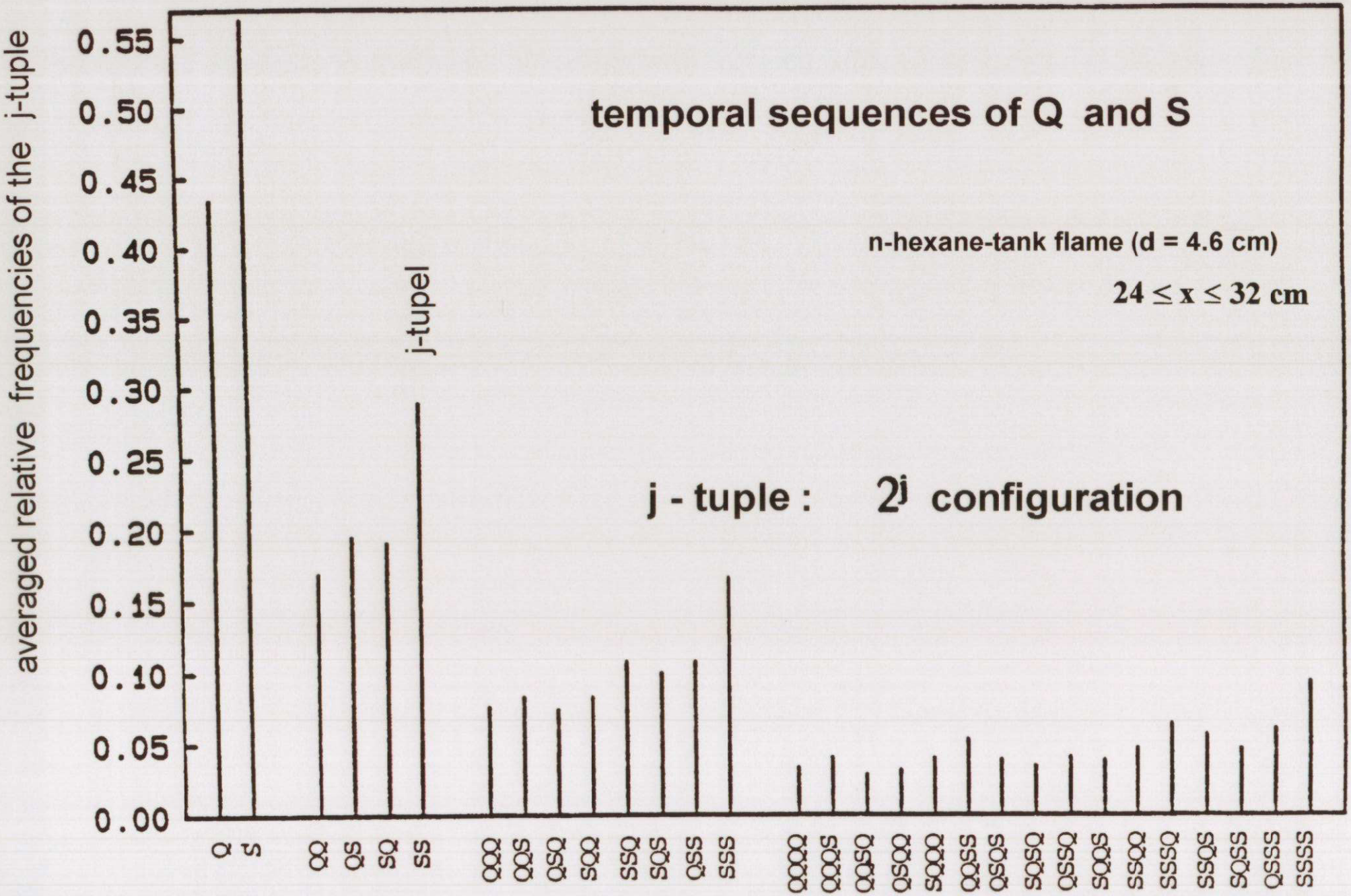
temporal sequences of Q and S
n-hexane-tank flame (d = 4.6 cm)
24 ≤ x ≤ 32 cm
j - tuple : 2^j configuration
averaged relative frequencies of the j-tuple
j-tupel
0.55
0.50
0.45
0.40
0.35
0.30
0.25
0.20
0.15
0.10
0.05
0.00
Q
S
QQ
QS
SQ
SS
QQQ
QQS
QSQ
SQQ
SSQ
SQS
QSS
SSS
QQQQ
QQQS
QQSQ
QSQQ
SQQQ
QQSS
QSQS
SQSQ
QSSQ
SQQS
SSQQ
SSSQ
SSQS
SQSS
QSSS
SSSS

5.3.7 Multiple combinations of Q and S (I)

communicative phenomena

Twins (ZW): (QQ), (SS), and (QS)

position: mainly in the region of the flame axis and less frequently at the contours of the flame field

$\bar{n}_{SS}^{max} \approx 18\%$: (SS) with a maximum probability

$\bar{\tau}_{(SS)} > \bar{\tau}_{(QQ)}$

(a) $\Delta x \uparrow : \bar{\tau}_{ZW} \downarrow \quad \overline{\Delta t}_{ZW} \downarrow \quad \bar{n}_{ZW} \uparrow (C_6H_{14}) \quad \downarrow (CH_3OH)$

(b) $d \uparrow : \bar{\tau}_{ZW} \downarrow \qquad\qquad \bar{n}_{ZW} \uparrow (C_6H_{14}) \quad \downarrow (CH_3OH)$

(c) $(\bar{\tau}_{ZW})_{CH_3OH} > (\bar{\tau}_{ZW})_{C_6H_{14}}$

$(\overline{\Delta t}_{ZW})_{CH_3OH} > (\overline{\Delta t}_{ZW})_{C_6H_{14}}$

$(\bar{n}_{ZW})_{CH_3OH} < (\bar{n}_{ZW})_{C_6H_{14}}$

Multiple combinations of Q and S (II)

Triplets (trip.): (QQQ), (QQS), (QSS)

position: as in the case of twins

$\overline{n}_{SSS}^{max} \approx 6.7\%$: (SSS) with a maximum probability

(a) $\Delta x \uparrow$: $\overline{\Delta t}_{trip.} \downarrow$ $\overline{n}_{trip.} \downarrow$

(b) $\left(\overline{\Delta t}_{trip.}\right)_{CH_3OH} > \left(\overline{\Delta t}_{trip.}\right)_{C_6H_{14}}$

$\left(\overline{n}_{trip.}\right)_{CH_3OH} > \left(\overline{n}_{trip.}\right)_{C_6H_{14}}$

Multiple combinations of Q and S (III)

quadru- and quintuplets:

(QQQQ), (QQQS), (QQSS), (QSSS), (SSSS)

$\bar{n}^{max}_{(SSSS)} \approx 2.3\%$: (SSSS) most probably

only (QSSSS)

$\bar{n}^{max}_{(QSSSS)} \approx 0.4\%$

(a) $\Delta x \uparrow$: $\overline{\Delta t}_{quadru} \downarrow$ $\bar{n}_{quadru} \uparrow$ (C_6H_{14}) $\downarrow$ (CH_3OH)

(b) $\left(\overline{\Delta t}_{quadru}\right)_{CH_3OH} > \left(\overline{\Delta t}_{quadru}\right)_{C_6H_{14}}$

$\left(\bar{n}_{quadru}\right)_{CH_3OH} > \left(\bar{n}_{quadru}\right)_{C_6H_{14}}$

5.3.8 Mono-, Bi- and Tri-periodicities of the thermal boundary layer wave

■ Mono-periodicities with harmonics

Experimental:

distance $y_G(t)$ between the thermal boundary layer and the flame axis

- Influencing quantities are:
  - Volume rate of the fuel
  - Premixedness
  - Fraction of inert gas (e.g. N_2, He)
  - O_2 and N_2 feed
  - type of fuel
    (depending on the number of C-atoms)
  - Pool diameter
  - Height region above the tank rim
- 5 mono-periodic phenomena with $f_i = 11.8$ Hz

  1 mono-periodic phenomenon with $f_{fG} = 8.5$ Hz

  (*for n-hexane tank flame, d = 4.6 cm*)

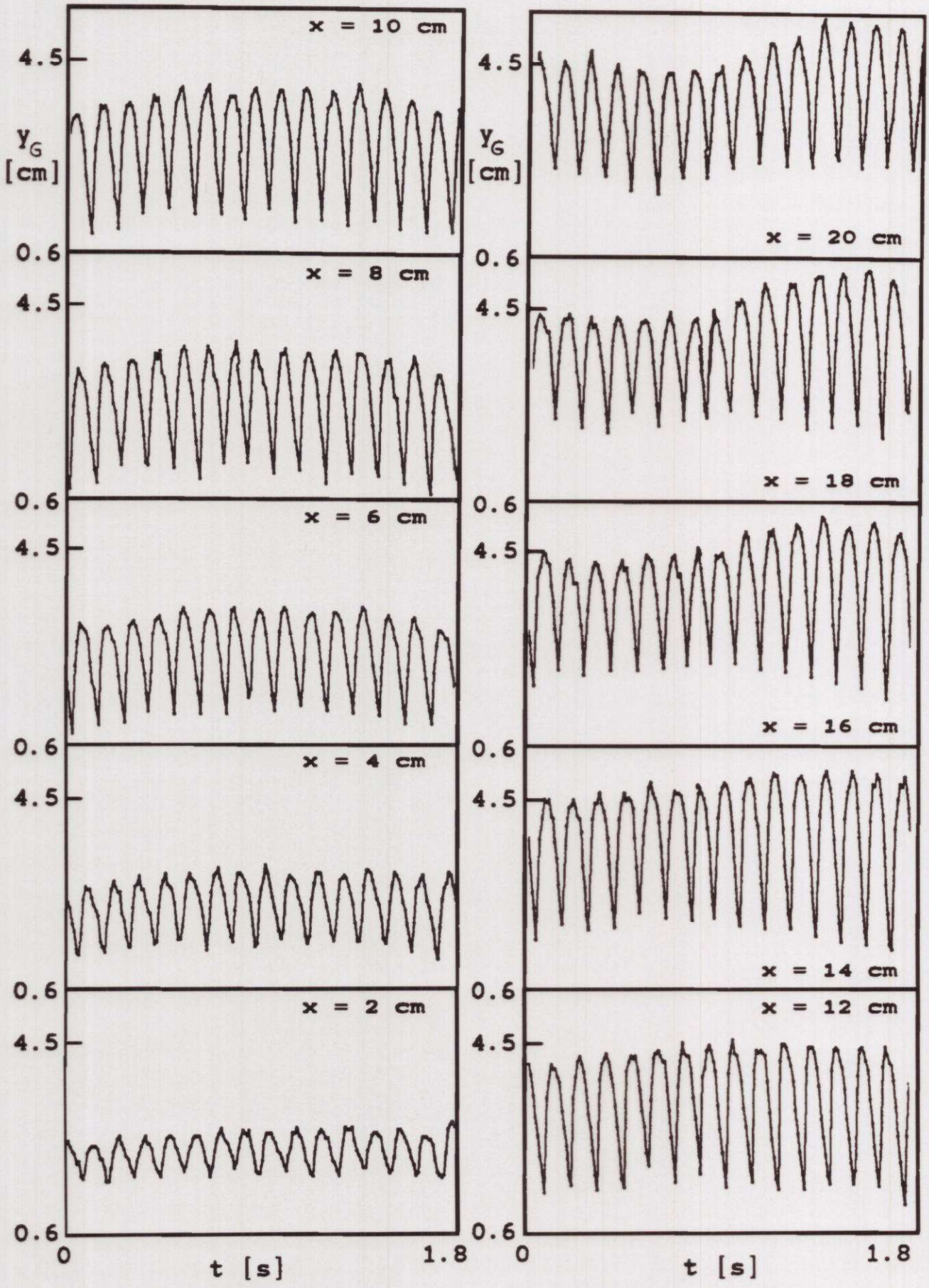

time series of $y_G(t)$ of the thermal boundary layer for a nonpremixed CH_4-tank flame $(\dot{V}_{CH_4} = 1.25 * 10^{-4}\ m^3/s)$

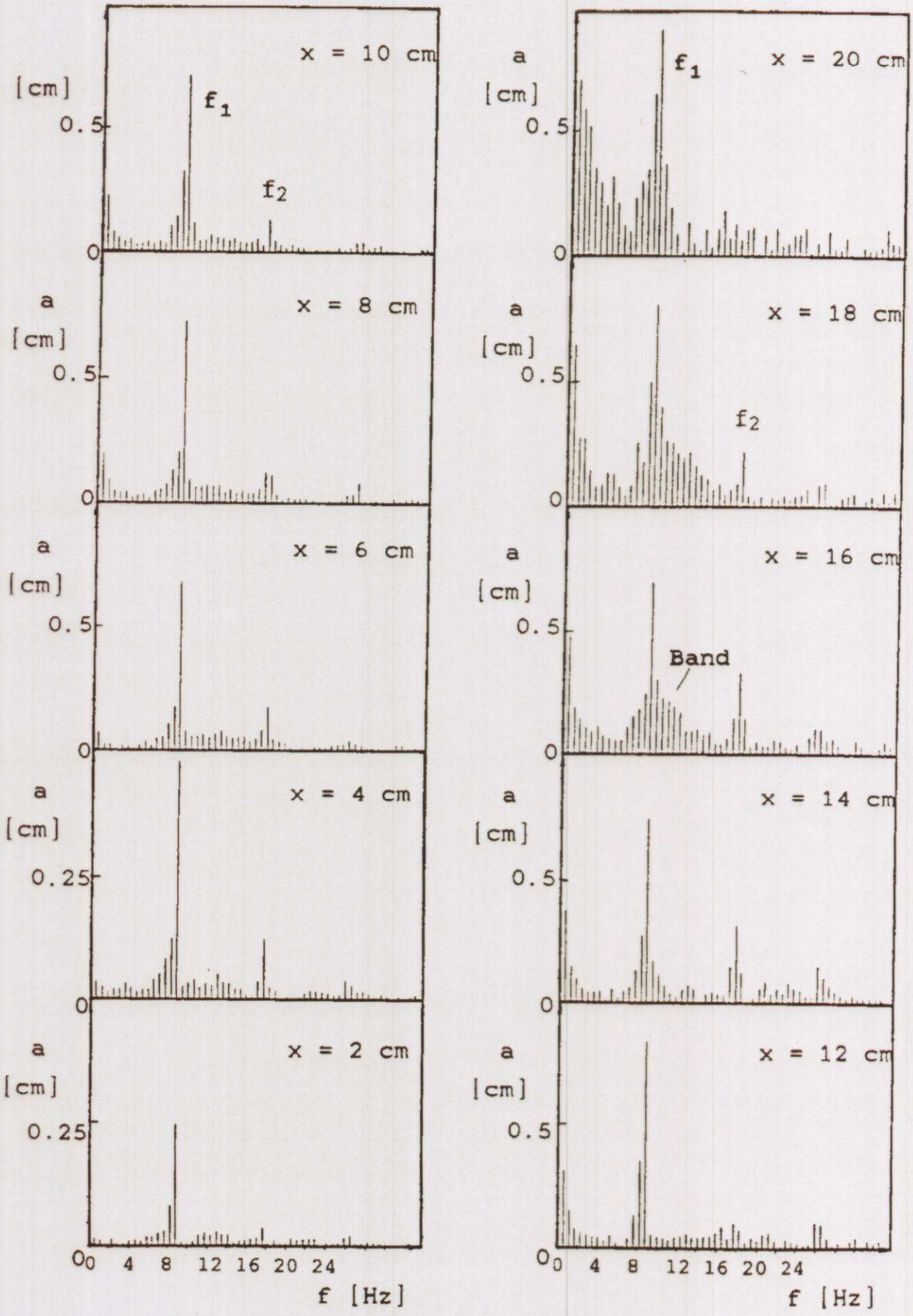

height dependent amplitude spectra of $y_G(t)$ for a nonpremixed CH_4-flame $(\dot{V}_{CH_4} = 1.25 * 10^{-4}\ m^3/s)$

- Qualitative *mechanism* of the mono-periodic phenomena

Example: CH_4/air tank flame (d = 4.6 cm)

In the case of air feed: $f_1 = 6.8$ Hz; $f_2 = 8.1$ Hz

$2 f_1 = 13.6$ Hz

In the case of O_2 feed: $f_1 = 7$ Hz

$2 f_1 = 14$ Hz

$3 f_1 = 21$ Hz

In the case of N_2-feed: $f_1 = 3.1$ Hz; $f_2 = 6.5$ Hz;

$2 f_1 = 6.2$ Hz

$f_3 = 7.8$ Hz

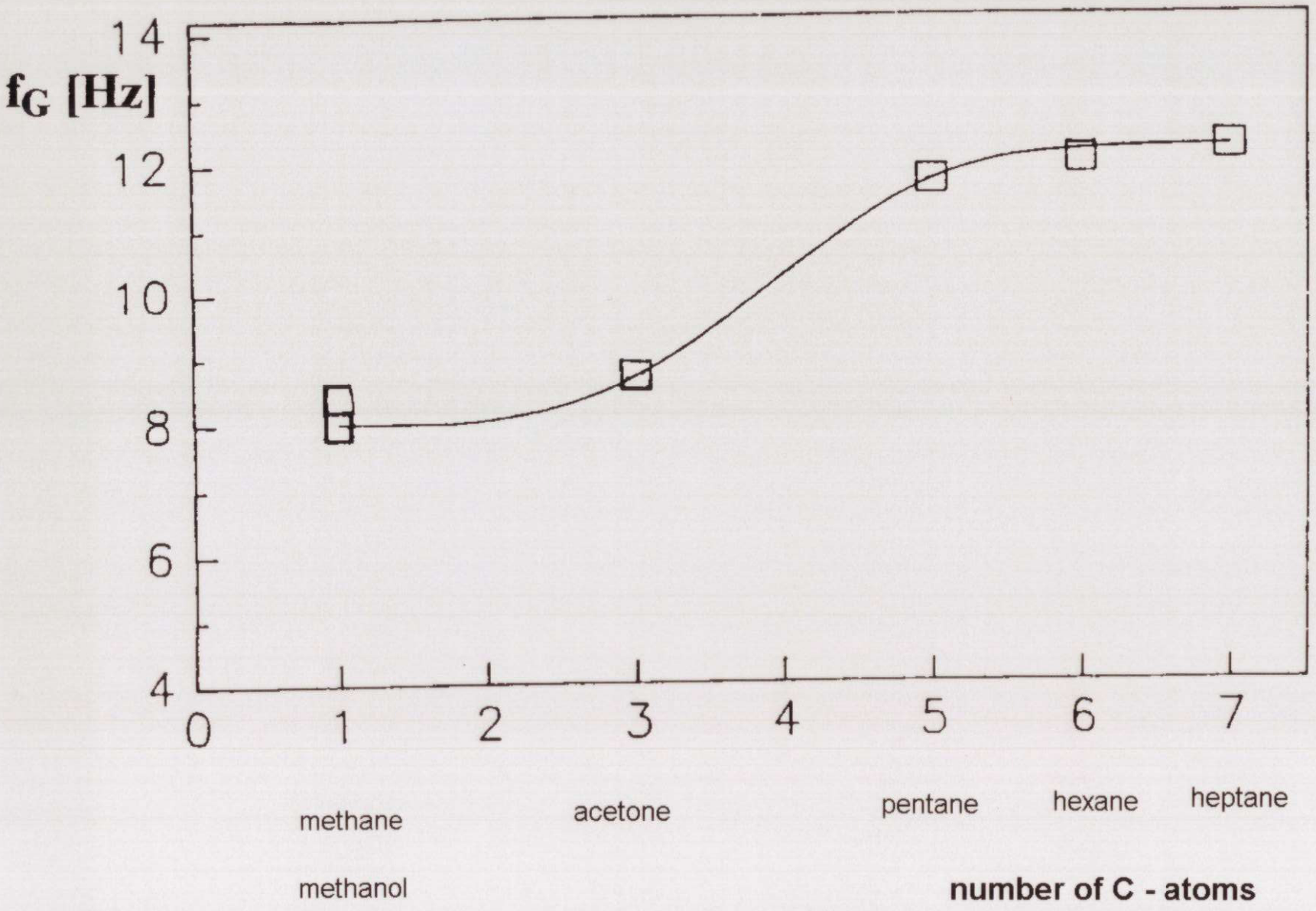

f_G: frequency of the thermal boundary layer of the flame

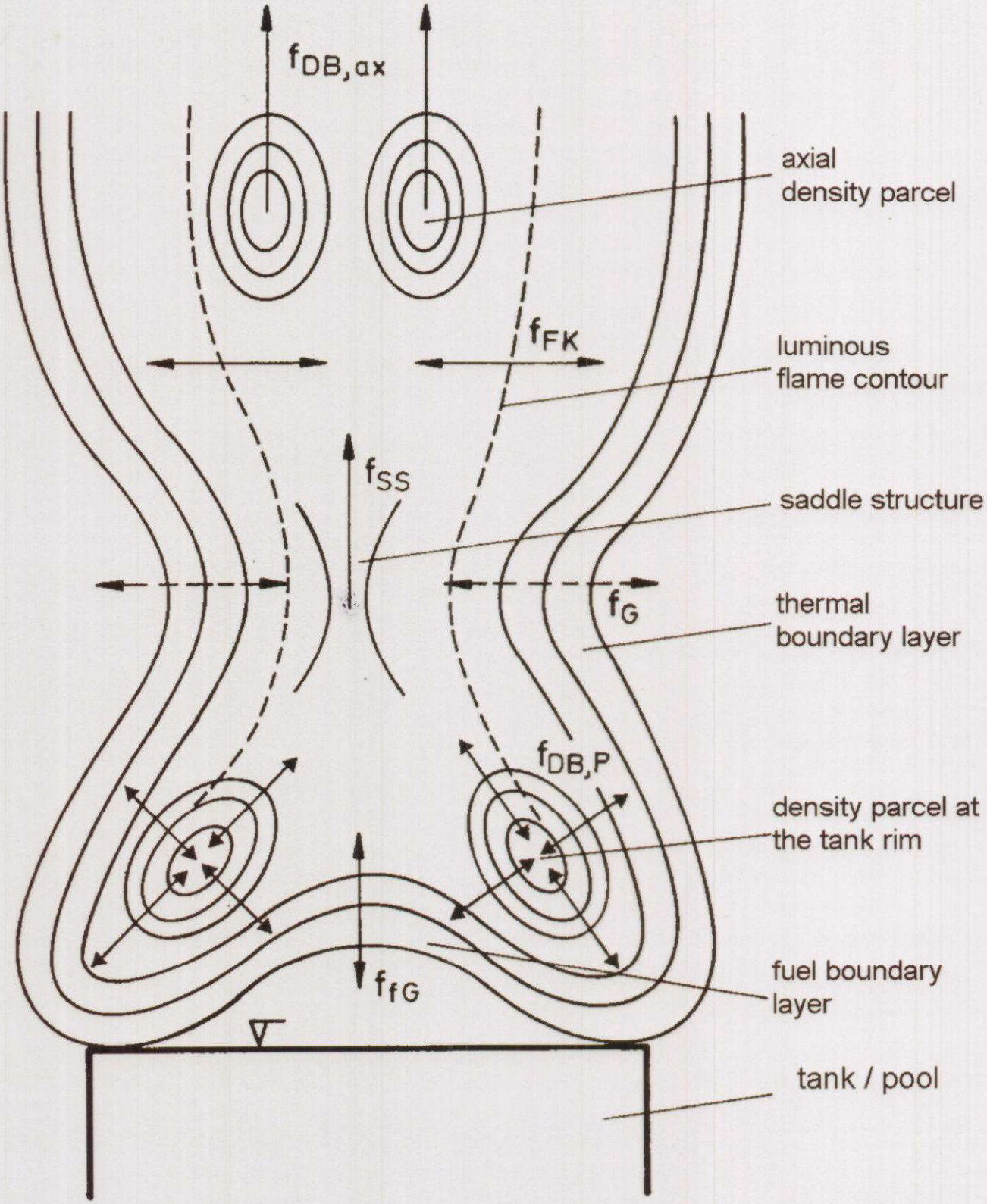

$f_G = f_{FK} = f_{DB,ax} = f_{DB,P} = f_{SS} \approx 11.8$ Hz

$f_{fG} = 8.5$ Hz

Schematical illustration of the periodic phenomena in the continuous flame zone of a tank flame (n-hexane, d = 4.6 cm)

■ Bi- and tri-periodicities

Experimental:

From $y_G(t)$ and from frequency spectra

- Influencing quantities are:
  - all quantities mentioned in the case of monoperiodic phenomena
  - regions of the height Δx

height-dependent curves of constant frequencies $f_i = \text{const}$

$i = 1, 2, 3$

$x > 5$ cm : bi- and tri-periodicities

($d > 7$ cm)

$10 < x < 15$ cm : amplitudes reach a maximum

if $x \uparrow$: low frequencies dominate at the loss of structures with higher frequencies

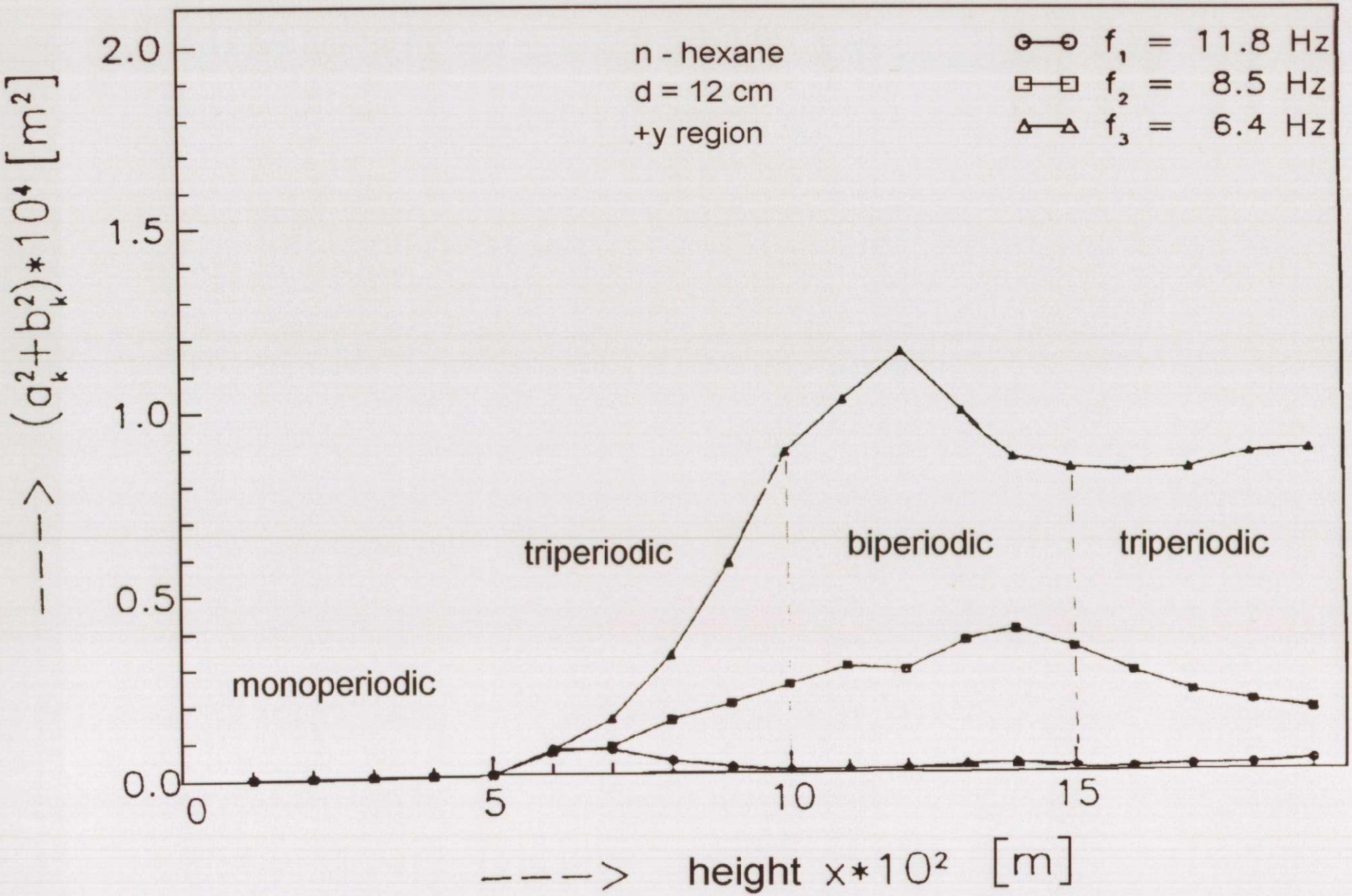
n - hexane
d = 12 cm
+y region
f1 = 11.8 Hz
f2 = 8.5 Hz
f3 = 6.4 Hz
monoperiodic
triperiodic
biperiodic
triperiodic
2.0
1.5
1.0
0.5
0.0
0
5
10
15
---> (ak2+bk2)*10⁴ [m²]
----> height x*10² [m]

- Dependence on tank diameter d (n- hexane)

d [cm]	f_1 [Hz]	f_2 [Hz]	f_3 [Hz]
4.6	11.8	8.5	-
7.0	10.8	6.9	-
8.0	10.5	6.0	3.0
9.0	10.5	7.0	2.6
12.0	11.8	8.5	6.4
15.0	11.3	6.6	4.7

5.3.9 Mono- and quasiperiodic phenomena of Q, S

- *Mono*periodic phenomena

- Formation of groups (i = 2, 3, 4, 5, 6) with the frequency f_{Gr} = 3 Hz at a constant sequence 3-2-5-6-4 (n - hexane, d = 4.6 cm):

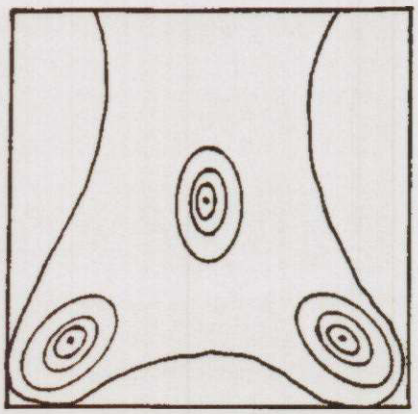

i = 3

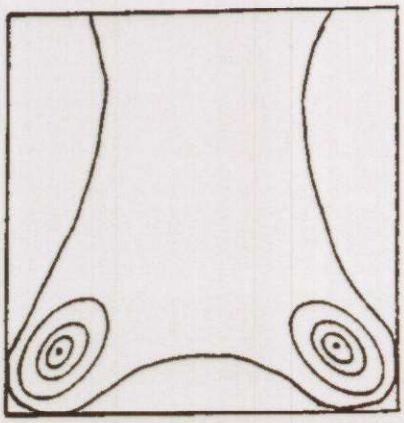

i = 2

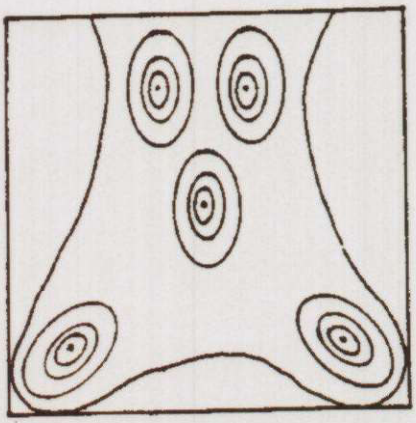

i = 5

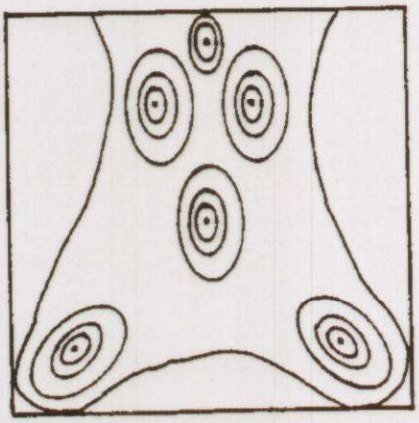

i = 6

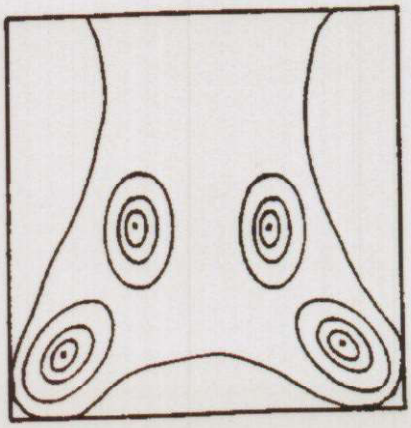

i = 4

- Influencing quantities are:

  - type of fuel
  - tank diameter d

- *Oscillations* of the density sources at the tank rim

  $f_{DB, P}$ = 11.8 Hz (n-hexane, d = 4.6 cm)

- *Periodical rise* of the axial density parcels in the region of the continuous flame zone

  $f_{DB, ax}$ = 11.8 Hz (n-hexane, d = 4.6 cm)

■ Quasiperiodic phenomena

- Formation times of Q and S

$p(\Delta t)$ PDF: exponential distribution

$$p(\Delta t) = \frac{1}{\overline{\Delta t}} \exp\left[-\frac{1}{\overline{\Delta t}}\,\Delta t\right]$$

(a) $\overline{\Delta t}_S < \overline{\Delta t}_Q$

(b) $\Delta x \uparrow : \overline{\Delta t} \downarrow$

(c) $d \uparrow : \overline{\Delta t} \downarrow$

(d) $\overline{\Delta t}_{CH_3OH} > \overline{\Delta t}_{C_6H_{14}}$

(e) number density: $\frac{w_{Q+S}}{A} = \frac{1}{A}\frac{\overline{\tau}_{Q+S}+1}{\overline{\Delta\tau}_{Q+S}} = 0.08$

A: observed aerea of the interference fringe pattern

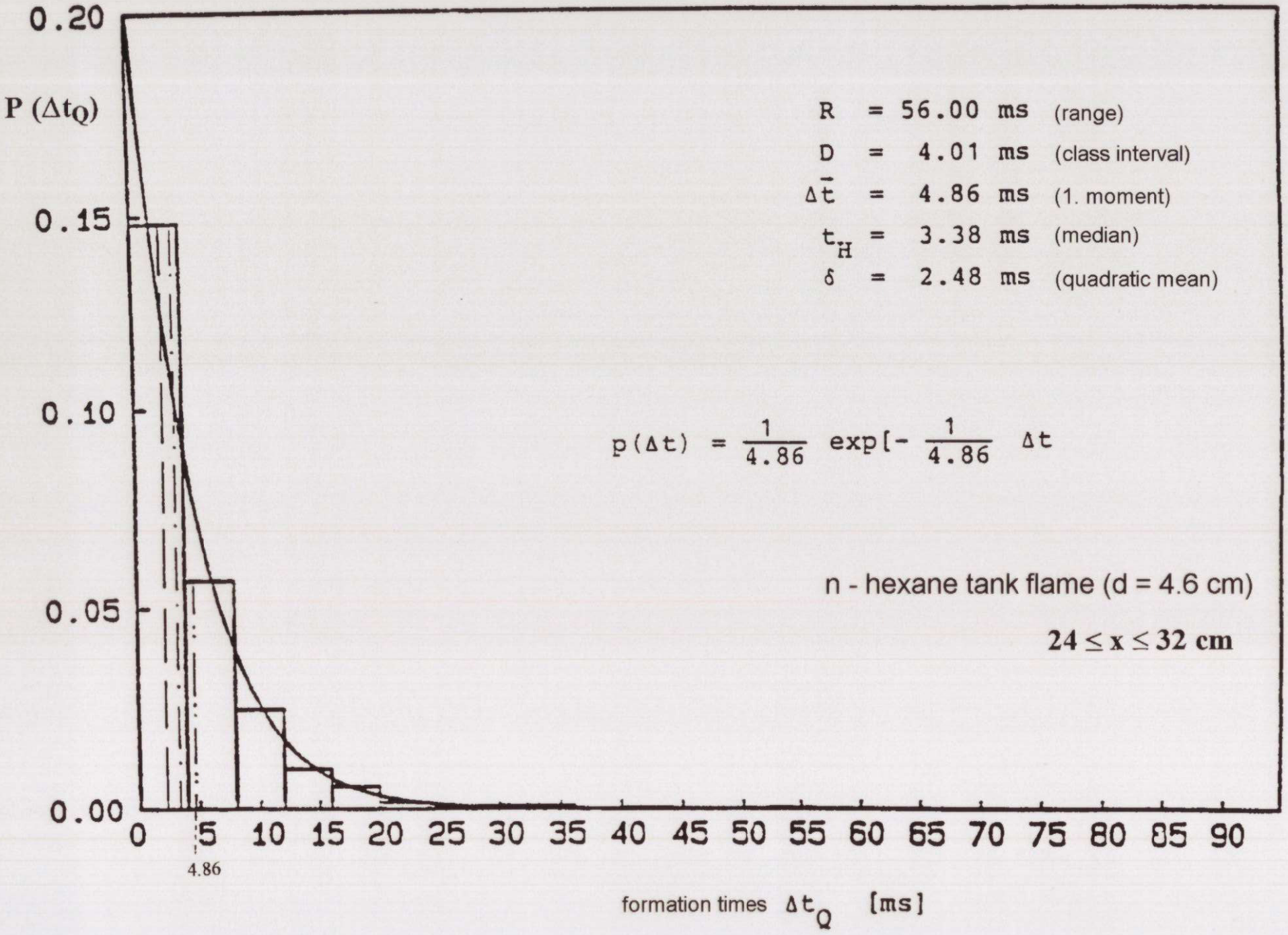
0.20
0.15
0.10
0.05
0.00
P (Δt_Q)
R = 56.00 ms (range)
D = 4.01 ms (class interval)
Δt̄ = 4.86 ms (1. moment)
t_H = 3.38 ms (median)
δ = 2.48 ms (quadratic mean)
p(Δt) = 1/4.86 exp[- 1/4.86 Δt
n - hexane tank flame (d = 4.6 cm)
24 ≤ x ≤ 32 cm
0 5 10 15 20 25 30 35 40 45 50 55 60 65 70 75 80 85 90
4.86
formation times Δt_Q [ms]

- *Formation frequencies of Q and S*

$$f_{BQ} \equiv \frac{1}{\Delta\bar{t}_Q}$$

$\Delta\bar{t}_Q$, $\Delta\bar{t}_S$: 1. moment of $P(\Delta t_Q)$ $P(\Delta t_S)$

$$f_{BS} \equiv \frac{1}{\Delta\bar{t}_S}$$

Example: n-hexane tank flame, d = 4.6 cm

$16 < x < 24$ cm : $f_{BQ} = 93$ Hz

$f_{BS} = 95$ Hz

$24 < x < 32$ cm : $f_{BQ} = 205$ Hz

$f_{BS} = 260$ Hz

5.4 Some new criteria for the formation of dissipative (coherent) structures

as $f(x)_d$ and $f(d)$

1. Changes in direction and beginning folding of the interference fringes

2. The thermal boundary layer starts rolling up and shows a strong constriction

3. Changes of the orientation (rotation) of axial density parcels

4. Occurrence of > 2 *incommensurable* frequencies

5. Broadening of the persistent line in the frequency spectra of the dynamic pressure

6. Formation of a mushroom in the VIS-radiance structure of the flame (flame mushroom)

7. Sequences of Q and S (j - Tuple)

$$2^j + j \leq w_Q + w_S + 1 \quad \rightarrow \quad j_{max} = 9$$

experimental: $j \leq 5$ $\rightarrow$ selection resp. partial order

8. Multiple combinations of Q and S

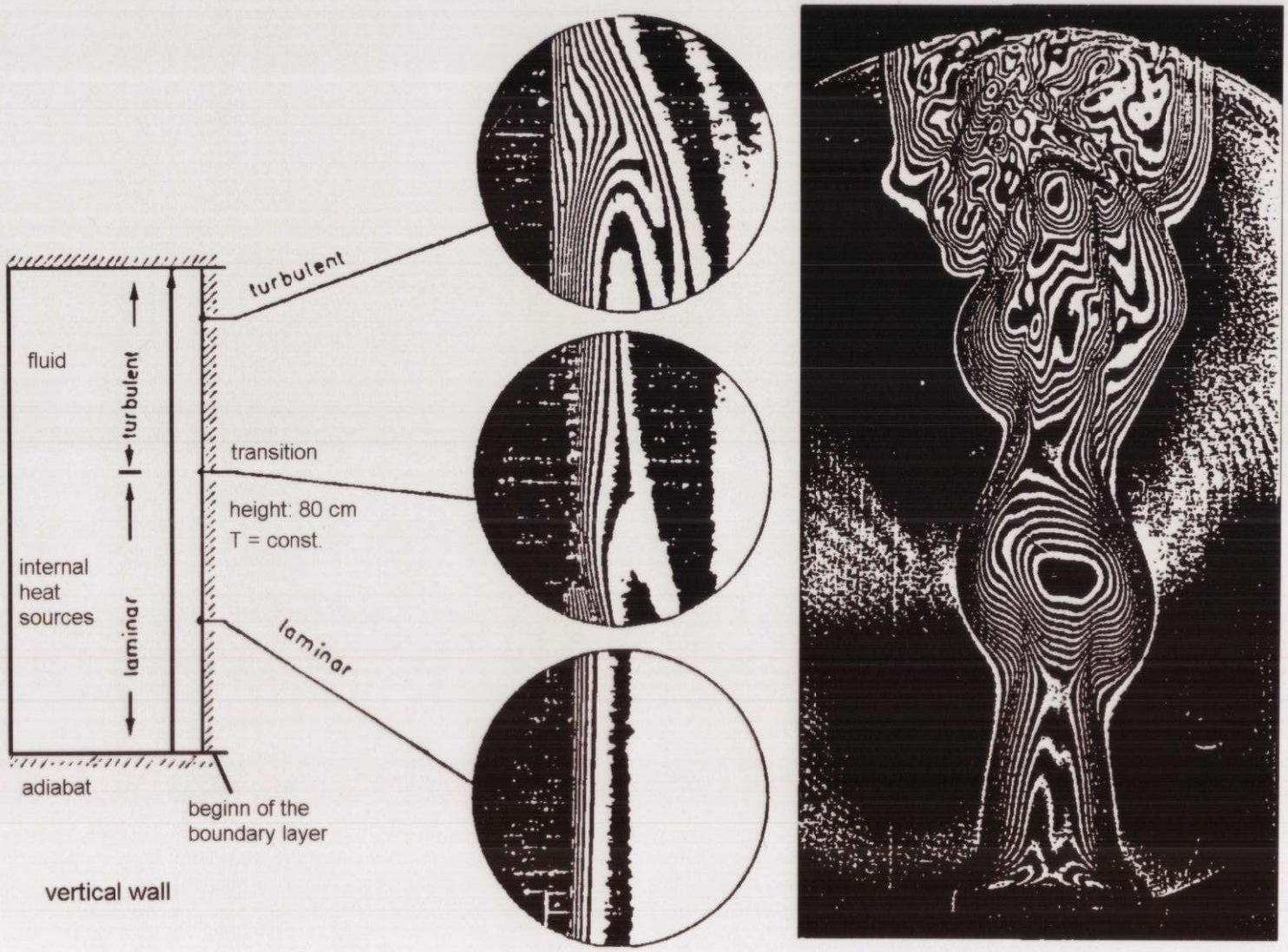

Characteristic structures of a vertical thermal boundary layer at different flow states in comparison to the interference fringe pattern of an n-hexane tank flame
(d = 4.6 cm, $0 \leqq x \leqq 25$ cm)

5.5 The influence of chemical reactions

Due to a definite variation of axial and radial feed of O_2, air and N_2, the ratio of r_R and the velocity r_T of the (turbulent) mass exchange is changed:
Essential changes of important characteristics of dissipative structures can be observed:

- **Density parcels at the tank rim**

  Formation of density sources in the region of the luminous reaction zones (RZ) as a function of the premixedness

  - In the case of axial, concentric feed of O_2

- **Distribution of the number of density parcels with the height x**

  - Considerable *increase* of the number of density *sources* near the tank rim and a strong *decrease* of the number of density sources in the transition zone and the flame plume, simultaneously,

    ⇒ shifting of the reaction zones to the lower region of the tank flame

- **Frequency distribution of the total number of density parcels per total height region**

  - At an increased O_2-fraction the averaged total number of density sources and also density sinks will be *diminished:*

    ⇒

    At increased O_2-fraction the fast chemical reactions are limited to a few (larger) regions

- **Frequency distribution of the length-scales**

  - The length-scales of density sources *increase*. The length-scales always (i.e. also with air, N_2-feed) increase in the continuous flame zone and decrease in the transition flame zone

    ⇒

    At increased O_2fraction the luminous flame fronts are *hotter* and *thinner*

- **Frequency distribution of lifetimes**

  - At increased O_2-fraction the averaged lifetime of the density sources increases strongly and the lifetime of the density sinks increases significantly

    ⇒

    The hotter reaction zones cause an intensive local heating of the flame gases, which exist correspondingly longer.

  - In the case of axial, concentric feed of N_2.

- **Distribution of the number of density parcels with height x**

  - Decrease of the number of density parcels in the total flame. The *first momentum* of the axial distribution shifts towards upper heights x.

    ⇒

    At increased N_2-fraction the reaction zones shift towards the upper regions of the flame.

- No density sinks exist in the continuous flame zone. The *first momentum* of the axial distribution shifts towards the upper heights within the flame.

  ⇒

  At increased N_2-fraction in the continuous flame zone, *no* density *sinks* are formed. With increasing height x in the region of the transition zone and flame plume a formation of density sinks (*decrease* of local *density*) is observed due to *cool-down* phenomena.

- **Frequency distribution of the total number of density parcels per total height region**

  - At increased N_2-fraction within the continuous flame zone the averaged total number of density sources decreases significantly, however, within the transition flame zone it increases strongly. The total number of density *sinks* increases slightly within the total flame:

    ⇒

    The reaction zones are distributed to the larger, turbulent region in the transition zone and flame plume.

- **Frequency distribution of length-scales**

  - The averaged length-scales of density *sources* decrease severely. Density sources exist only within the transition flame zone:

    ⇒

    At increased N_2-fraction the luminous flame fronts are less hot and less thin

- **Frequency distribution of lifetimes**

  At increased N_2-fraction the averaged lifetimes of density sources and sinks are significantly *shortened*:

  ⇒

  An additional shortening of the lifetime of the reaction zones occurs because these are predominantly located in the turbulent transition zone and flame plume.

■ Frequencies of the thermal boundary layer

At O_2-feed:

Increase of r_R, so that a *transport*-controlled ($r_R >> r_{transport}$) e.g. CH_4/air tank flame exists with a relatively *high* temperature and *high* density gradients:

⇒

A strong periodic bulging of the thermal boundary layer occurs, with a fundamental oscillation of a high amplitude with the frequency f_1 and its harmonics:

CH_4/air tank flame
(with O_2-feed): $f_1 = 7$ Hz (laminating effect)

$2 f_1 = 14$ Hz

$3 f_1 = 21$ Hz

CH_4/air tank flame
(with air-feed): $f_1 = 6.8$ Hz; $f_2 = 8.1$ Hz

$2 f_1 = 13.6$ Hz

At N_2-feed:

Decrease of r_R so that a *kinetic*-controlled ($r_R << r_{transport}$) e.g. CH_4/air tank flame exists with a relatively *low* temperature and relatively *small* density gradients:

⇒ No strong bulging of the thermal boundary layer occurs, and thus also no significant fundamental oscillation:

CH_4/tank flame
(with N_2-feed): $f_1 = 3.1$ Hz; $f_2 = 6.5$ Hz;
$2 f_1 = 6.2$ Hz
$f_3 = 7.8$ Hz

- Investigated phase objects and their dimensions

Non-reacting flows:	He, hot air
Reacting flows:	Hydrocarbons,
(nonpremixed tank flames, partially premixed tank flames)	alcohols, H_2

$$1 \leq d \leq 25 \text{ cm}$$

6. Conclusions and outlook (I)

6.1 Characteristics and technical importance of phase objects

Buoyant, laminar slow flows *with* and *without* chemical reactions: formation of soot particles and gaseous pollutants

New concept: coflow, nonpremixed flame, considered as a nonlinear dissipative system

6.2 Experimental methods

- *Visualisation* of dissipative structures with the holographic real-time interferometry (25 cm laser beam expanding): instantaneous density fields simultaneous to the luminous flame fronts

Conclusions and outlook (II)

- Interpretation of the interference fringes from tank flames as lines of constant mass density of the flame gas mixture

- Types of structures: e.g. density *sources*, density *sinks*, *thermal boundary* layer

DVD-video: "Tank flames, Dynamics of dissipative Structures"

6.3 Dynamic properties of dissipative structures

Spatial-temporal structures

Sources: local temperature *increase* (e.g. due to the presence of reaction zones)

Sinks: local temperature *decrease* (e.g. due to interaction with the cooler ambient air)

Conclusions and outlook (III)

- Existence of *two length scales directly* from the interference fringe pattern in agreement with the corresponding values from frequency spectra of p'_{dyn} , $L_{\Delta\lambda}$
  - Classification of tank flames ($d \leq 10$ cm) within the *Borghi* diagram
  - Small folded to wrinkled flamelets
- Turbulent momentum-, mass- and heat exchange coefficients directly from the interference fringe patterns (K_I) and also from *measured* concentration profiles ($K_{\gamma i}$), and measured temperature profiles (K_w)
- K_I, $K_{\gamma i}$, K_w : $\approx$ 10 to 70 fold larger than the molecular transport coefficients

- From the dynamic properties of *density* parcels can be concluded:

$0.2 \leq Pr_t \leq 0.4$
$0.2 \leq Sc_t \leq 0.4$ for $x \geq 10$ cm

$\Rightarrow$

momentum transport < mass transport

heat transport

$0.8 \leq Le_t \leq 1.0$ for $10 \leq x \leq 16$ cm

$\Rightarrow$

mass transp. > heat transp.

$1.0 \leq Le_t \leq 1.5$ for $x \geq 16$ cm

$\Rightarrow$

mass transp. < heat transp.

Conclusions and outlook (IV)

- **Number of Q and S**

  $w_S > w_Q$; $w_S = f(\Delta x, d, \text{fuel})$

- **Growth and decay of Q, S**

  as a function of height x and fuel

- **Lifetimes τ of Q and S**

$$\bar{\tau}_S > \bar{\tau}_Q \; ; \quad \bar{\tau}_S = f(\Delta x, d, \text{fuel})$$

- **Transitions between Q and S**

  (*communicative* phenomena)

  $Q \rightarrow S$: local *cool-down* or local density increase, respectively

  $S \rightarrow Q$: local *heating* or local density decrease, respectively

  $Q \rightarrow S \rightarrow Q \rightarrow S$ and $S \rightarrow Q \rightarrow S \rightarrow Q \rightarrow S$

Conclusions and outlook (V)

- **Temporal sequences of Q and S**

  (*communicative* phenomena)

  2^j configurations: j = 1 1-tupel: Q, S

  j = 2 2-tupel: QQ, QS, SQ, SS

  j = 3 3-tupel: QQQ, SSS, ...

  Relative frequency of 2 to 4-tupel

  Most probable *configuration:*

  The tupel which consists only of sinks S

  Most probable *composition:*

  Q_2S_3 (d = 4.6 cm, n-hexane)

  QS_3 (d = 10 cm, n-hexane)

Conclusions and outlook (VI)

- Multiple combinations of Q and S (*communicative* phenomena)

  Twins (e.g. SS) up to *quintuples* (e.g. SSSSS)

  18 % 4 %

  Especially in the region of the flame axis

Conclusions and outlook (VII)

- ***Mono-, Bi- and Tri-periodicities***

Mono- and bi-periodicities:

e.g. n-hexane tank flame (d = 4.6 cm)

$f_{FK} = f_{DB,\,ax} = f_{DP,\,P} = f_{SS} = 11.8$ Hz

$f_{fG} = 8.5$ Hz

Tri-periodicity of the wave of the thermal boundary layer:

e.g. n-hexane flame (d = 12 cm)

$6 < x < 19$ cm : $f_1 = 11.8$ Hz

$1 < x < 19$ cm : $f_2 = 8.5$ Hz

$7 < x < 19$ cm : $f_3 = 6.4$ Hz.

Conclusions and outlook (VIII)

- **Mono- and quasi-periodic phenomena of the source and sink structures**

n-hexane d = 4.6 cm, 0 < x < 8 cm

Mono-periodic (f_K = 3 Hz):

Formation of i-groups with constant sequence

3-2-5-6-4

Quasi-periodic:

Frequencies of formation of density sources and density sinks

f_{BQ} = 93 Hz; f_{BS} = 95 Hz

16 < x < 24 cm

f_{BQ} = 205 Hz; f_{BS} = 260 Hz

24 < x < 32 cm

6.4 Experimental criteria for the formation of dissipative structures

- Specific properties of the thermal boundary layer:

  Particularly beginning roll-up and quasi-periodic oscillations

- Formation of a flame mushroom in the VIS-spectral range

- Appearance of multiples of Q and S

- Sequences of Q and S (j-tupel)

  $$2^j + j \leq w_Q + w_S + 1 \quad \Rightarrow \quad j_{max} = 9$$

  Experimental: $j \leq 5$ $\Rightarrow$ selection or partial order, respectively.

6.5 *Chemical reactions* have influence on

- Density parcels at the tank rim
- Distribution of the number of density parcels as a function of height
- Frequency distribution of the total number per total height region
- Frequency distribution of length-scales
- Frequency distribution of lifetimes
- Frequencies of the thermal boundary layer

6.6 Concepts of modeling

- Nonpremixed flames show a typical *complex behaviour*
  - *Physics of nonequilibrium states*
    Nonlinear science
    - Concept of *dissipative structures*
      (→ *I. Prigogine*, Brussels)
    - Concept of *synergetics*
      (→ *H. Haken*, Stuttgart)

6.7 Outlook

- *Modeling of the dissipative structures* in laminar and turbulent tank flames, respectively in other nonpremixed flames

- *Multidirectional* recording of *asymmetric* refractive index fields, e.g. *turbulent* tank flames for d ≈ 20 - 50 cm and *nonreacting* turbulent flows

  - Holographic interferometry by methods of computer aided tomography, e.g. with 4 illuminating rays (expanded beams) passing the phase object.

Conclusions and outlook (XIII)

- Using *additional* optical measurement techniques, especially for

  - flow and *concentration* measurements, e.g. Laser-Doppler-velocimetry (LDA),
  - CARS spectroscopy,
  - Laser Induced Fluorescence (LIF), measurement of particle sizes [e.g. line-of-sight extinction of a laser beam as it penetrates through a cloud of particles; dynamic light scattering].

- *Simultaneous* diagnostics

  e.g. of major and minor species and temperature from a *combination* of *Raman* scattering and LIF